ISSN 2436-5173 (Online)

Metallomics Research

SPECIAL ISSUE

Trends in Selenium Research

Vol.2/No.3
December 2022

JSBRTE
Japan Society for
Biomedical Research on Trace Elements

Metallomics Research

Vol.2/No.3
December 2022
ISSN 2436-5173 (Online)

Japan Society for
Biomedical Research on Trace Elements

Index

SPECIAL ISSUE

Trends in Selenium Research

Editorial Office

Seishinsha, co. Ltd.,
Japan society for Biomedical Research on Trace Elements
2-8-13 Fukashi, Matsumoto-shi, Nagano 390-0815, Japan
Tel: +81-263-32-2301
Fax: +81-263-36-4691
Editorial Office: brte-post@seisin.cc
URL: https://www.brte.org/
https://metallomicsresearch.brte.org/

Metallomics Research 2022 (3) #MR202206

Review https://metallomicsresearch.brte.org

Redox Chemistry of Selenols and Diselenides as Potential Manipulators for Structural Maturation of Peptides and Proteins

Kenta Arai [1, 2*], Rumi Mikami [1]

[1] Department of Chemistry, School of Science, Tokai University, Kitakaname, Hiratsuka-shi, Kanagawa 259-1292, Japan

[2] Institute of Advanced Biosciences, Tokai University, Kitakaname, Hiratsuka-shi, Kanagawa 259-1292, Japan

Summary

Oxidative folding is an essential process for polypeptide chains containing cysteine (Cys) residues to form a bioactive three-dimensional structure. During this process, the folded state with the correct disulfide (SS) combination, which is found in the native state, cannot be obtained at 100% yield because various byproducts, such as misfolded states with mispaired SS bonds, oligomers, and aggregates are simultaneously produced. The formation of misfolded states *in vivo* has been suggested to cause critical human diseases such as neurodegenerative disorders. Therefore, the development of methods to promote the correct structural maturation of polypeptides, including Cys residues, both *in vivo* and *in vitro*, is a challenging task in protein synthesis, medicine, and drug discovery. To rapidly form correctly folded proteins at high yields, two potential strategies are available. First, called the *outside strategy*, is to control oxidative folding from the *outside* of proteins using artificial small molecules as catalyst and a reagent that mimics the function of protein disulfide isomerase, which catalyzes SS-related reactions during oxidative folding in cells. Second, called the *inside strategy*, is to insert mimics of SS linkage(s) into the *inside* of polypeptides to form a rigid covalent bond chemoselectively, thereby avoiding the formation of a misfolded state having mispaired SS bonds. In this review, recent developments and trends based on the unique redox properties of selenols and diselenides, which are selenium analogs of thiols and disulfides, respectively, are outlined, and their future prospects are discussed.

Key words: protein folding, cysteine, selenocysteine, enzyme mimic, catalyst, misfolding

Statements about COI: There are no conflicts of interest to declare.

*Correspondence:
Kenta Arai
Department of Chemistry, School of Science, Tokai University,
Kitakaname, Hiratsuka-shi, Kanagawa 259-1292, Japan
Tel: +81 463 58 1211
E-mail: k-arai4470@tokai-u.jp

Received: October 06, 2022
Accepted: November 21, 2022
Released online: December 12, 2022

1. Introduction

Proteins are first synthesized as polypeptide chains through transcription from genetic information in DNA into mRNA and subsequent translation, during which amino acids corresponding to three specific bases (codons) in mRNA are sequentially elongated (i.e., central dogma, **Fig. 1**). For the synthesized polypeptide chains to exert their physiological functions as proteins, they must gain a unique three-dimensional structure through protein folding. In classical protein science, polypeptide chains spontaneously fold into their most stable conformation in an aqueous solution under properly controlled reaction

conditions (**Fig. 1**, *in vitro* folding) [1]. However, only a few proteins strictly follow the basic principle of biophysics, known as the Anfinsen's dogma. In cells with high concentrations of biomolecules, intermolecular interactions and the resulting irreversible aggregation are inevitable; thus, correct folding is inhibited. Therefore, in modern protein science, it is important to understand the structures and functions of enzymes that promote correct folding [2].

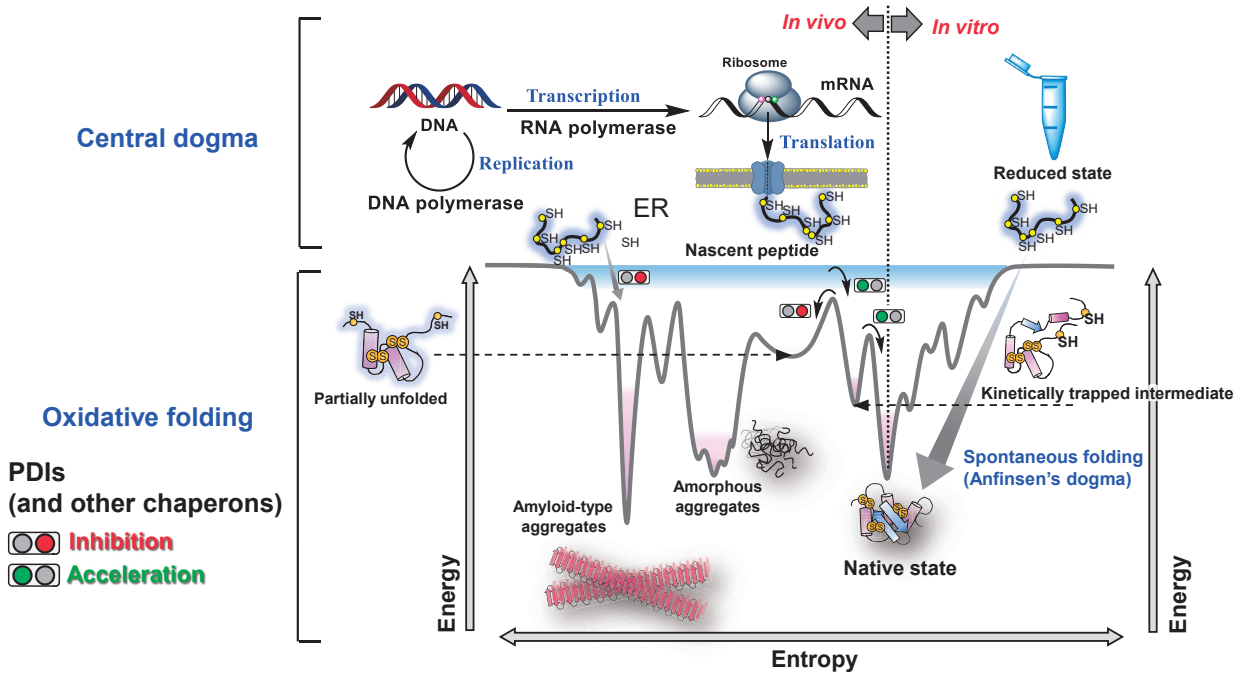

Fig. 1. Biosynthesis of polypeptides following the central dogma and subsequent oxidative protein folding controlled by protein disulfide isomerase family members (PDIs). For oxidative folding, two-dimensional energy landscapes (folding funnels) for *in vivo* and *in vitro* folding are shown, which represent the relationship of energy and entropy (i.e., diversity of peptidyl conformation).

Oxidative cross-linking between cysteinyl thiol (SH) groups to form disulfide (SS) bond(s) is a typical and important posttranslational modification, particularly for secreted proteins; folding coupled with SS formation is commonly termed oxidative folding [3]. Synthesized nascent polypeptides undergo oxidative folding in the endoplasmic reticulum (ER), where the oxidative environment is maintained. Protein disulfide isomerase (PDI), a typical ER-resident SS-based oxidoreductase, cooperatively controls proteostasis together with more than 20 PDI family enzymes (PDIs) in the ER (**Fig. 1**) [4]. PDI has four functional cysteine (Cys) residues that are important for its enzymatic activity (see below). The generation and accumulation of reactive nitrogen species (RNS) due to excessive oxidative stress in the ER leads to undesired oxidative modifications of Cys residues in PDI and significantly decreases enzymatic activity [5]. Dysfunction of PDI leads to disruption of proteostasis in the ER, resulting in misfolding, oligomerization, aggregation, and amyloidogenesis of proteins (**Fig. 1**), eventually triggering various fatal human diseases such as cancer, neurodegenerative disorders, diabetes, and atherothrombotic stroke [6–12].

Oxidative folding is also an essential process for chemically synthesized polypeptides to exert their physiological functions. The solid-phase peptide synthesis (SPPS) method pioneered by Merrifield enabled the synthesis of polypeptides with arbitrary amino acid sequences [13]. Consequently, rare proteins, non-natural proteins, and peptide-based formulations have been easily synthesized, and related fields such as structural biology, medicine, and drug discovery have progressed remarkably [14]. Generally, oxidative folding of synthetic polypeptides can be completed within a reasonable reaction time (hours to days) under mild oxidative conditions. However, considerable effort is often required to determine the optimal reaction conditions. While the use of PDI as a catalyst is effective for efficient folding, it is costly, and separation of the folded protein from PDI is usually difficult. In addition, peptide chains containing three or more Cys residues generally convert to isomeric species with non-native SS bonds (scrambled species) in addition to the native state during oxidative folding. Because the SS bonding pattern depends on the thermodynamic stability of the peptide loop, it is impossible to achieve 100% folding yield, even under precisely optimized

conditions. Therefore, purification of the target protein by high-performance liquid chromatography (HPLC) is usually required after oxidative folding, thus reducing cost and time efficiency of the overall protein synthesis.

Consequently, developing tools for efficient oxidative folding, which has troublesome aspects both *in vivo* and *in vitro*, should be valuable in medicinal science and drug discovery where protein misfolding is a concern. Currently, two chemical strategies are available for this purpose:

a) Indirect control of oxidative folding from the *outside* of protein molecules using an artificial organocatalyst with PDI-like functions (called the *outside strategy*; **Fig. 2a**).

b) Insertion of regioselective covalent bond(s), instead of SS bond(s), and promotion of structural maturation of proteins directly from the *inside* of the protein molecule (called the *inside strategy*; **Fig. 2b**).

In this review, the outside and inside strategies utilizing the redox properties of organoselenium molecules and peptides are discussed. First, the latest research trends and important achievements, in addition to some significant pioneering studies for each strategy, are outlined, and future perspectives of these strategies for artificial manipulation of *in vivo* and *in vitro* oxidative folding are discussed.

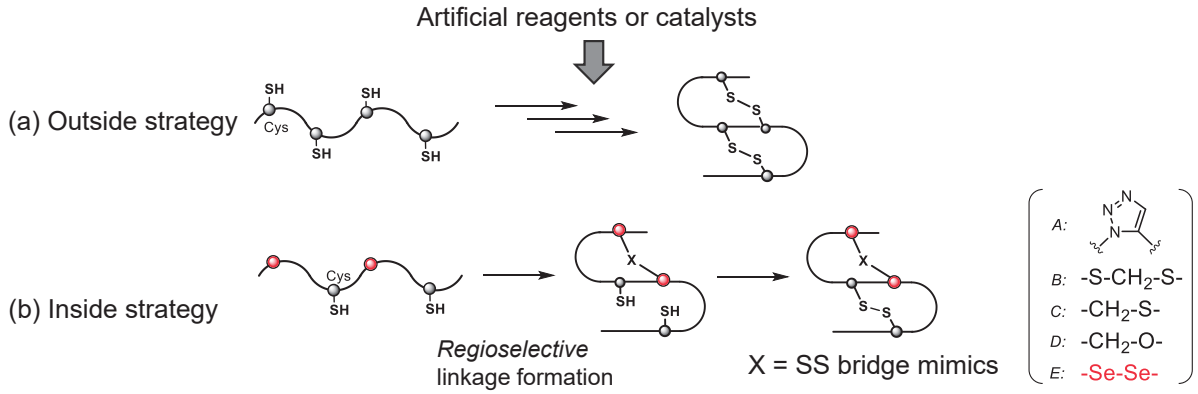

Fig. 2. Potential manipulation strategies for oxidative folding.
(a) Control of oxidative folding using artificial reagents and catalysts (*outside strategy*).
(b) Regioselective covariant bond formation in peptides and proteins by substituting native SS bonds with its representative mimics (*inside strategy*). Disulfide (SS) mimic E (diselenide bridge) was discussed in this review. For SS mimics A, B, C, and D, see the reports in Refs. [15], [16], [17], and [18], respectively.

2. Protein folding coupled with disulfide bond formation

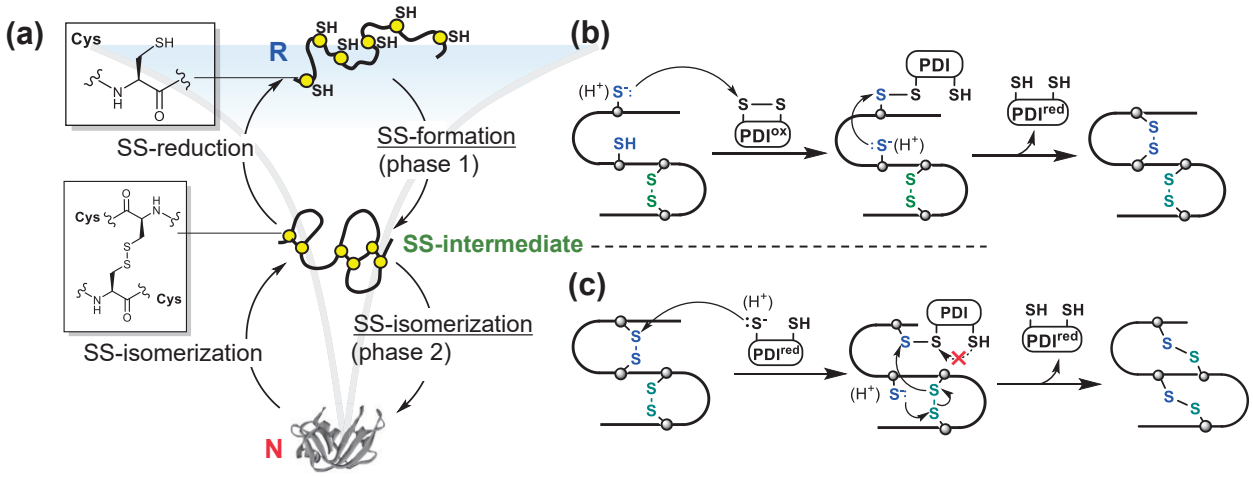

Fig. 3. Chemical perspective of oxidative folding.
(a) Structural maturation coupled with SS-formation (phase 1) and subsequent SS-isomerization (phase 2).
(b) SS-formation promoted by PDI^{ox} via an intermolecular bond exchange reaction.
(c) SS-isomerization catalyzed by PDI^{red} via a temporal SS-cleavage in substrate proteins.

Generally, during *in vitro* oxidative folding, two chemical reaction phases, SS-formation (phase 1) and SS-isomerization (phase 2), are observed (**Fig. 3a**). In phase 1, a reduced protein (R) loses its chain entropy with the hydrophobic collapse of the polypeptide, accompanied by the formation of intramolecular non-native SS bonds. In phase 2, the SS intermediates (scrambled species) generated in the first phase undergo conformational folding accompanied by rearrangement of SS bonds to search for correctly paired SS bonding patterns found in the native state. PDI accelerates the overall rate of oxidative folding by exhaustively catalyzing SS-related reactions in these phases (**Fig. 3b, c**) [19–22].

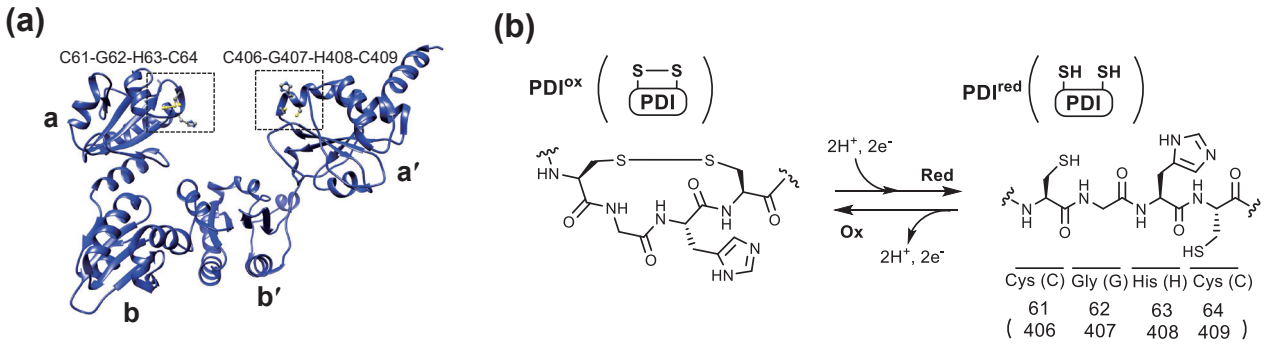

Fig. 4. Protein disulfide isomerase (PDI).
(a) Molecular structure of PDI composed of four tandem thioredoxin (Trx)-like domains.
(b) Reversible redox state of CGHC motif as the redox active sequence of PDI.

PDI is composed of four tandem thioredoxin (Trx)-like domains, in which the N- and C-terminal domains (a and a′, respectively) contain a redox active sequence, namely Cys-Gly-His-Cys (CGHC) (**Fig. 4a**). Under physiological conditions, CGHC sequences are in equilibrium between the two redox states, disulfide (PDI^{ox}) and dithiol (PDI^{red}) states (**Fig. 4b**). During phase 1, PDI^{ox} rapidly introduces SS bonds to substrate proteins via an intermolecular bond exchange reaction (**Fig. 3b**). On the other hand, PDI^{red} catalyzes SS-isomerization during phase 2 by temporarily cleaving the miscrossed SS bonds due to the superior nucleophilic capability of the SH groups in CGHC (**Fig. 3c**). CGHC in PDI^{ox} and PDI^{red} have two crucial physicochemical properties so that PDI effectively catalyzes these reactions. First, the SS reduction potential ($E^{o\prime}$) of PDI^{ox} (–180 mV) is considerably higher than that of the CXXC motifs in other PDI family members except for ERdj5 [23]. This indicates that PDI^{ox} possesses a strong oxidizing capability, which is an ideal property for promoting phase 1. Furthermore, the pK_a values (ca. 6.7) of the SH groups in CGHC are substantially lower than those of general cysteinyl SH groups in proteins (ca. 8.3) due to the effect of the neighboring basic His residue. Thus, for phase 2, which is initiated by nucleophilic attack from the SH group in CGHC, PDI also has ideal reactivity. Moreover, the high $E^{o\prime}$ indicates that PDI^{red} is less likely to be ring-closed (oxidized) to PDI^{ox}, indicating that PDI^{red} promotes SS-isomerization rather than SS-reduction (**Fig. 3c**).

Since organothiols (RSH) exist in redox equilibrium states with coexisting disulfide (R′SSR′) compounds in an aqueous solution (Eq. 1), they can promote SS-related reactions via a PDI-like catalytic activity during oxidative folding.

$$2RSH + R'SSR' \rightleftharpoons RSSR + 2R'SH \quad \cdots (1)$$

In addition to monothiol glutathione (GSH) and its oxidized form (GSSG), which have been conventionally used as oxidative folding reagents, a number of sulfur-based compounds that mimic the physicochemical properties and catalytic functions of PDI active centers have been reported [24–29]. However, their catalytic ability is remarkably lower than that of PDI, and compounds must be added at a molar ratio of 10 to 100-fold with respect to the substrate proteins to achieve reasonable folding yields and rates.

3. Redox chemistry of diselenides and selenols

Table 1. | Physicochemical properties of conventional thiols and selenols.

Compound	Analog	pK_a	Diselenide reduction potential $E^{\circ\prime}$ (mV)
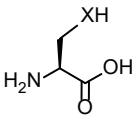	X = S (Cys)	8.22 [a]	–238 [b]
	X = Se (Sec)	ca. 5.2 [c]	–383 [b]
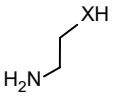	X = S (CA)	8.37 [d]	–236 [b]
	X = Se (SeCA)	ND [a]	–352 [b]
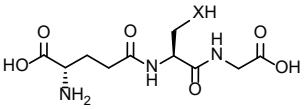	X = S (GSH)	9.42 [a]	–256 [b]
	X = Se (GSeH)	ND [b]	–407 [b]
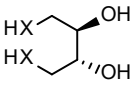	X = S (DTT^{red})	9.21/10.1 [e]	–327 [f]
	X = Se (DST^{red})	ND [b]	–396 [g]

Values are from Refs. [a] [30], [b] [31], [c] [32], [d] [33], [e] [34], [f] [35], and [g] [36]. [h] No data.

Selenium, an essential micronutrient in living organisms, is incorporated into selenocysteine (Sec). Sec is an analog of Cys, in which the SH group in cysteine is replaced by a selenol (SeH) group. Sec is a building block in proteins that functions as an active center in various reductases to reduce various biological substrates, due to the excellent two-electron-donating ability of the SeH groups. Various organoselenols (RSeH), including Sec, can also be in redox equilibrium with coexisting disulfide compounds (R'SS R'), as RSH (Eq. 2).

$$RSeSeR + 2R'SH \rightleftharpoons 2RSeH + R'SSR' \quad \bullet\bullet\bullet (2)$$

In general, the pK_a value of RSeH is considerably lower than that of RSH. Although there are few reports on the pK_a of a SeH group because the isolation and purification of organoselenols are generally difficult due to their enormously high reactivity, the pK_a values of Cys and Sec residues have been reported to be 8.22 and ca. 5.2, respectively (**Table 1**). Thus, the SeH group almost exists as a deprotonated state (selenolate; Se^-) under physiological conditions and functions as a superior nucleophile. The acidity of the SeH group exceeds that of Cys residues in the active centers of PDI, indicating that organoselenols have more ideal chemical properties as reagents for promoting SS-isomerization (phase 2, **Fig. 3c**). On the other hand, the reduction potential of the diselenide (SeSe) bond ($E^{\circ\prime}_{SeSe}$) is generally lower than that of the SS bond (**Table 1**), and the oxidation of SH groups to SS bonds with SeSe compounds (eq. 2, forward reaction) is thermodynamically unfavorable [37]. Therefore, molecular design to increase the $E^{\circ\prime}_{SeSe}$ values is important for improving the function of organodiselenides as PDI mimics.

4. Outside strategy

4.1. Selenoglutathione: The first selenocompound as an oxidative folding catalyst

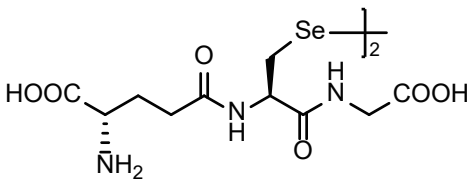

Fig. 5. | Oxidized selenoglutathione (GSeSeG) as the first diselenide-based folding catalyst.

Selenoglutathione (GSeSeG, **Fig. 5**), in which Cys residues in glutathione disulfide (GSSG) are replaced by Sec residues, was first reported as a water-soluble diselenide-based reagent used in oxidative folding [31]. Hilvert *et al*. used GSeSeG as an oxidant to the oxidative folding of the reduced state of ribonuclease A (RNase A) with no SS bond, and found that GSeSeG promoted oxidative folding at a higher rate than GSSG. They further demonstrated that in the oxidative folding of the reduced state of bovine pancreatic trypsin inhibitor (BPTI), GSeSeG promoted early SS-formation events (phase 1, **Fig. 3b**) more effectively and provided a higher final folding yield than GSSG. GSeSeG, despite having a considerably lower reduction potential ($E^{\circ\prime}_{SeSe} = -407$ mV) than GSSG ($E^{\circ\prime}_{SS} = -256$ mV), exerts a higher oxidizing ability for SS-formation than GSSG. The nucleophilic attack of an SH group on the SeSe bond was previously shown to be up to four orders of magnitude faster than the attack on the SS bond, indicating that the kinetics of organodiselenides make them more favorable SS-forming reagents [38,39]. In addition, monoselenol GSeH, which is produced as a byproduct during SS-formation (GSeSeG + Protein[SH,SH] → $2GSe^- + 2H^+$ + Protein[S-S]), promotes SS-isomerization reactions (phase 2, **Fig. 3c**) more effectively than GSH because of its higher nucleophilicity, which accelerates the overall folding rate.

In the oxidative folding of BPTI, the accumulation of two kinetically trapped SS-intermediates decelerates the overall folding rate and reduces the yield of the folded state (see section 5-2). Metanis and Hirvert *et al*. previously showed that GSeH promotes SS-isomerization of SS-intermediates on unproductive pathways, thus improving folding efficiency [40]. Furthermore, the addition of catalytic amounts of GSeSeG can substantially promote oxidative folding under aerobic conditions because the GSeH generated during the reaction is readily reoxidized by molecular oxygen to GSeSeG (i.e., $4GSeH + O_2 \rightarrow 2GSeSeG + 2H_2O$) as an SS-forming agent [41]. GSeSeG was applied to the oxidative folding of various reduced proteins, and its wide substrate scope has been demonstrated [42].

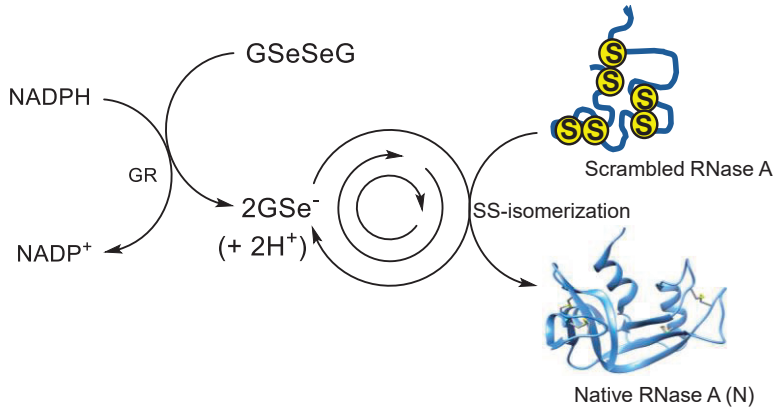

Fig. 6. | Refolding of scrambled RNase A coupled with GSeSeG reduction by glutathione reductase (GR).

Recently, Iwaoka *et al*. reported an effective synthetic route for preparing GSeSeG using a liquid-phase peptide synthesis method [43]. Furthermore, they showed that scrambled RNase A with four non-native SS bonds can be quickly repaired to the native state by treatment with NADPH and glutathione reductase (GR) in the presence of catalytic amounts of GSeSeG (1 mol%) (**Fig. 6**). This is because GSeSeG is reduced to GSeH, which catalyzes SS-isomerization, with NADPH in the presence GR that can recognize both GSSG and GSeSeG as substrates [44].

4.2. Modification of chemical structures

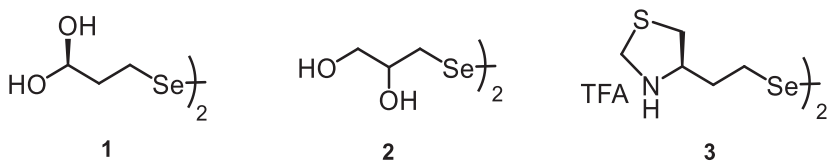

Fig. 7. | Structures of small molecule diselenides **1–3** as oxidative folding catalysts.

Metanis *et al*. synthesized small-molecule diselenides **1–3** as second-generation dimeric-type diselenide compounds to replace GSeSeG (**Fig. 7**) [45]. These compounds can be synthesized more easily and at a higher yield than peptide-based compounds through a short synthetic route using inexpensive starting materials. Furthermore, the compound is smaller than GSeSeG, improving the probability of contact with free cysteinyl SH groups buried in kinetically trapped SS-intermediates, and consequently accelerating the overall velocity of oxidative folding. Indeed, in the oxidative folding of BPTI, selenol states generated from corresponding diselenide compounds smoothly mediated SS-isomerization of the kinetically trapped SS-intermediates generated during the folding, and remarkably improved the oxidative folding rate and yield more than GSSG. Notably, the capability of compounds **2** and **3** as folding promoters was comparable to or slightly higher than that of GSeSeG.

4.3. Cyclic diselenides

Not only dimeric diselenides as shown above but also cyclic diselenide compounds are frequently used to manipulate the structural maturation of denatured and reduced proteins. Raines *et al*. reported that the diselenolate form (**4a**) produced by the reduction of (*S*)-1,2-diselenan-4-amine (**4**) can rapidly reduce protein SS bonds [46] (**Fig. 8**). Arai *et al*. extended the potential application of compound **4** to oxidative folding [36]. In addition to **4**, analogs **5** and **6**, which differ in ring size and functional groups, respectively, were also synthesized, and the ability of the oxidative folding catalyst was compared by folding experiments with reduced RNase A. Five-membered ring diselenide **5** was found to have the highest SS-formation and SS-isomerization abilities [36]. Among the six-membered ring diselenides (**4** and **6**) (**Fig. 8**), the $E^{\circ\prime}_{SeSe}$ value of **4**, which has an amino group, is higher than that of **6**, which has two hydroxy groups. This may be due to the ammonium ($-NH_3^+$) group in the aqueous solution that stabilizes the chain-opened (diselenol) form (**4a**) by electrostatic interactions with the Se^- group in the molecule. Moreover, compound **5**, which has a stronger ring strain, had a significantly higher $E^{\circ\prime}_{SeSe}$ value than compound **4**. These results suggest that the $E^{\circ\prime}_{SeSe}$ value, and thus the folding catalytic activity of the cyclic diselenides, can be modulated by changing the ring size and functional groups.

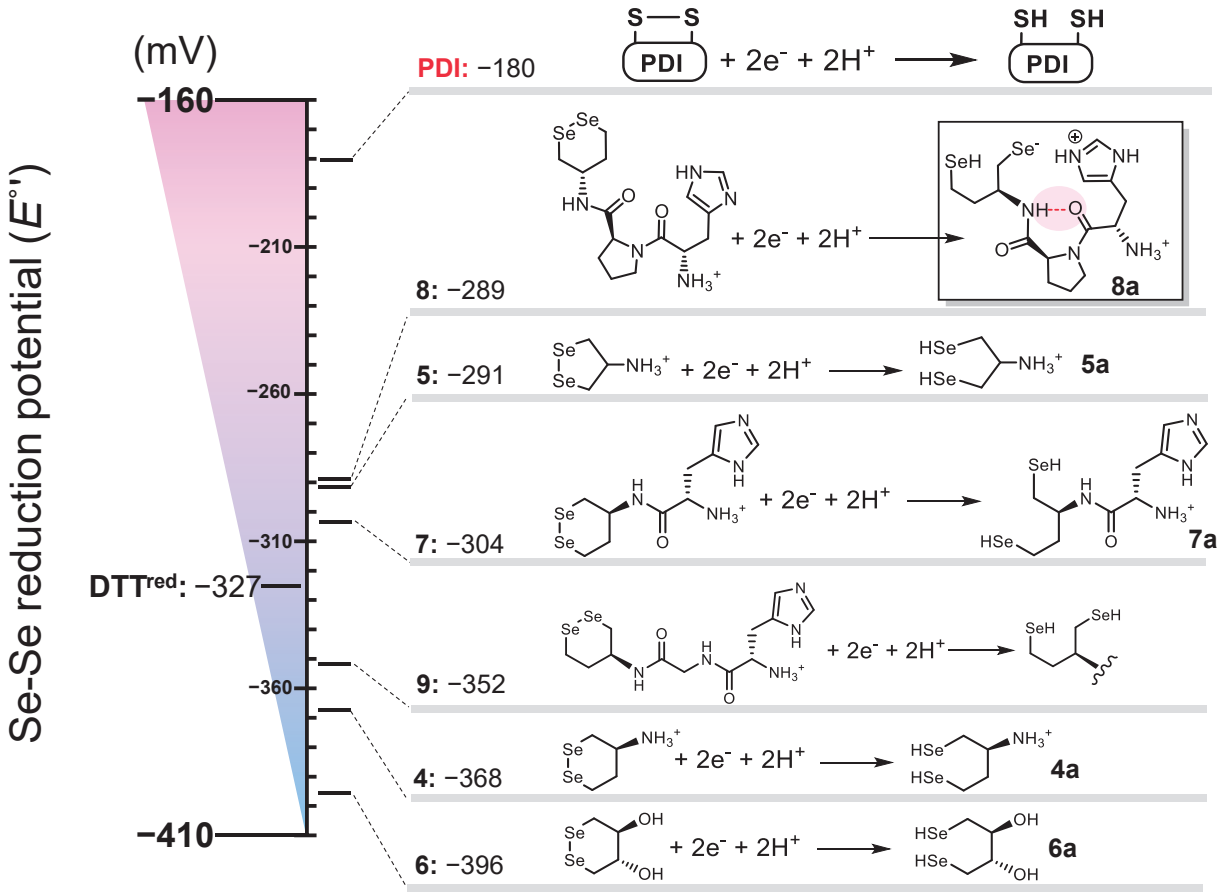

Fig. 8. | Comparison of reduction potentials of cyclic diselenide compounds.

However, such structural modifications of simple Se-containing aliphatic compounds have not been readily achieved in practical organic syntheses [47]. Meanwhile, we also reported that the $E^{\circ\prime}_{SeSe}$ values could be easily increased by conjugating His via an amide bond with compound **4** [48] (**Fig. 8**). This result may be attributed to the stabilization of the reduced form due to the formation of NH•••Se hydrogen bonds between the selenium atom in the diselenol state and the imidazole ring of His in **7a** (**Fig. 8**) [49]. Consequently, in the oxidative folding of hen egg-white lysozyme (HEL), compound **7** showed higher catalytic activity than the parent compound (**4**) for both oxidative folding of the reduced state without SS bonds and repair of the misfolded state (scrambled species) with non-native SS bonds. Importantly, the addition of compound **7** (0.3–0.5 mM) also efficiently inhibited the aggregation of HEL (1.4 mg/mL) induced by thermal denaturation. In the oxidative folding of high concentrations of reduced HEL (0.7 mg/mL), correct folding of the monomeric protein was also accompanied with undesired aggregation and oligomerization in a redox buffer solution containing common glutathione (GSH/GSSG, 1.0 mM/0.2 mM), finally recovering only 25% yield of biologically active state. In contrast, the coexistence of compound **7** (0.2 mM) instead of GSSG inhibited intermolecular contacts of proteins, accelerated the oxidative folding rate, and improved the folding yield to 55% [48]. Thus, these results strongly suggest that the conjugation of His with compound **4** simultaneously enhances its redox reactivity as a PDI-like catalyst and chaperone-like capability to suppress protein aggregation.

More recently, compound **8**, in which Pro is inserted as a spacer amino acid between compound **4** and His, had a significantly higher $E^{\circ\prime}_{SeSe}$ value than **7** and **9** without or with Gly spacer instead of Pro residue, respectively (**Fig. 8**) [50,51]. Detailed structural analyses of the compounds by circular dichroism (CD) and 2-dimensional nuclear magnetic resonance (NMR) spectroscopy clearly showed that reductive cleavage of the SeSe bond in **8** induces transformation of the peptide backbone into a rigid γ-turn structure. Therefore, the SeH and imidazole groups are spatially close to each other in the reduced state, forming NH•••Se hydrogen bonds (or salt bridges) that thermodynamically stabilize the diselenol moiety. Thus, compound **8** functions as an excellent oxidative folding catalyst. Moreover, aliphatic cyclic diselenols are promising regulators of intracellular redox balance in cells because they function as good two-electron donors and are effective not only in SS-related reactions during folding, but also in the reduction of reactive oxygen/nitrogen species, such as peroxides and nitrosothiols, which cause protein misfolding [51,52].

4.4. Enhancement of oxidative folding in cells by selenocystamine

Hilvert *et al*. previously reported that selenocystamine ($[SeCA]_2$), an oxidized state of SeCA (**Table 1**) and a smaller diselenide compound than GSeSeG, also significantly accelerates the oxidative folding of RNase A. However, its catalytic ability is slightly lower than that of GSeSeG. [41]. They further reported that low concentrations (1–10 μM) of $[SeCA]_2$ administered to *Escherichia coli* lacking disulfide bond isomerase A (DsbA), a typical CXXC motif-containing folding enzyme in the periplasm of gram-negative bacteria, promoted oxidative protein folding instead of DsbA [53].

Recently, eukaryotic green algae have attracted attention as platforms for the production of recombinant proteins. The rate-limiting step in the accumulation of recombinant proteins is the structural maturation of proteins coupled with SS-formation and SS-isomerization in chloroplasts, which contain protein-folding enzymes, such as chaperones, peptidyl prolyl isomerases, and PDIs. Interestingly, the addition of $[SeCA]_2$ was found to improve the accumulation of SS-containing proteins in the chloroplasts, suggesting that the selenocompound would be promising for effective protein production by genetic engineering [54].

5. Inside strategy

5.1. Folding pathway kinetically controlled by insertion of Sec residues

Because SS-boding patterns in proteins with multiple Cys residues are essentially governed by the thermodynamics of polypeptide chains, it is impossible to form SS bonds at arbitrary positions at 100% yield without direct modification of peptide chains in the synthetic process. Moloder *et al*. pioneered a method to kinetically govern oxidative protein folding by internalizing the physicochemical properties of the SeH group into the polypeptide itself [55]. Endothelin-1 (ET1; 21 amino acids), a vasoconstrictive peptide, is a mini protein stabilized by two intramolecular SS bonds (Cys1–Cys15 and Cys3–Cys11). Under optimal conditions, oxidation of reduced ET1 without SS bond by O_2 provides a regioisomer with two non-native SS bonds (isomer A) and native ET1 (isomer B) in a 1:3 ratio, depending on the relative thermodynamic stability of the peptide loops (**Fig. 9a**) [56]. Moroder *et al*. synthesized an ET1 analog ([C3U,C11U]-ET1), in which the two Cys residues (Cys3 and Cys11) that form SS bonds in the native state were substituted by Sec residues to selectively yield correctly folded ET1. Because the pK_a

value of the SeH groups in the reduced state is significantly lower than that of the cysteinyl SH groups (**Table 1**), SeSe bond formation proceeds preferentially even when multiple Cys residues coexist in the peptide chain. In addition, the SeSe bond in the peptide chain is more thermodynamically stable than the SS bond [37], and thus bond isomerization via SH-SeSe exchange is thermodynamically less likely to proceed. Consequently, the generation of a misfolded state with incorrect bonding pairs was inhibited during the oxidative folding of [C3U,C11U]-ET1 (**Fig. 9a**). Notably, replacing SS with SeSe did not affect the biological activity and folded structure of ET1.

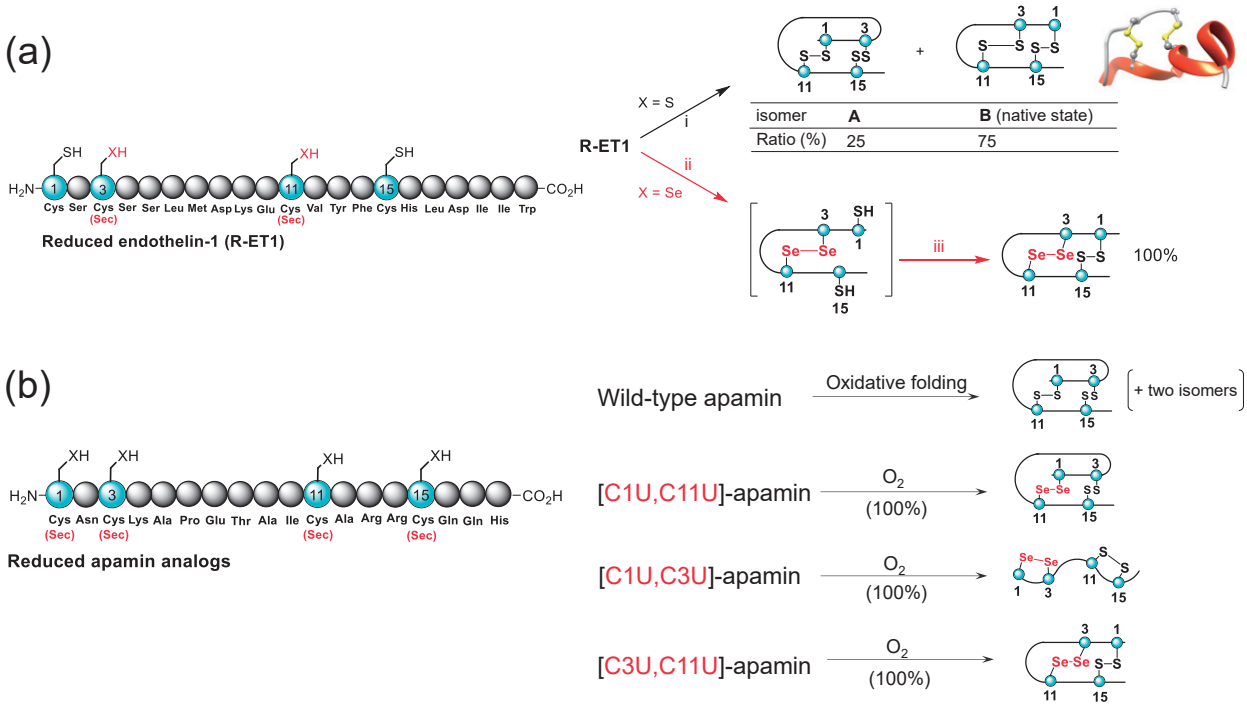

Fig. 9. Oxidative folding of mini proteins kinetically controlled by highly reactive selenol (SeH) groups in selenocysteine (Sec) residues.
(a) Predominant oxidation of Sec residues and selective production of folded endothelin-1 (ET1) analog ([C3U,C11U]-ET1).
(b) Regioselective diselenide- (SeSe) and SS-formation to produce possible apamin isomers.

Apamin, a bee toxin protein, has the same SS bond topology as ET1. Moroder *et al*. selectively synthesized three possible isomers, including the native state, by utilizing the Sec-substituting strategy (**Fig. 9b**) [57,58]. The results strongly suggest that beyond the structural information encoded in the primary sequence, the kinetic and thermodynamic properties of the SeH groups and SeSe bonds, respectively, contribute more strongly to the folding pathway and SS-bonding pattern in the final product. Consequently, Sec was also utilized to generate misfolded forms in a purposeful manner [55]. Since then, this method has been applied to structural analysis of protein folding intermediates, elucidation of the folding pathway, and effective production of peptide formulations, as described below.

5.2. Enhancement of the foldability of conotoxins

SS-rich bioactive peptides, such as neurotoxins, plant cyclotides, antimicrobial peptides, and protease inhibitors, are potential therapeutic agents for analgesics, antihypertensives, antiarrhythmics, antitumor medicines, antivirals, and antibiotics. SS-rich conotoxins, known as neurotoxins from *Conus*, are peptide drug candidates that have been explored to enhance the foldability and structural stability of their native states by the Sec-substituting strategy. Multiple SS bonds in conotoxins are readily reduced or isomerized in the presence of an SH-based reductant, such as GSH, thioredoxin, and albumin, thus easily degrading them in the blood. Alewood *et al*. synthesized α-selenoconotoxins, in which one or two SS bonds in wild-type α-conotoxin were replaced by SeSe bonds [59]. Due to regioselective SeSe bonding, the folded state of α-selenoconotoxins is effectively produced at high yields, and all analogs exhibited remarkable stability against SH-based biomolecules [59,60]. Similarly, for pharmacologically

relevant conotoxins containing three SS bonds, such as μ-conotoxin [61], ω-selenoconotoxin GVIA [62], μ-conotoxin KIIIA [63], and μO-conotoxin MrVIB [64], the folding yield was improved by replacing one SS bond with a SeSe bond. In both cases, the substitution of SeSe bonds did not alter the 3D structure and reduce the biological activity. Furthermore, Bulaj *et al*. compared the overall folding rates of seleno-analogs of ω-conotoxin GVIA and μ-conotoxin SIIIA with wild types. Both selenopeptides, in which one of the three SS bonds was replaced by SeSe bond, promoted SS-formation and SS-isomerization during oxidative folding at a higher rate than the wild-type peptides, even in the absence of chemical redox reagents. This is due to the autocatalytic functions of inserted Sec residues in the peptides (**Fig. 10**). [65].

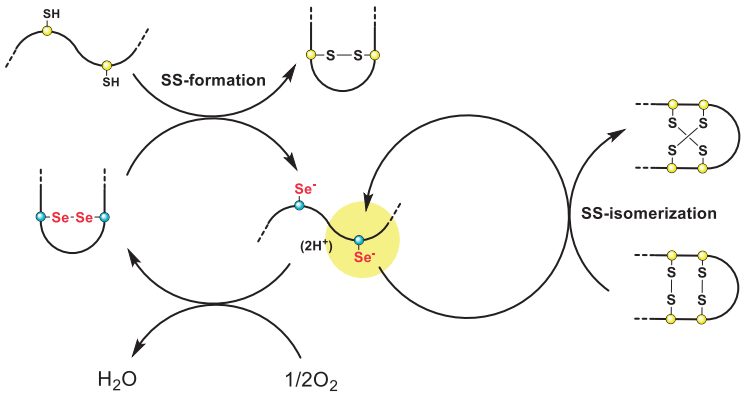

Fig. 10. | Redox reagent-free oxidative folding of conotoxins catalyzed by intramolecular Sec residues.

5.3. Steering of the folding pathway by inserting Sec residues

A detailed oxidative folding pathway has been reported for wild-type BPTI (58 amino acids), which has long been employed as a benchmark protein in folding studies (**Fig. 11a**) [66–68]. In the key intermediates, N* and N′, which have native-like structures, free SH groups are buried inside the molecules. Generation of these kinetically trapped intermediates consequently decelerates the overall folding rate of BPTI. Conversely, if the formation of N* and N′ could be avoided, reduced BPTI (R) could lead to rapid and high-yield formation of the native state (N).

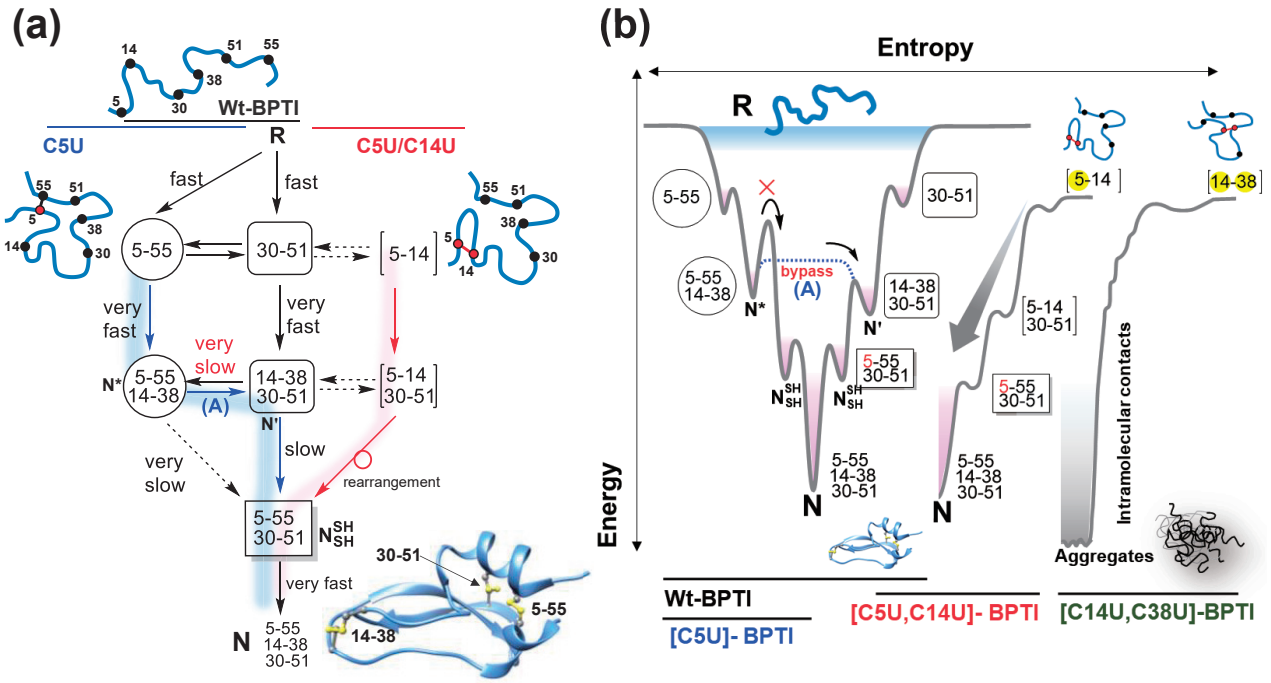

Fig. 11. | Oxidative folding of bovine pancreatic trypsin inhibitor (BPTI).
(a) Major oxidative folding pathways of BPTI and its Sec-substituted analogs.
(b) Modification of energy landscape for oxidative folding of BPTI by insertion of Sec, instead of cysteine (Cys) residues.

Based on this concept, Hilvert *et al*. proposed a new strategy to efficiently yield N by replacing Cys5 and Cys14 of BPTI with Sec residues, preferentially undergoing a pathway in which N* and N′ are not involved (**Fig. 11a**, pathways highlighted in pink) [69]. Indeed, the seleno-analog, [C5U,C14U]-BPTI, folded into N at 70–80% yield at a higher rate than wild-type BPTI under weakly basic and aerobic conditions, whereas oxidative folding of wild-type BPTI produced N* and N′ as the major products (80%) with N at a low yield. This result indicates that [C5U,C14U]-BPTI can selectively undergo a reaction pathway with smaller activation barriers than those in wild-type BPTI by preferentially forming the non-native crosslink via the SeSe bond at the early folding phase (**Fig. 11b**, middle funnel). On the other hand, for [C14U,C38U]-BPTI, intermolecular contacts preferentially form aggregates because of the formation of an unfoldable intermediate with a SeSe bond at the non-native position (**Fig. 11b**, right funnel) [70]. In the case of [C5U]-BPIT, in which only one Cys residue (Cys5) is replaced by Sec, the folding pathway is essentially unaltered (**Fig. 11a**, pathways highlighted in blue), but N* can be quickly converted to N′, which is accessible to the precursor (N^{SH}_{SH}) through a bypass with a small activation barrier (**Fig. 11a**, path A), resulting in an increased overall folding rate (**Fig. 11b**, left funnel) [70]. Since a single Sec residue can be artificially introduced into a protein by genetic engineering, the result that the single Sec insertion instead of Cys reasonably enhances folding efficiency would be advantageous for the biological production of peptide-based formulations containing SS bonds [70–74].

5.4. Simplification of the oxidative folding pathway involving diverse SS-intermediates

A detailed oxidative folding pathway of hirudin (65 amino acid residues), a thrombin inhibitor with three SS bonds (Cys6–Cys14, Cys16–Cys28, and Cys22–Cys39), was reported in the 1990s by Chang *et al*. [75–77]. While hirudin has almost the same number of amino acid residues as BPTI with three SS bonds, their oxidative folding phenomena are completely different [78]. BPTI achieves oxidative folding through a limited number of SS-intermediates with native-like structures (**Fig. 11a**). In contrast, the oxidative folding of hirudin involves SS-intermediates (scrambled species), 1SS, 2SS, and 3SS, which have one, two, and three non-native SS bonds in the molecule, respectively. These intermediates are sequentially generated from the reduced state (R) (i.e., R→1SS→2SS→3SS), accompanied by the hydrophobic collapse of the polypeptide. 3SS subsequently undergoes SS-isomerization with conformational folding to obtain the native SS-bonding pattern and folded structure (**Fig. 12**).

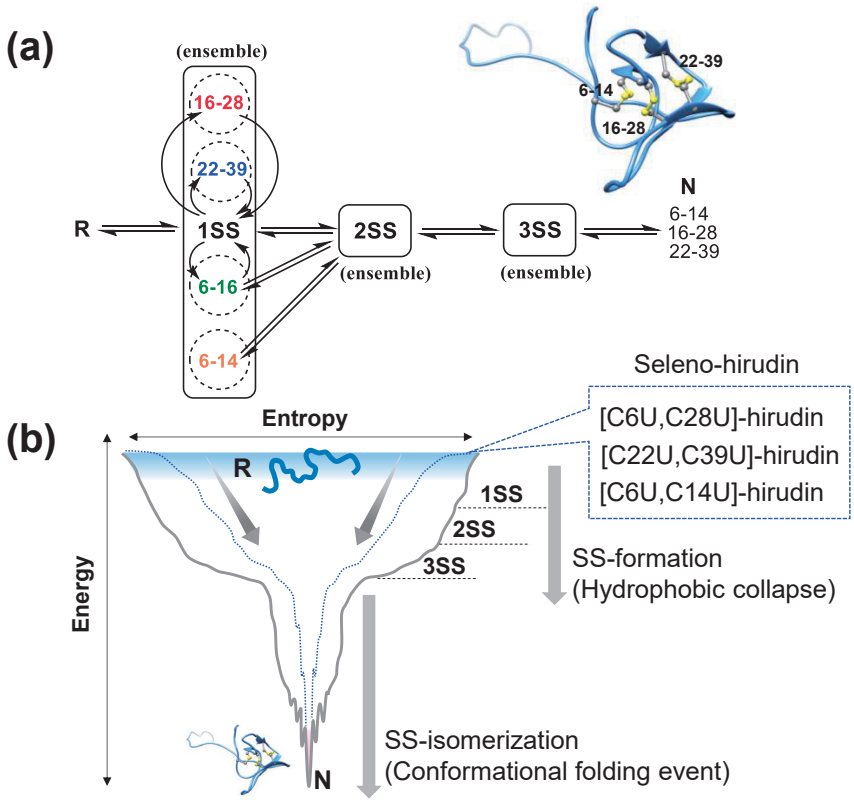

Fig. 12. Oxidative folding of hirudin with three SS bonds.
(a) Oxidative folding pathway of hirudin and seleno-hirudin via scrambled SS-intermediates. Heterogeneous ensembles with one (1SS), two (2SS), and three (3SS) SS bonds in the molecule are shown.
(b) Energy landscape for oxidative folding of wild-type hirudin (gray) and seleno-hirudin (blue).

Metanis *et al*. prepared seleno-hirudins ([C6U,C14U], [C16U,C28U] and [C22U,C39U]), in which one of the three native SS bonds was replaced by SeSe bond, and investigated their folding behavior [79]. All analogs folded into the native state at a higher rate than the wild type. During the early oxidative folding event (SS-formation) of wild-type hirudin, heterogeneous 1SS ensembles, including various isomers, are generated as scrambled species, whereas for seleno-hirudin, the components in the scrambled species are biased, decreasing the heterogeneity. Particularly, [C6U,C14U]-hirudin with the SeSe bond directly gained an additional SS bond without conversion into the scrambled species via the SH-SeSe exchange reaction (**Fig. 12a**). In contrast, [C6U,C16U]-hirudin with the SeSe bond at the non-native position rapidly isomerized to a heterogeneous ensemble. These results indicate that the introduction of the SeSe bond in the appropriate position significantly reduces the diversity (i.e., peptidyl entropy) of the folding intermediates (**Fig. 12b**) and that the folding rate is accelerated by undergoing a simpler pathway.

5.5. Potent tool for interchain cross-coupling

Insulin, an important peptide-based drug, is widely known as a hypoglycemic agent for diabetic patients. Its native structure is stabilized by two interchain SS bonds (Cys7^{A}–Cys7^{B} and Cys20^{A}–Cys19^{B}) between the A-chain (21 amino acid residues) and the B-chain (30 amino acid residues), in addition to the intrachain SS bond (Cys6^{A}–Cys11^{A}) in the A-chain. Direct coupling of the unprotected A-chain and B-chain via SS linkages in an oxidative environment to obtain the native form is the simplest and most rational synthetic method. However, intramolecular SS cross-linking in each peptide chain is usually preferred, producing a folding yield of less than 5% [80–82]. Although several efforts have been directed toward developing innovative synthetic methodologies, a technology that involves a simple synthetic process and exhibits high product yield is yet to be developed [83].

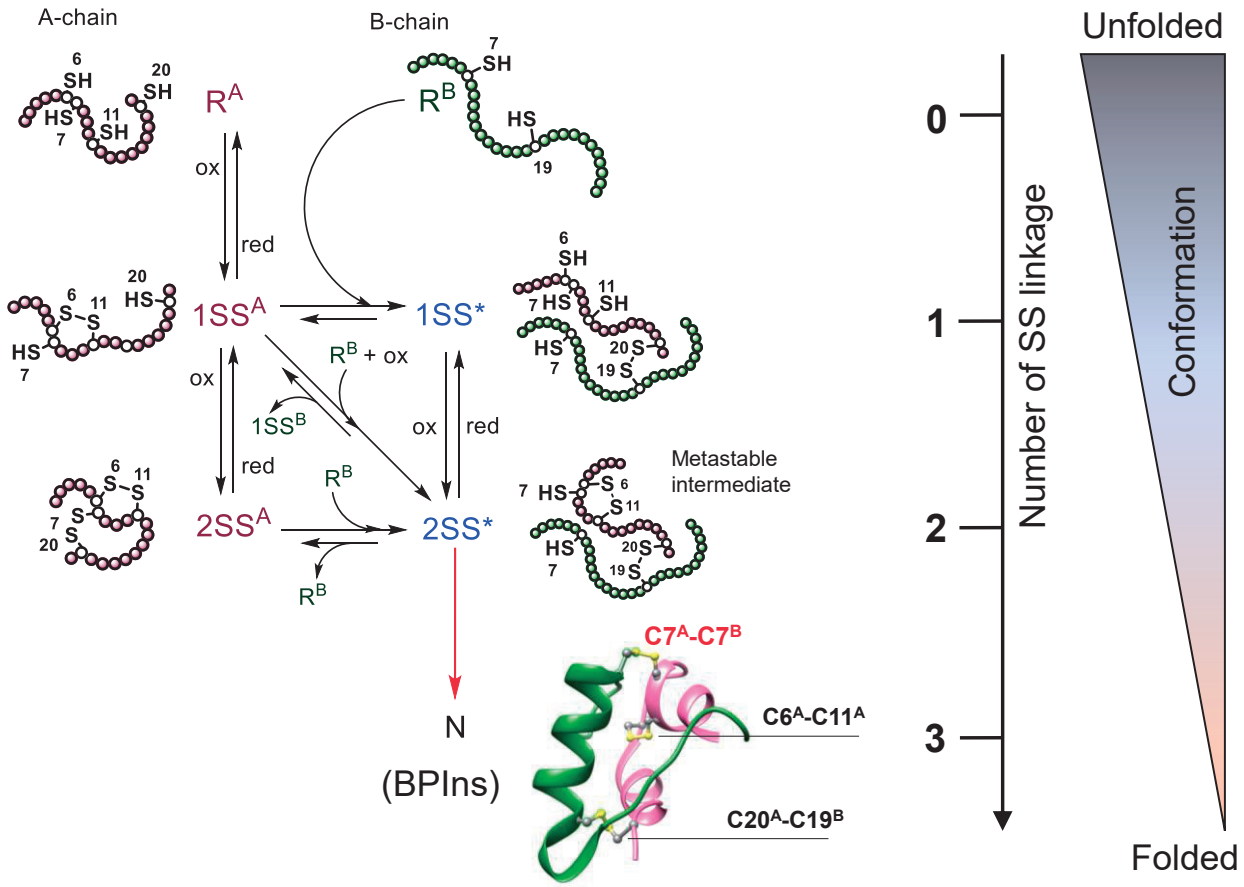

Fig. 13. Chain combination pathways of unprotected bovine pancreatic insulin (BPIns) A-chain and B-chain (native chain assembly; NCA).

Arai *et al*. predicted that the A-chain and B-chain could be coupled directly and effectively by utilizing the Sec-substituting strategy, which has been applied to single-chain polypeptide folding (see above). Prior to the trial of this strategy, an exhaustive mechanistic investigation on oxidative folding of the unprotected A-chain and B-chain, namely native chain assembly (NCA), was performed to determine the appropriate positions for inserting Sec residues [84]. The results revealed that the NCA pathway of insulin includes several pathways, all of which involve a common metastable precursor (2SS*) that lacks one interchain SS bond ($Cys7^A$–$Cys7^B$) (**Fig. 13**). Furthermore, $Cys7^A$–$Cys7^B$, which is solvent-exposed in the native structure, was found to be the most kinetically and thermodynamically unstable among the three native SS bonds.

Consequently, Arai *et al*. synthesized the [C7U]-A-chain and [C7U]-B-chain, which are seleno-analogs of the component peptides of bovine pancreatic insulin (BPIns) [85]. The A-chain and B-chain were isolated as 2-pyridylsulfanyl- (Pys) protected derivatives with one SeS bond and an oxidized form including one SeS bond, respectively (**Fig. 14a**). The peptide chains were activated to reactive species containing SH and SeH groups under weakly reductive conditions, and the chains gradually coupled with each other by O_2 as an oxidant to form the [$C7U^A$,$C7U^B$] variant of BPIns, namely selenoinsulin (SeIns), at up to 27% isolated yield. SeIns has almost the same biological activity and 3D structure as the wild type. More notably, SeIns exhibited much higher resistance against insulin-degrading enzyme (IDE), which is found in the liver and pancreas in mammals, than wild-type insulin (i.e., $\tau_{1/2} \approx 8$ h vs. ≈ 1 h for BPIns), and was found to have potential as a long-acting formulation that could circulate in the body for a long time. X-ray crystallographic analysis of SeIns suggests that the SeSe bond ($Sec7^A$–$Sec7^B$) has enhanced native interactions in the N-terminal region of the B-chain, resulting in increased stability of the monomeric state, which may explain the high IDE resistances.

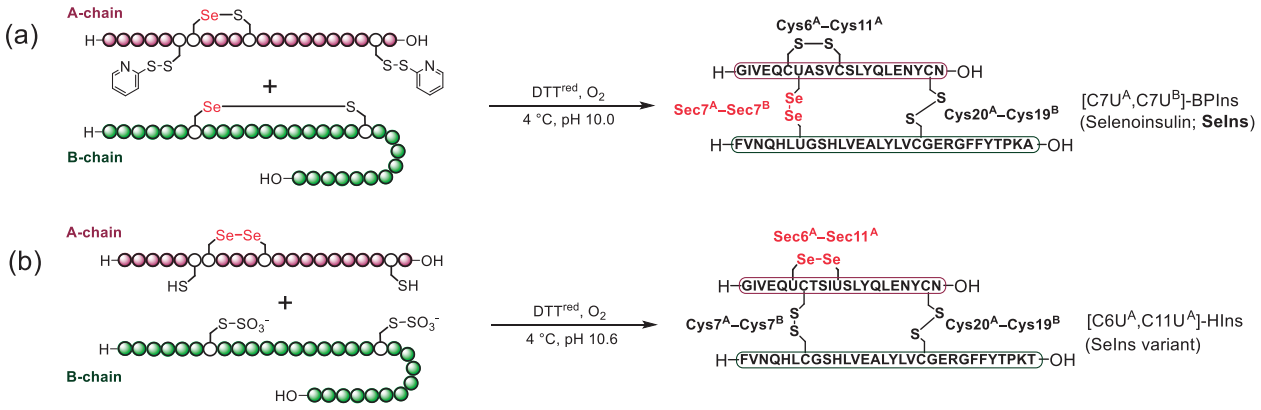

Fig. 14. Preparation of selenoinsulins. Components and primary sequences of selenoinsulin series are shown.
(a) [$C7U^A$,$C7U^B$]-bovine pancreatic insulin (SeIns) with external SeSe bond reported by Arai *et al*.
(b) Human selenoinsulin with internal SeSe bond reported by Metanis *et al*.

The second selenoinsulin [$C6U^A$,$C11U^A$] variant of human insulin (HIns) (**Fig. 14b**) was synthesized by Metanis *et al*. [86]. They focused on $Cys6^A$–$Cys11^A$, which is formed as a major SS component in $1SS^A$ during the early NCA event (**Fig. 13**), and prepared [$C6U^A$,$C11U^A$]-A-chain through SPPS. Interestingly, the A-chain analog, which has an intrachain SeSe bond, coupled effectively with the wild-type B-chain to produce [$C6U^A$,$C11U^A$]-HIns with a correctly folded structure at 31% isolation yield. Importantly, the replacement of internal SS bond, which is buried in the hydrophobic core of the molecule, enhanced thermodynamic stability against guanidinium chloride (GdmCl) and improved resistance to peptide hydrolysis by Glu-V8 protease and reductive unfolding by GSH. These results suggest that replacement of SS bonds with SeSe bonds in proteins enable effective oxidative folding and improve the pharmacological effects of peptide formulations.

6. Future prospective and concluding remark

In vivo folding studies over the past decades have revealed that the oxidative folding pathway of proteins can be flexibly changed to non-native pathways that are not encoded in the primary amino acid sequence by regulating the environment, such as the additives, pH, temperature, and peptide modifications [87]. As described above, the unique redox properties of the SeSe bond and SeH groups can also modify the energy landscape of oxidative folding and accelerate folding velocity by avoiding a pathway

involving a kinetically trapped intermediate, or by altering the unproductive pathway to a productive pathway with lower energetic barriers. The addition of a catalytic amount of small molecule diselenide to the oxidative folding of wild-type peptides greatly improves both the rate and yield despite its ease of use; however, its catalytic activity is still lower than that of PDI. One reason for the enormously high catalytic activity of PDI is that it aggressively incorporates structurally immature proteins, which have exposed hydrophobic regions in the molecules, into its own hydrophobic cavity [88]. To further enhance the catalytic activity of SeSe-based catalysts, it is necessary to improve their redox properties and design novel molecules to selectively recognize undesired species that prohibit oxidative folding, such as misfolded states, kinetically trapped intermediates, and oligomers, and finally lead them to productive pathways.

In addition, although diselenide compounds may be promising in regulating protein quality control in cells, there are only a few reports on their biological applications (see Section 4.4). This is probably because SeSe-based compounds are highly reactive, and therefore, often highly toxic to cells. To develop diselenide-based therapeutics for protein misfolding diseases, it is also necessary to design molecules that can exert appropriate catalytic activity at the target organelles. Furthermore, disulfides/thiols redox reactions are involved in a variety of biological phenomena related to protein quality control as well as oxidative folding in the ER. For example, inositol-requiring enzyme 1 (IRE1), which is an ER transmembrane protein, can detect misfolded proteins, and subsequently assembles with other IRE1 molecules via intermolecular SS bonds, eventually activating the unfolded protein response (UPR) mechanisms [89]. To avoid excessive accumulation and prolonged retention of IRE1-oligomers that cause undesired UPR-associated apoptosis, PDI family A member 6 (PDIA6 or P5) cleaves the intermolecular SS bonds in the oligomers to reproduce monomeric IRE1 [90,91]. Organoselenol compounds are also well known to function as a potent reductant for protein SS bonds due to their high nucleophilic potency [36,46,50], and thus could also be expected to possess the capability to chemically mimic the SS-reductase activity of PDIA6, which attenuates the IRE1 activity.

Meanwhile, the replacement of SS bonds with SeSe bonds in peptides provides various advantages, such as the promotion of oxidative folding, enhancement of structural stability, improvement of intrinsic bioactivity, and introduction of a novel biological function. However, although many SeSe-containing peptides have been reported as potential candidates for practical formulations, their clinical application has not yet been achieved. For drug discovery, further knowledge of the toxicity and pharmacokinetics, as well as the chemical phenomena of the SeSe bond *in vivo*, is necessary.

Acknowledgements

This work was supported by the Promotion and Mutual Aid Corporation (PMAC) for Private Schools of Japan [The Science Research Promotion Fund] and the Research and Study Project of Tokai University, Educational System General Research Organization.

References

[1] Anfinsen CB: Principles that govern the folding of protein chains. Science 181: 223-230, 1973.

[2] Kanemura S, Matsusaki M, Inaba K, Okumura M: PDI family members as guides for client folding and assembly. Int J Mol Sci 21: 9351, 2020.

[3] Matthias JF, Ineke B, Linda MH. Disulfide bonds in protein folding and stability. Matthias JF (ed): Oxidative Folding of Proteins. Royal Society of Chemistry, United Kingdom, 2018, 1-33.

[4] Matsusaki M, Kanemura S, Kinoshita M, Lee YH, Inaba K, Okumura M: The protein disulfide isomerase family: from proteostasis to pathogenesis. Biochim Biophys Acta Gen Subj 1864: 129338, 2020.

[5] Uehara T, Nakamura T, Yao D, Shi ZQ, Gu Z, Ma Y, Masliah E, Nomura Y, Lipton SA: S-nitrosylated protein-disulphide isomerase links protein misfolding to neurodegeneration. Nature 441: 513-517, 2006.

[6] Gaut JR, Hendershot LM: The modification and assembly of proteins in the endoplasmic reticulum. Curr Opin Cell Bio 5: 589-595, 1993.

[7] Ellgaard L, Helenius A: Quality control in the endoplasmic reticulum. Nat Rev Mol Cell Biol 4: 181-191, 2003.

[8] Meusse B, Hirsch C, Jarosch E, Sommer T: ERAD: The long road to destruction. Nat Cell Biol 7: 766-772, 2005.

[9] Chaudhuri TK, Paul S: Protein-misfolding diseases and chaperone-based therapeutic approaches. FEBS J 273: 1331-1349, 2006.

[10] Wu J, Kaufman RJ: From Acute ER stress to physiological roles of the unfolded protein response. Cell Death Differ 13: 374-384, 2006.

[11] Kim I, Xu W, Reed JC: Cell death and endoplasmic reticulum stress: disease relevance and therapeutic opportunities. Nat Rev Drug

Discov 7: 1013-1030, 2008.

[12] Verfaillie T, Garg AD, Agostinis P: Targeting ER stress induced apoptosis and inflammation in cancer. Cancer Lett 332: 249-264, 2013.

[13] Merrifield RB: Solid phase peptide synthesis. I. the synthesis of a tetrapeptide. J Am Chem Soc. 85: 2149-2154, 1963.

[14] Jaradat DMM: Thirteen decades of peptide synthesis: key developments in solid phase peptide synthesis and amide bond formation utilized in peptide ligation. Amino Acids 50: 39-68, 2018.

[15] Empting M, Avrutina O, Meusinger R, Fabritz S, Reinwarth M, Biesalski M, Voigt S, Buntkowsky G, Kolmar H: "Triazole bridge": disulfide-bond replacement by ruthenium-catalyzed formation of 1,5-disubstituted 1,2,3-triazoles. Angew Chem Int Ed Engl 50: 5207-5211, 2011.

[16] Kourra CMBK, Cramer N: Converting disulfide bridges in native peptides to stable methylene thioacetals. Chem Sci. 7: 7007-7012, 2016.

[17] Wang T, Fan J, Chen XX, Zhao R, Xu Y, Bierer D, Liu L, Li YM, Shi J, Fang GM: Synthesis of peptide disulfide-bond mimics by using fully orthogonally protected diaminodiacids. Org Lett 20: 6074-6078, 2018.

[18] Zhao R, Shi P, Chen J, Sun S, Chen J, Cui J, Wu F, Fang G, Tian C, Shi J, Bierer D, Liu L, Li YM: Chemical synthesis and biological activity of peptides incorporating an ether bridge as a surrogate for a disulfide bond. Chem Sci 11: 7927-7932, 2020.

[19] Wilkinson B, Gilbert HF: Protein disulfide isomerase. Biochim Biophys Acta - Proteins Proteom 1699: 35-44, 2004.

[20] Gruber CW, Čemažar M, Heras B, Martin JL, Craik DJ: Protein disulfide isomerase: the structure of oxidative folding. Trends Biochem Sci 31: 455-464, 2006.

[21] Oka OBV, Bulleid NJ: Forming disulfides in the endoplasmic reticulum. Biochim Biophys Acta - Mol Cell Res 1833: 2425-2429, 2013.

[22] Wang L, Wang X, Wang CC: Protein disulfide–isomerase, a folding catalyst and a redox-regulated chaperone. Free Radic Biol Med 83: 305-313, 2015.

[23] Hagiwara M, Maegawa K, Suzuki M, Ushioda R, Araki K, Matsumoto Y, Hoseki J, Nagata K, Inaba K: Structural basis of an ERAD pathway mediated by the ER-resident protein disulfide reductase ERdj5. Mol Cell 41: 432-444, 2011.

[24] Lees WJ: Small-molecule catalysts of oxidative protein folding. Curr Opin Chem Biol 12: 740-745, 2008.

[25] Madar DJ, Patel AS, Lees WJ: Comparison of the oxidative folding of lysozyme at a high protein concentration using aromatic thiols versus glutathione. J Biotechnol 142: 214-219, 2009.

[26] Potempa M, Hafner M, Frech C: Mechanism of gemini disulfide detergent mediated oxidative refolding of lysozyme in a new artificial chaperone system. Protein J 29: 457-465, 2010.

[27] Lukesh III JC, Andersen KA, Wallin KK, Raines RT: Organocatalysts of oxidative protein folding inspired by protein disulfide isomerase. Org Biomol Chem 12: 8598-8602, 2014.

[28] Okada S, Matsusaki M, Arai K, Hidaka Y, Inaba K, Okumura M, Muraoka T: Coupling effects of thiol and urea-type groups for promotion of oxidative protein folding. Chem Commun 55: 759-762, 2019.

[29] Okada S, Matsusaki M, Okumura M, Muraoka T: Conjugate of thiol and guanidyl units with oligoethylene glycol linkage for manipulation of oxidative protein folding. Molecules 26: 879, 2021.

[30] Tajc SG, Tolbert BS, Basavappa R, Miller BL: Direct determination of thiol pK_a by isothermal titration microcalorimetry. J Am Chem Soc 126: 10508-10509, 2004.

[31] Beld J, Woycechowsky KJ, Hilvert D: Selenoglutathione: efficient oxidative protein folding by a diselenide. Biochemistry 46: 5382-5390, 2007.

[32] Huber RE, Criddle RS: Comparison of the chemical properties of selenocysteine and selenocystine with their sulfur analogs. Arch Biochem Biophys 122: 164-173, 1967.

[33] Connett PH, Wetterhahn KE: Reaction of chromium (VI) with thiols: pH dependence of chromium(VI) thio ester formation. J Am Chem Soc 108: 1842-1847, 1986.

[34] Whitesides GM, Lilburn JE, Szajewski RP: Rates of thiol-disulfide interchange reactions between mono- and dithiols and Ellman's reagent. J Org Chem 42: 332-338, 1977.

[35] Lees WJ, Whitesides GM: Equilibrium constants for thiol-disulfide interchange reactions: a coherent, corrected set. J Org Chem 58: 642-647, 1993.

[36] Arai K, Ueno H, Asano Y, Chakrabarty G, Shimodaira S, Mugesh G, Iwaoka M: Protein folding in the presence of water-soluble cyclic diselenides with novel oxidoreductase and isomerase activities. ChemBioChem 19: 207-211, 2018.

[37] Besse D, Siedler F, Diercks T, Kessler H, Moroder L: The redox potential of selenocystine in unconstrained cyclic peptides. Angew Chem Int Ed Engl 36: 883-885, 1997.

[38] Metanis N, Keinan E, Dawson PE: Synthetic seleno-glutaredoxin 3 analogues are highly reducing oxidoreductases with enhanced catalytic efficiency. J Am Chem Soc 128: 16684-16691, 2006.

[39] Steinmann D, Nauser T, Koppenol WH: Selenium and sulfur in exchange reactions: a comparative study. J Org Chem 75: 6696-6699, 2010.

[40] Metanis N, Foletti C, Beld J, Hilvert D: Selenoglutathione-mediated rescue of kinetically trapped intermediates in oxidative protein

folding. Isr J Chem 51: 953-959, 2011.

[41] Beld J, Woycechowsky KJ, Hilvert D: Catalysis of oxidative protein folding by small-molecule diselenides. Biochemistry 47: 6985-6987, 2008.

[42] Beld J, Woycechowsky KJ, Hilvert D: Diselenides as universal oxidative folding catalysts of diverse proteins. J Biotechnol 150: 481-489, 2010.

[43] Shimodaira S, Asano Y, Arai K, Iwaoka M: Selenoglutathione diselenide: unique redox reactions in the GPx-like catalytic cycle and repairing of disulfide bonds in scrambled protein. Biochemistry 56: 5644-5653, 2017.

[44] Yoshida S, Kumakura F, Komatsu I, Arai K, Onuma Y, Hojo H, Singh BG, Priyadarsini KI, Iwaoka M: Antioxidative glutathione peroxidase activity of selenoglutathione. Angew Chem Int Ed Engl 50: 2125-2128, 2011.

[45] Reddy PS, Metanis N: Small Molecule Diselenide Additives for in Vitro Oxidative Protein Folding. Chem Commun 52: 3336-3339, 2016.

[46] Lukesh JC, VanVeller B, Raines RT: Thiols and selenols as electron-relay catalysts for disulfide-bond reduction. Angew Chem Int Ed 52: 12901-12904, 2013.

[47] Arai K, Kumakura F, Takahira M, Sekiyama N, Kuroda N, Suzuki T, Iwaoka M: Effects of ring size and polar functional groups on the glutathione peroxidase-like antioxidant activity of water-soluble cyclic selenides. J Org Chem 80: 5633-5642, 2015.

[48] Tsukagoshi S, Mikami R, Arai K: Basic amino acid conjugates of 1,2-diselenan-4-amine with protein disulfide isomerase-like functions as a manipulator of protein quality control. Chem Asian J 15: 2646-2652, 2020.

[49] Arai K, Matsunaga T, Ueno H, Akahoshi N, Sato Y, Chakrabarty G, Mugesh G, Iwaoka M: Modeling thioredoxin reductase-like activity with cyclic selenenyl sulfides: participation of an NH•••Se hydrogen bond through stabilization of the mixed Se–S intermediate. Chem Eur J 25: 12751-12760, 2019.

[50] Mikami R, Tsukagoshi S, Arai K: Abnormal enhancement of protein disulfide isomerase-like activity of a cyclic diselenide conjugated with a basic amino acid by inserting a glycine spacer. Biology 10: 1090, 2021.

[51] Mikami R, Tsukagoshi S, Oda Y, Arai K: S-denitrosylase-like activity of cyclic diselenides conjugated with Xaa-His dipeptide: role of proline spacer as a key activity booster. ChemBioChem 23: e202100394, 2022.

[52] Arai K, Sato Y, Nakajima I, Saito M, Sasaki M, Kanamori A, Iwaoka M: Glutathione peroxidase-like functions of 1,2-diselenane-4,5-diol and its amphiphilic derivatives: switchable catalytic cycles depending on peroxide substrates. Bioorg Med Chem 29: 115866, 2021.

[53] Beld J, Woycechowsky KJ, Hilvert D: Small-molecule diselenides catalyze oxidative protein folding in vivo. ACS Chem Biol 5: 177-182, 2010.

[54] Ferreira-Camargo LS, Tran M, Beld J, Burkart MD, Mayfield SP: Selenocystamine improves protein accumulation in chloroplasts of eukaryotic green algae. AMB Expr 5: 39, 2015.

[55] Moroder L, Musiol HJ, Götz M, Renner C: Synthesis of single- and multiple-stranded cystine-rich peptides. Biopolymers 80: 85-97, 2005.

[56] Pegoraro S, Fiori, S, Rudolph-Böhner S, Watanabe TX, Moroder L: Isomorphous replacement of cystine with selenocystine in endothelin: oxidative refolding, biological and conformational properties of [Sec3,Sec11,Nle7]-endothelin-1. J Mol Biol 284: 779-792, 1998.

[57] Pegoraro S, Fiori S, Cramer J, Rudolph-Böhner S, Moroder L: The disulfide-coupled folding pathway of apamin as derived from diselenide-quenched analogs and intermediates. Protein Sci 8: 1605-1613, 1999.

[58] Fiori S, Pegoraro S, Rudolph-Böhner S, Cramer J, Moroder L: Synthesis and conformational analysis of apamin analogues with natural and non-natural cystine/selenocystine connectivities. Biopolymers 53: 550-564, 2000.

[59] Armishaw CJ, Daly NL, Nevin ST, Adams DJ, Craik DJ, Alewood PF: α-selenoconotoxins, a new class of potent A7 neuronal nicotinic receptor antagonists. J Biol Chem 281: 14136-14143, 2006.

[60] Muttenthaler M, Nevin ST, Grishin AA, Ngo ST, Choy PT, Daly NL, Hu SH, Armishaw CJ, Wang CIA, Lewis RJ, Martin JL, Noakes PG, Craik DJ, Adams DJ, Alewood PF: Solving the α-conotoxin folding problem: efficient selenium-directed on-resin generation of more potent and stable nicotinic acetylcholine receptor antagonists. J Am Chem Soc 132: 3514-3522, 2010.

[61] Walewska A, Zhang MM, Skalicky JJ, Yoshikami D, Olivera BM, Bulaj G: Integrated oxidative folding of cysteine/selenocysteine containing peptides: improving chemical synthesis of conotoxins. Angew Chem Int Ed Engl 48: 2221-2224, 2009.

[62] Gowd KH, Yarotskyy V, Elmslie KS, Skalicky JJ, Olivera BM, Bulaj G: Site-specific effects of diselenide bridges on the oxidative folding of a cystine knot peptide, ω-selenoconotoxin GVIA. Biochemistry 49: 2741-2752, 2010.

[63] Han TS, Zhang MM, Gowd KH, Walewska A, Yoshikami D, Olivera BM, Bulaj G: Disulfide-depleted selenoconopeptides: simplified oxidative folding of cysteine-rich peptides. ACS Med Chem Lett 1: 140-144, 2010.

[64] de Araujo AD, Callaghan B, Nevin ST, Daly NL, Craik DJ, Moretta M, Hopping G, Christie MJ, Adams DJ, Alewood PF: Total synthesis of the analgesic conotoxin MrVIB through selenocysteine-assisted folding. Angew Chem Int Ed Engl 50: 6527-6529, 2011.

[65] Steiner AM, Woycechowsky KJ, Olivera BM, Bulaj G: Reagentless oxidative folding of disulfide-rich peptides catalyzed by an intramolecular diselenide. Angew Chem Int Ed 51: 5580-5584, 2012.

[66] Creighton TE: Experimental studies of protein folding and unfolding. Prog Biophys Mol Biol 33: 231-297, 1978.

[67] Creighton TE, Goldenberg DP: Kinetic role of a meta-stable native-like two-disulphide species in the folding transition of bovine pancreatic

trypsin inhibitor. J Mol Biol 179: 497-526, 1984.

[68] Weissman JS, Kim PS: Reexamination of the folding of BPTI: Predominance of native intermediates. Science 253: 1386-1393, 1991.

[69] Metanis N, Hilvert D: Strategic use of non-native diselenide bridges to steer oxidative protein folding. Angew Chem Int Ed Engl 51: 5585-5588, 2012.

[70] Metanis N, Hilvert D: Harnessing selenocysteine reactivity for oxidative protein folding. Chem Sci 6: 322-325, 2014.

[71] Jiang Z, Arnér ESJ, Mu Y, Johansson L, Shi J, Zhao S, Liu S, Wang R, Zhang T, Yan G, Liu J, Shen J, Luo G: Expression of selenocysteine-containing glutathione s-transferase in *Escherichia coli*. Biochem Biophys Res Commun 321: 94-101, 2004.

[72] Aldag C, Gromov IA, García-Rubio I, von Koenig K, Schlichting I, Jaun B, Hilvert D: Probing the Role of the Proximal Heme Ligand in Cytochrome P450cam by recombinant incorporation of selenocysteine. Proc Natl Acad Sci U S A 106: 5481-5486, 2009.

[73] Bröcker MJ, Ho JML, Church GM, Söll D, O'Donoghue P: Recoding the genetic code with selenocysteine. Angew Chem Int Ed Engl 53: 319-323, 2014.

[74] Liu J, Chen Q, Rozovsky S: Utilizing Selenocysteine for expressed protein ligation and bioconjugations. J Am Chem Soc 139: 3430-3437, 2017.

[75] Chatrenet B, Chang JY: The folding of hirudin adopts a mechanism of trial and error. J Biol Chem 267: 3038-3043, 1992.

[76] Chatrenet B, Chang JY: The disulfide folding pathway of hirudin elucidated by stop/go folding experiments. J Biol Chem 268: 20988-20996, 1993.

[77] Chang JY: The properties of scrambled hirudins. J Biol Chem 270: 25661-25666, 1995.

[78] Arolas JL, Aviles FX, Chang JY, Ventura S: Folding of small disulfide-rich proteins: clarifying the puzzle. Trends Biochem Sci 31: 292-301, 2006.

[79] Mousa R, Hidmi T, Pomyalov S, Lansky S, Khouri L, Shalev DE, Shoham G, Metanis N: Diselenide crosslinks for enhanced and simplified oxidative protein folding. Commun Chem 4: 1-9, 2021.

[80] Meienhofer J, Schnabel E, Bremer H, Brinkhoff O, Zabel R, Sroka W, Klostermayer H, Brandenburg D, Okuda T, Zahn H: Synthesis of insulin chains and their combination to insulin-active preparations. Z Naturforsch B 18: 1120-1121, 1963.

[81] Katsoyannis PG, Fukuda K, Tometsko A, Suzuki K, Tilak M: Insulin Peptides. X. The synthesis of the b-chain of insulin and its combination with natural or synthetic a-chain to generate insulin activity. J Am Chem Soc 86: 930-932, 1964.

[82] Kung YT, Du YC, Huang WT, Chen CC, Ke LT: Total Synthesis of crystalline bovine insulin. Sci Sin 14: 1710-1716, 1965.

[83] Karas JA, Wade JD, Hossain MA: The Chemical synthesis of insulin: an enduring challenge. Chem Rev 121: 4531-4560, 2021.

[84] Arai K, Takei T, Shinozaki R, Noguchi M, Fujisawa S, Katayama H, Moroder L, Ando S, Okumura M, Inaba K, Inaba K, Iwaoka M: Characterization and optimization of two-chain folding pathways of insulin via native chain assembly. Commun Chem 1: 1-11, 2018.

[85] Arai K, Takei T, Okumura M, Watanabe S, Amagai Y, Asahina Y, Moroder L, Hojo H, Inaba K, Iwaoka M: Preparation of selenoinsulin as a long-lasting insulin analogue. Angew Chem Int Ed 56: 5522-5526, 2017.

[86] Weil-Ktorza O, Rege N, Lansky S, Shalev DE, Shoham G, Weiss MA, Metanis N: Substitution of an internal disulfide bridge with a diselenide enhances both foldability and stability of human insulin. Chem Eur J 25: 8513-8521, 2019.

[87] Arai K, Iwaoka M: Flexible folding: disulfide-containing peptides and proteins choose the pathway depending on the environments. Molecules 26: 195, 2021.

[88] Okumura M, Noi K, Kanemura S, Kinoshita M, Saio T, Inoue Y, Hikima T, Akiyama S, Ogura T, Inaba K: Dynamic assembly of protein disulfide isomerase in catalysis of oxidative folding. Nat Chem Biol 15: 499-509, 2019.

[89] Chen Y, Brandizzi F: IRE1: ER stress sensor and cell fate executor. Trends Cell Biol 23: 547-555, 2013.

[90] Eletto D, Eletto D, Dersh D, Gidalevitz T, Argon Y: Protein disulfide isomerase A6 controls the decay of IRE1α signaling via disulfide-dependent association. Mol Cell 53: 562-576, 2014.

[91] Okumura M, Kanemura S, Matsusaki M, Kinoshita M, Saio T, Ito D, Hirayama C, Kumeta H, Watabe M, Amagai Y, Lee Y-H, Akiyama S, Inaba K: A unique leucine-valine adhesive motif supports structure and function of protein disulfide isomerase P5 via dimerization. Structure 29: 1357-1370.e6, 2021.

Metallomics Research 2022 (3) #MR202209

Review https://metallomicsresearch.brte.org

Metal-binding properties of selenoprotein P—its relation to structure and function

Takashi Toyama, Takayuki Kaneko, Kotoko Arisawa, Yoshiro Saito*

Laboratory of Molecular Biology and Metabolism, Graduate School of Pharmaceutical Sciences, Tohoku University, Sendai, Miyagi 980-8578, Japan

Abstract

Selenoprotein P (SeP), encoded by the *SELENOP* gene, is the major selenium-containing protein in human plasma. SeP has 10 residues of selenocysteine (Sec, cysteine analog in which the sulfur is replaced by selenium), and Sec plays a significant role in the multifunctional properties of SeP. The one Sec residue on the N-terminal side functions for the redox reaction that reduces lipid hydroperoxides, while the 9 Sec residues on the C-terminal side are responsible for the selenium supplying activity. In the middle of SeP, the domain rich in basic amino acids containing consecutive histidine is present. SeP has been reported to have multiple metal-binding abilities such as Hg, Cd, Cu, Ni, Zn, and Co; however, its physiological significance and the effects on SeP functions remain unclear. In this review, the findings to date on the metal-binding properties of SeP and its structural relevance are summarized, particularly for methylmercury. The binding of other selenoproteins to metals is also described. Finally, the interactions of selenoproteins with various metals and its significance for biological defense are discussed.

Key words: Selenoprotein P, Methylmercury, Selenium, Histidine, Selenocysteine

Statements about COI: No potential conflicts of interest were disclosed.

*Correspondence:
Laboratory of Molecular Biology and Metabolism, Graduate School of Pharmaceutical Sciences, Tohoku University
C301, 6-3 Aoba, Aramaki, Aoba-ku, Sendai, Miyagi 980-8578, Japan
TEL: +81 22 795 6870
FAX: +81 22 795 6870
E-mail: yoshiro.saito.a8@tohoku.ac.jp

Received: October 29, 2022
Accepted: December 13, 2022
Released online: December 26, 2022

Abbreviations:

GPx, glutathione peroxidase; GSH, glutathione; LRP, lipoprotein receptor-related protein; PL-OOH, phospholipid hydroperoxide; ROS, reactive oxygen species; Sec, selenocysteine; SECIS, Sec-insertion sequence; SeP, Selenoprotein P; SeMet, selenomethionine; Trx, Thioredoxin; TrxR, thioredoxin reductase

1. Introduction

Selenium (Se) is a type of chalcogen in Group 16 of the periodic table with a large electron orbital compared with oxygen and sulfur, which facilitates the emission and reception of electrons. Selenium is known to be highly toxic, while it is an essential trace element[1]. A particularly narrow appropriate range between deficiency and excess is a characteristic property of selenium. The physiological role of selenium is mediated by

selenoproteins, containing selenocysteine (Sec), an amino acid in which the sulfur in cysteine is replaced by selenium[2,3]. Twenty-five kinds of human selenoproteins are identified, and are a key factor in the antioxidant system, which plays a significant role in the removal of reactive oxygen species (ROS) and redox regulation[4,5]. Sec is encoded by the UGA codon, known as a stop (opal) codon, and is called the 21st amino acid in the genetic code. In eukaryotes, the Sec insertion sequence (SECIS), which is a specific hairpin structure located in the 3′ untranslated region (3′UTR) of selenoprotein mRNA, is essential for the incorporation of Sec during the biosynthesis of selenoproteins[3]. SECIS binds the SECIS-binding protein 2 (SBP2) and forms a complex for Sec incorporation via the recruitment of the Sec-specific eukaryotic elongation factor (eEFsec) and Sec-tRNA^{Sec} (an anticodon complementary to the UGA codon)[6,7].

Glutathione peroxidase (GPx), the identified first selenoprotein, is an enzyme that reduces and detoxifies hydroperoxides in the presence of glutathione (GSH), and Sec forms its active site[8]. Thioredoxin reductase (TrxR) is a selenoprotein that is responsible for redox control[9]. TrxR is an NADPH-dependent flavin enzyme that consumes NADPH and reduces Trx by using Sec in its active site. Selenoproteins are also involved in growth/development and energy metabolism; iodothyronine deiodinase (DI), which activates or inactivates the thyroid hormone, is a selenoprotein, and Sec is used for the elimination/addition of iodide[10].

Selenoprotein P (SeP) accounts for 50% of human plasma selenium with the 'P' derived from its presence in 'plasma.' SeP is synthesized mainly in the liver and secreted into plasma[11]. SeP is the unique selenoprotein containing 10 Sec residues in the polypeptide chain. SeP is multifunctional with GPx-like reducing activity for lipid hydroperoxides and with a selenium transporting activity that efficiently delivers selenium to the cells[12,13]. Further, SeP binds heavy metals such as copper (Cu) and cadmium (Cd) and is also identified as a major methylmercury-binding protein in plasma, suggesting its role in the detoxication of heavy metals[14,15].

This review focused on the metal-binding properties of SeP and its structural relevance, particularly on methylmercury. The binding of other selenoproteins to various metals is also described. The interactions of selenoproteins with metals and their biological role in the defense against environmental pollution are discussed.

2. Structure and function of selenoprotein P

The structure–function relationship in SeP is shown in **Fig. 1** [13,16]. The mRNA of SeP contains ten UGA codons in the open reading frame and two SECIS in the 3′UTR, while other selenoprotein mRNAs have only one SECIS element[17]. SeP possesses several biological functions ascribed with 10 Sec residues; one N-terminal Sec residue forms an active site of enzyme

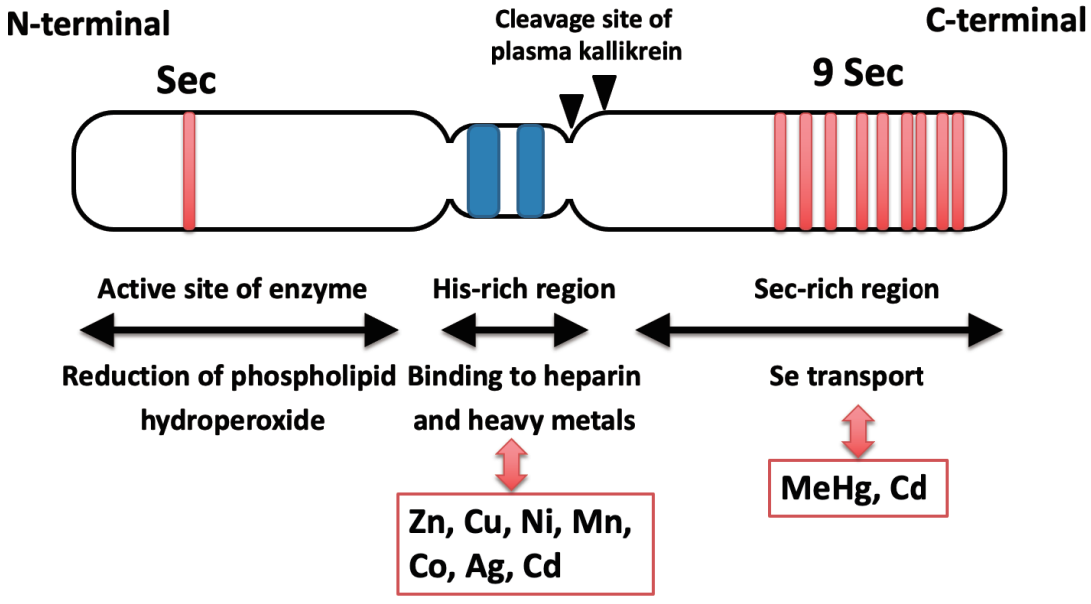

Fig. 1. **Structure and function of selenoprotein P.**
Domain structure and function of selenoprotein P. Possible interaction between each region and metal is indicated.

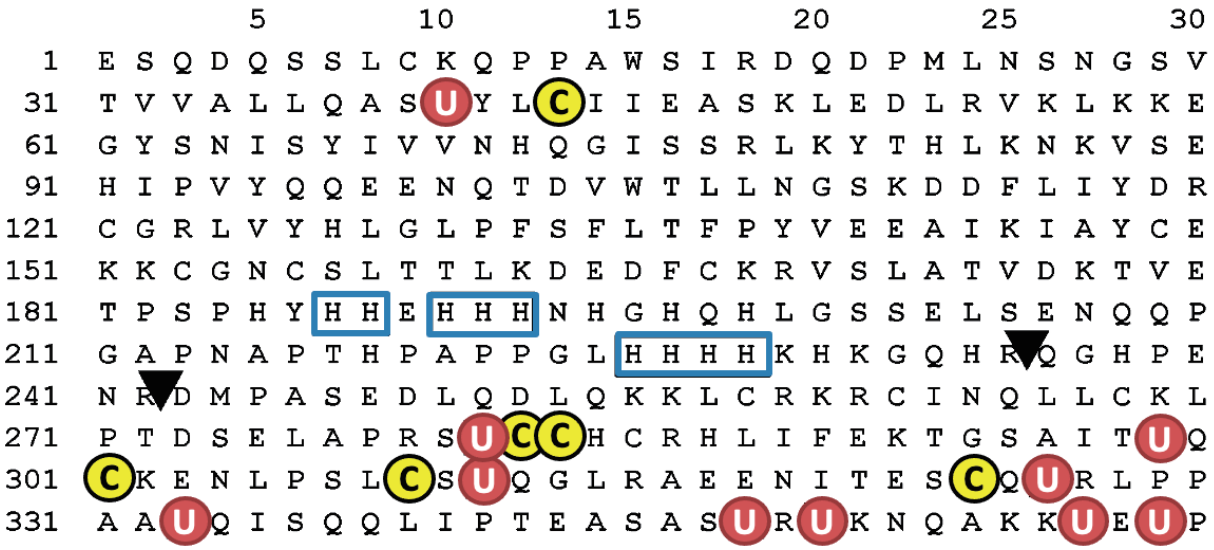

Fig. 2. **The properties of the amino acid sequence of human Selenoprotein P.**
U: selenocysteine. C (yellow color): cysteine near selenocysteine. Sequential histidine is shown in the box. Triangle indicates the cleavage sites of plasma kallikrein.

activity to reduce lipid hydroperoxide, while the nine C-terminal Sec residues function as a Se transporter. Plasma kallikrein cleaves SeP in limited proteolysis with Arg-235–Gln-236 and Arg-242–Asp-243, generating the N-terminal fragments (residues 1–235) with enzyme activity and C-terminal fragment (residues 243–361) exhibiting Se-supply activity[18]. Based on the biological function of these SeP fragments, a domain structure of SeP is proposed (**Fig. 1**).

The amino acid sequence of human selenoprotein P (SeP) is shown in **Fig. 2**. N-terminal, a possible catalytic center of SeP, has U(Sec)XXC motif, similar to the active site of thioredoxin (CXXC), which suggests the reactivity of SeP against the protein thiols. The interaction between the C-terminal domain of SeP and the YWTD β-propeller domain of SeP receptor, ApoER2, has been reported, and the importance of this interaction, particularly in maintaining selenium levels in the brain and testes, has been manifested in the phenotypes of these KO mice[19–21]. Both Sec and Cys have been found to be abundant in the C-terminal region of human SeP (**Fig. 2**). These residues are known to be relatively well conserved between human, rats and mice [22]. If Sec and Cys are considered together, an almost complete conservation of Sec and Cys residues is observed. When the CC or CXC sequences (i.e., the metal-binding motif in metallothionein [23]) are adapted to the C-terminal part of SeP, it has the following sequences: one UCC, one UXC, two CXU, and two UXU. This suggests that SeP will bind metals via C-terminal Sec residues; however, details are unknown.

A His-rich region containing a typical heparin-binding motif XBBXB (B: a basic amino acid) is located in the middle of SeP (**Fig. 1**). This His-rich region functions like a naturally occurring His-tag to bind nickel–nitrilotriacetic acid (Ni–NTA) agarose; namely, SeP binds strongly to nickel-chelating agarose in the same manner as six constitutive His-tagged recombinant proteins and it is eluted by competition with imidazole, a His analog [13,24]. Interestingly, it has been reported that SeP can bind to heavy metals *in vivo* and *in vitro* in a His-dependent manner (details are described later). SeP is also identified as a major methylmercury-binding protein in plasma, suggesting that it plays a role in the detoxication of heavy metals; however, the physiological significance of the metal-binding property of SeP is still under consideration.

3. Role of selenium on mercury distribution toxicity and metabolisms

Selenide ion (Se^{2-} or hydrogen selenide ion; HSe^-) and selenolate ion (RSe^-) show potent nucleophilicity; thus, selenide and selenocysteine can bind electrophilic metals, e.g., mercury. In addition, selenium can also form coordination bonds through noncovalent electron pairs similar to the sulfide group. Based on these chemical properties, several effects of selenium on the distribution and toxicity of metals have been reported.

One of the earliest and most representative studies on selenium and metal interaction has been on mercury (Hg). Mercury is distributed in the earth's crust at 0.05 mg/kg and is naturally found as mercuric salts, e.g., HgCl, HgO, HgS, and HgSe[25,26]. Unlike most other metallic compounds, mercuric compounds tend to involve covalent bonding rather than ionic bonding[26]. These inorganic mercury compounds are methylated by microorganisms and biologically concentrated in large predatory fish and marine mammals (whales, dolphins, and seals)[27,28]. Indeed, the most abundant chemical speciation of mercury in fish is mono-methylmercury (MeHg) and its assumed to consist of approximately 84% of total mercury[29]. Thus, humans are predominantly exposed to mercury as methylmercury from seafood[30,31], except for occupational exposure to inorganic mercury. Methylmercury and inorganic mercury are bound with S and Se in an aqueous solution and the binding energy between Hg and Se is relatively stronger than S[32,33]. Recent computational chemistry suggested that binding of methylmercury to selenocysteine would facilitate spontaneous Se-elimination reaction from selenocysteine to produce dehydroalanine in selenoenzymes[34]; however, it is not known whether this reaction is observed *in vivo*.

Several studies suggested that selenium antagonizes mercury toxicity, both inorganic mercury and methylmercury. Parizek and Ostadalova demonstrated that Se protects against mercury-induced neurotoxicity in rats[35]. This similar detoxification of mercury by selenium was reported in Japanese quails, rats, aquatic organisms, and bacteria[36]. The concentrations of mercury and selenium are frequently found in a 1:1 molar ratio in tissues of marine life[37,38]. Recent studies suggest that consuming fish with Hg:Se ratios lower than 1:1 may reduce the risk of mercury toxicity[39,40]. Interestingly selenium toxicity was rescued by mercury; thus, it has been known that selenium and mercury cancel each other's toxicity via the formation of a stable adduct. Although selenium protects against mercury and methylmercury toxicity, the effect of selenium on mercury concentration in organs is controversial and it is not explainable by the effect of mercury excretion alone[41]. This indicates selenium can detoxify mercury and methylmercury toxicity via the formation of stable and less-toxic adducts, which is independent of excretion. Naganuma et al. reported the formation of bis-methylmercuric selenide, $(MeHg)_2Se$, by the reaction product of methylmercury, glutathione, and selenide. This compound is unstable and readily degraded to HgSe[36,42,43]. HgS and HgSe complex was found in the liver of mammals, and some studies suggest that selenium can facilitate the demethylation of methylmercury[44]. Little is known about the biological fate of HgS and HgSe; however, it may contribute to the excretion of mercury because methylmercury is reabsorbed in the kidney and intestine to form enterohepatic and intrarenal circulation[45]. The biological absorption of inorganic mercury is less than methylmercury; thus, it has been thought that the demethylation process is the detoxification of methylmercury[46,47]. However, Takanezawa et al. recently reported that ectopic expression of the demethylation enzyme for methylmercury, which is the microbial origin MerB, to mammalian cell line-enhanced methylmercury toxicity[48]. These findings suggest that methylmercury demethylation inside or outside of the cells may be important for toxicity, or the presence of a counter ion (Se^{2-} or S^{2-}), which eliminates the reactivity of inorganic mercury may also be crucial. Again, selenium is thought to be an important factor in the understanding of the distribution and demethylation of methylmercury, and the subsequent toxicity.

Selenoproteins were also important for mercury toxicity. Several studies have reported decreased GPx activity, a selenoprotein that plays a significant role in antioxidative defense, by methylmercury. Methylmercury containing water at a concentration of 40 mg/L and bred mice *ad libitum* for 15–17 days resulting in a decrease in GPx activity and an increase in oxidative stress were observed in the brain with Purkinje cell injury[49]. Franco et al. also found that the free drinking of 40 mg/L methylmercury for 21 days in mice (male Swiss mice) resulted in a 50–60% decrease in GPx activity in the brain[50]. Usuki et al. reported that methylmercury administration to rats for 4 weeks decreased GPx1 mRNA in the skeletal muscle[51]. Using cultured neurons, it was also shown that mercaptosuccinic acid (GPx inhibitor) potentiates the toxicity of methylmercury, while overexpression of GPx1 in mouse cerebellar granule cells suppressed methylmercury-induced cell death, suggesting that GPx1 plays a protective role in methylmercury-induced neuronal injury[52]. The effect of methylmercury on the activity of purified GPx protein has been investigated[53], and methylmercury may inhibit its enzymatic activity by binding to selenocysteine; however, direct evidence that indicates the formation of the covalent bond (Se-mercuration) has not been shown.

4. Selenoprotein P, a major target of methylmercury in plasma

Interestingly, recent studies suggest that SeP can be a major target of methylmercury in plasma. Although SeP is known as a selenium transporting protein and anti-oxidative enzyme, the effect of Se-mercuration of SeP on its functions is not well

understood. This chapter introduces some evidence that shows the strong interaction of SeP and mercury and discusses its contribution to mercury toxicity.

In human plasma, there are two kinds of selenoproteins: SeP and extracellular GPx (GPx3), possessing Se as Sec residue, and 53% and 19% of plasma selenium is derived from SeP and GPx3, respectively. The residual 28% of selenium might be derived from selenomethionine (SeMet) in albumin, and/or low molecular selenium compounds, which have in part been identified as selenosugars. The Nunavik Inuit is one of the groups that are exposed to relatively high concentrations of methylmercury and selenium because the Nunavik Inuit people consume seafood and marine mammals daily. Achebe et al. challenged LC-ICP/MS analysis of Inuit plasma and found that the highest concentration of mercury is found at the same fraction of SeP[54]. In the case of mercury miners in China who were occupationally exposed to inorganic mercury, it was found that both SeP and GPx3 were bound with mercury in serum[55]. An animal study was also conducted by Liu et al. and SeP was found as a predominant target of methylmercury in the plasma of rats administrated with methylmercury-containing water (4 mg/kg as Hg for 4 weeks). They concluded that 73% of total mercury in plasma is bound with SeP and this is the major mercury transporting protein in plasma, despite albumin being abundant[15]. The SeP level in plasma is decreased by methylmercury intoxication for a 4-week exposure of 20 ppm of MeHg to rat, while not by Pb and Cd exposure[56].

Administration of inorganic mercury ($HgCl_2$) and selenite simultaneously and equimolar prevent toxicity; this led many researchers to suggest the formation of an equimolar $(HgSe)_n$ that is bound to the specific plasma protein in the bloodstream[57,58], and later this was identified as SeP[59]. In this case, inorganic mercury or selenite itself failed to bind with SeP, indicating that the $(HgSe)_n$ cluster ionically electrostatically interacted with SeP, but not Hg^{2+}. The estimated number of HgSe complex that is bound with SeP is approximately 100, and at least 35 binding sites on SeP was suggested[60].

In all studies, the effects of methylmercury and inorganic mercury on the selenium transporting function in SeP were not addressed at all and will need to be examined in the future.

5. Interaction of several selenoproteins with various metals

As mentioned above, SeP binds to several divalent cation metals due to its His-rich domain[14]. Sidenius et al. found that Cu^{2+}, Ni^{2+}, Zn^{2+}, Co^{2+}, and Cd^{2+} bind to SeP in human plasma by metal ion affinity chromatography, and among these, Co^{2+} binds most strongly to SeP[14]. The relationship between Zn, an essential trace element, and SeP has been well studied in these metals[61,62]. Zn is an important metal for the neurodevelopment of brains and spermatogenesis in testes similar to selenium and SeP[63,64]. In the brains of Alzheimer's disease patients, it has been reported that the amount of SeP protein expression in cerebrospinal fluid is slightly increased, and it is also known that Zn promotes protein aggregation and that Zn concentrations are heterogeneous[65,66]. In the brains of SeP KO mice, Zn concentration in the hippocampus was increased[67]. Xiubo et al. reported that the binding of SeP to Zn inhibits Aβ aggregation and reduces the resulting neuropathy[62]. These results may suggest that SeP contributes to Zn utilization in the brain via directly binding through its His-rich domain[67]. ApoER2, which is the SeP receptor, is also known as the ApoE receptor in the brain[21]. Polymorphism in the ApoE gene is one of the most well-known risk factors for Alzheimer's disease[68]. Zn exacerbates Alzheimer's disease by cleaving ApoE and reducing the normal full-length ApoE[69]. In addition to suppressing Aβ aggregation by Zn as described above, SeP may suppress Alzheimer's disease by maintaining full-length ApoE. In some cohort studies related to selenium and aging including Alzheimer's disease, the involvement of selenium in Alzheimer's disease was found to be still controversial, but we are hopeful that a more detailed role may be found by focusing on SeP rather than selenium.

The relevance between selenium/SeP and toxic metals known as environmental pollutants, such as methylmercury, As, and Cd, has been well studied[70,71]. Cd and its binding proteins have long been well studied, and metallothionein has been extensively investigated[72]. Cd and metallothionein are bound by CXXC, or CXC motif, and also SeP has CXU, UXC, and UXU in its C-terminal Sec-rich domain. On the other hand, computer calculations also suggest binding to His-rich plasma glycoproteins[73,74]. Sasakura et al. found that SeP fractions, purified from human plasma, bind Cd, and the molar ratios of SeP to Cd are 1:1[75]. It is not clear whether the binding of SeP to Cd is in the His-rich domain or the C-terminal domain (or both), but we expect this to be clarified.

Cd induces oxidative stress and injures kidneys and testes, while it has been demonstrated that selenium reduces this toxicity[76]. Recently, it was shown that lipid peroxide accumulates in the testes of mice treated with low concentrations of Cd, inducing

ferroptosis[77]. We have found that GPx4 expression, which plays a role in the reduction of phospholipid hydroperoxidase, is almost abolished in the testes of SeP KO mice (data not shown). Additionally, exposure of high-dose Cd to the HepG2 cell, hepatocarcinoma cell line, decreases SeP expression[78]. These results imply that when Se is sufficiently greater than Cd, the expression of SeP is enough to protect against toxicity caused by ROS in the testes, but when Cd is excessively increased, SeP production from the liver decreases, resulting in oxidative stress and ferroptosis.

Other selenoproteins containing selenocysteine such as TrxR and GPx have also been suggested to bind metals. As mentioned above, some metals may inhibit its enzymatic activity by binding to Sec[79,80]. In particular, several studies suggest that Au binds to TrxR and inhibits its activity[81–83]. TrxRs have a redox active Sec residue [84]. Mass spectrometry studies suggest that TrxRs bind to approximately four Au (I) cations[85], while biochemical assays show that the Au compound greatly alters the active Sec site of the enzymes[86–89]. Though conclusive evidence of direct metal binding to Sec has not been achieved yet, the study examining the reaction of TrxR1 mutant lacking Sec (Sec498→Cys mutant) with Au compounds supported this hypothesis[90]. Particularly in cancers, TrxR inhibition leads to an increased intracellular oxidative stress and induces apoptosis[91]. TrxR overexpression is associated with aggressive tumor progression and poor survival in patients with breast, ovarian, and lung cancers[85,92,93]. The thioredoxin system may represent an attractive target for the development of new cancer treatments. The Au complex auranofin inhibits the activity of TrxR and was developed as an oral therapy for rheumatoid arthritis. Recently, it has been studied as a potent anticancer agent due to its TrxR inhibitory effect[79]. Other metals, such as Ag, Pt, Ru, and Rh, are also used in anticancer drugs, and many of them are designed specifically for targeting TrxR[94,95].

Direct binding of free selenium to various metals may modulate metal toxicity. It has been suggested that administration of inorganic selenium may be protective against metal toxicity of Pb, Hg, As, Cd, etc. Overall, it is thought that selenium is used as a source of selenoprotein and protects cells by scavenging ROS, but it has been suggested that selenium directly binds to some metals and inhibits their toxicity[96]. Human studies have demonstrated that selenium may reduce As accumulation in the organism and protect against As-related skin lesions[97]. In another study examining the effect of As on ultraviolet radiation (UVR)-induced carcinogenesis in mouse skin, dietary selenium blocked the cancer enhancement effects of As[98]. This study suggested that selenium prevented As retention in mouse skin probably by formation of an As–Se metabolite, a seleno-bis (S-glutathionyl) arenium ion, whose traces were identified in the liver of mice. The authors concluded that formation of this compound was more likely to be responsible for the As-blocking effect of Se than was a mechanism based on oxidative stress reduction. Another study implicated that selenium compounds prevent metal-mediated oxidative damage through binding to copper and iron[99]. Selenium compounds such as selenocysteine directly inhibited Cu- and Fe-induced DNA damage *in vitro* despite their low GPx activity, suggesting that metal binding to selenium compounds is the primary mechanism.

While there is much evidence suggesting protective/ameliorative effects of selenium against metal toxicity, it should be noted that selenium interaction with several toxic elements may prolong their persistence in animal tissues, leading to long-term effects of toxic elements[100].

6. Conclusion

This review focuses on the binding of several metals for selenium/selenoproteins, particularly SeP in plasma. The list of metals binding to SeP were shown in **Table 1**. SeP binds metals in at least two ways: Sec- and His-rich sequences. At present,

Table 1. | Binding patterns of selenoproteins and selenium to various metals

		binding site	metal	reference
Selenoprotein P				
		His-rich domain	Zn, Cu Ni, Mn, Co, Ag, Cd	[14,62,75,101]
		Sec	MeHg, Cd	[15,78]
Other selenoproteins				
	TrxR	Sec	Au, Pt, Pd	[81,83]
	GPx	Sec	Au	[80,81]
Selenium			Hg, Ag, Pb, As, Mn, Cu, Fe	[96,98,99]

the precise effects of heavy metals on SeP functions are not fully understood, which is an important subject to understanding the molecular mechanisms of the toxicity of these metals. It will also be an exciting study that reveals the relationship between the metal-binding properties of SeP and its related diseases, including type 2 diabetes. Further research is necessary to show the interaction between selenium/selenoproteins and metals in physiological and toxicological conditions.

Acknowledgment

This work was supported in part by JSPS KAKENHI (grant number 20H00488, 20H05491, and 21K19321) and Japan Agency for Medical Research and Development (AMED, grant number JP20ek0210144).

References

[1] Lockitch G. Selenium: clinical significance and analytical concepts. Crit Rev Clin Lab Sci 1989;27:483–541.

[2] Commans S, Böck A. Selenocysteine inserting tRNAs: an overview. FEMS Microbiol Rev 1999;23:335–351.

[3] Böck A, Forchhammer K, Heider J, et al. Selenocysteine: the 21st amino acid. Mol Microbiol 1991;5:515–520.

[4] Kryukov GV, Castellano S, Novoselov SV, et al. Characterization of mammalian selenoproteomes. Science 2003;300:1439–1443.

[5] Reeves MA, Hoffmann PR. The human selenoproteome: recent insights into functions and regulation. Cell Mol Life Sci 2009;66:2457–2478.

[6] Copeland PR, Driscoll DM. RNA binding proteins and selenocysteine. Biofactors 2001;14:11–16.

[7] Copeland PR, Fletcher JE, Carlson BA, et al. A novel RNA binding protein, SBP2, is required for the translation of mammalian selenoprotein mRNAs. EMBO J 2000;19:306–314.

[8] Brigelius-Flohé R, Maiorino M. Glutathione peroxidases. Biochim Biophys Acta 2013;1830:3289–3303.

[9] Mustacich D, Powis G. Thioredoxin reductase. Biochem J 2000;346 Pt 1:1–8.

[10] St Germain DL, Galton VA. The deiodinase family of selenoproteins. Thyroid 1997;7:655–668.

[11] Carlson, Novoselov, Kumaraswamy. Specific excision of the selenocysteine tRNA [Ser] Sec (Trsp) gene in mouse liver demonstrates an essential role of selenoproteins in liver function. Boll Soc Ital Biol Sper 2004;

[12] Saito Y. Selenoprotein P as a significant regulator of pancreatic β cell function. J Biochem 2020;167:119–124.

[13] Saito Y, Hayashi T, Tanaka A, et al. Selenoprotein P in human plasma as an extracellular phospholipid hydroperoxide glutathione peroxidase. Isolation and enzymatic characterization of human selenoprotein p. J Biol Chem 1999;274:2866–2871.

[14] Sidenius U, Farver O, Jøns O, et al. Comparison of different transition metal ions for immobilized metal affinity chromatography of selenoprotein P from human plasma. J Chromatogr B Biomed Sci Appl 1999;735:85–91.

[15] Liu Y, Zhang W, Zhao J, et al. Selenoprotein P as the major transporter for mercury in serum from methylmercury-poisoned rats. J Trace Elem Med Biol 2018;50:589–595.

[16] Saito Y, Takahashi K. Characterization of selenoprotein P as a selenium supply protein. Eur J Biochem 2002;269:5746–5751.

[17] Saito Y. Selenium Transport Mechanism via Selenoprotein P-Its Physiological Role and Related Diseases. Front Nutr 2021;8:685517.

[18] Saito Y, Sato N, Hirashima M, et al. Domain structure of bi-functional selenoprotein P. Biochem J 2004;381:841–846.

[19] Hill KE, Zhou J, McMahan WJ, et al. Deletion of selenoprotein P alters distribution of selenium in the mouse. J Biol Chem 2003;278:13640–13646.

[20] Olson GE, Winfrey VP, Nagdas SK, et al. Apolipoprotein E receptor-2 (ApoER2) mediates selenium uptake from selenoprotein P by the mouse testis. J Biol Chem 2007;282:12290–12297.

[21] Burk RF, Hill KE, Motley AK, et al. Selenoprotein P and apolipoprotein E receptor-2 interact at the blood-brain barrier and also within the brain to maintain an essential selenium pool that protects against neurodegeneration. FASEB J 2014;28:3579–3588.

[22] Hill KE, Lloyd RS, Burk RF. Conserved nucleotide sequences in the open reading frame and 3' untranslated region of selenoprotein P mRNA. Proc Natl Acad Sci U S A 1993;90:537–541.

[23] Romero-Isart N, Vasák M. Advances in the structure and chemistry of metallothioneins. J Inorg Biochem 2002;88:388–396.

[24] Tujebajeva RM, Harney JW, Berry MJ. Selenoprotein P expression, purification, and immunochemical characterization. J Biol Chem 2000;275:6288–6294.

[25] Kim CS, Bloom NS, Rytuba JJ, et al. Mercury Speciation by X-ray Absorption Fine Structure Spectroscopy and Sequential Chemical Extractions: A Comparison of Speciation Methods. Environ Sci Technol 2003;37:5102–5108.

[26] O'Connor D, Hou D, Ok YS, et al. Mercury speciation, transformation, and transportation in soils, atmospheric flux, and implications for risk management: A critical review. Environ Int 2019;126:747–761.

[27] de Wit HA, Kainz MJ, Lindholm M. Methylmercury bioaccumulation in invertebrates of boreal streams in Norway: Effects of aqueous methylmercury and diet retention. Environ Pollut 2012;164:235–241.

[28] Harding G, Dalziel J, Vass P. Bioaccumulation of methylmercury within the marine food web of the outer Bay of Fundy, Gulf of Maine. PLoS One 2018;13:e0197220.

[29] Clémens S, Monperrus M, Donard OFX, et al. Mercury speciation in seafood using isotope dilution analysis: A review. Talanta 2012;89:12–20.

[30] Airey D. Mercury in human hair due to environment and diet: a review. Environ Health Perspect 1983;52:303–316.

[31] Rice G, Swartout J, Mahaffey K, et al. Derivation of U.S. EPA's oral Reference Dose (RfD) for methylmercury. Drug Chem Toxicol 2000;23:41–54.

[32] Madabeni A, Nogara PA, Bortoli M, et al. Effect of Methylmercury Binding on the Peroxide-Reducing Potential of Cysteine and Selenocysteine. Inorg Chem 2021;60:4646–4656.

[33] Rabenstein DL. The aqueous solution chemistry of methylmercury and its complexes. Acc Chem Res 1978;11:100–107.

[34] Nogara PA, Madabeni A, Bortoli M, et al. Methylmercury Can Facilitate the Formation of Dehydroalanine in Selenoenzymes: Insight from DFT Molecular Modeling. Chem Res Toxicol 2021;34:1655–1663.

[35] Parízek J, Ostádalová I. The protective effect of small amounts of selenite in sublimate intoxication. Experientia 1967;23:142–143.

[36] Khan MAK, Wang F. Mercury-selenium compounds and their toxicological significance: toward a molecular understanding of the mercury-selenium antagonism. Environ Toxicol Chem 2009;28:1567–1577.

[37] Koeman JH, Peeters WHM, Koudstaal-Hol CHM, et al. Mercury-Selenium Correlations in Marine Mammals. Nature 1973;245:385–386.

[38] Koeman JH, van de Ven WS, de Goeij JJ, et al. Mercury and selenium in marine mammals and birds. Sci Total Environ 1975;3:279–287.

[39] Ralston NVC. Selenium health benefit values as seafood safety criteria. Ecohealth 2008;5:442–455.

[40] Burger J, Gochfeld M. Selenium and mercury molar ratios in commercial fish from New Jersey and Illinois: variation within species and relevance to risk communication. Food Chem Toxicol 2013;57:235–245.

[41] Cuvin-Aralar MLA, Furness RW. Mercury and selenium interaction: A review. Ecotoxicol Environ Saf 1991;21:348–364.

[42] Naganuma A, Nakajima E, Shigehara E, et al. Mercury distribution in mouse brain after i.v. administration of bis(methylmercuric) selenide. Toxicol Lett 1983;15:175–179.

[43] Naganuma A, Imura N. Bis(methylmercuric) selenide as a reaction product from methylmercury and selenite in rabbit blood. Res Commun Chem Pathol Pharmacol 1980;27:163–173.

[44] Takahashi H, Suetomi K, Konishi T. Differential Determination of Ionizable and Unionizable (Inert) Forms of Inorganic Mercury in Animal Tissues. In: Suzuki T, Imura N, Clarkson TW, editors. Advances in Mercury Toxicology. Boston, MA: Springer US; 1991. p. 181–189.

[45] Urano T, Iwasaki A, Himeno S, et al. Absorption of methylmercury compounds from rat intestine. Toxicol Lett 1990;50:159–164.

[46] Rowland IR, Robinson RD, Doherty RA. Effects of diet on mercury metabolism and excretion in mice given methylmercury: role of gut flora. Arch Environ Health 1984;39:401–408.

[47] Vázquez M, Calatayud M, Vélez D, et al. Intestinal transport of methylmercury and inorganic mercury in various models of Caco-2 and HT29-MTX cells. Toxicology 2013;311:147–153.

[48] Takanezawa Y, Nakamura R, Matsuda H, et al. Intracellular Demethylation of Methylmercury to Inorganic Mercury by Organomercurial Lyase (MerB) Strengthens Cytotoxicity. Toxicol Sci 2019;170:438–451.

[49] Carvalho MC, Franco JL, Ghizoni H, et al. Effects of 2,3-dimercapto-1-propanesulfonic acid (DMPS) on methylmercury-induced locomotor deficits and cerebellar toxicity in mice. Toxicology 2007;239:195–203.

[50] Franco JL, Posser T, Dunkley PR, et al. Methylmercury neurotoxicity is associated with inhibition of the antioxidant enzyme glutathione peroxidase. Free Radic Biol Med 2009;47:449–457.

[51] Usuki F, Yamashita A, Fujimura M. Post-transcriptional defects of antioxidant selenoenzymes cause oxidative stress under methylmercury exposure. J Biol Chem 2011;286:6641–6649.

[52] Farina M, Campos F, Vendrell I, et al. Probucol increases glutathione peroxidase-1 activity and displays long-lasting protection against methylmercury toxicity in cerebellar granule cells. Toxicol Sci 2009;112:416–426.

[53] Hirota Y, Yamaguchi S, Shimojoh N, et al. Inhibitory effect of methylmercury on the activity of glutathione peroxidase. Toxicol Appl Pharmacol 1980;53:174–176.

[54] Achouba A, Dumas P, Ouellet N, et al. Plasma levels of selenium-containing proteins in Inuit adults from Nunavik. Environ Int 2016;96:8–15.

[55] Chen C, Yu H, Zhao J, et al. The roles of serum selenium and selenoproteins on mercury toxicity in environmental and occupational exposure. Environ Health Perspect 2006;114:297–301.

[56] Usuki F, Fujimura M. Decreased plasma thiol antioxidant barrier and selenoproteins as potential biomarkers for ongoing methylmercury intoxication and an individual protective capacity. Arch Toxicol 2016;90:917–926.

[57] Burk RF, Foster KA, Greenfield PM, et al. Binding of simultaneously administered inorganic selenium and mercury to a rat plasma protein. Proc Soc Exp Biol Med 1974;145:782–785.

[58] Naganuma A, Ishii Y, Imura N. Effect of administration sequence of mercuric chloride and sodium selenite on their fates and toxicities in mice. Ecotoxicol Environ Saf 1984;8:572–580.

[59] Yoneda S, Suzuki KT. Equimolar Hg-Se complex binds to selenoprotein P. Biochem Biophys Res Commun 1997;231:7–11.

[60] Suzuki KT, Sasakura C, Yoneda S. Binding sites for the (Hg-Se) complex on selenoprotein P. Biochim Biophys Acta 1998;1429:102–112.

[61] Yue C, Shan Z, Tan Y, et al. His-Rich Domain of Selenoprotein P Ameliorates Neuropathology and Cognitive Deficits by Regulating TrkB Pathway and Zinc Homeostasis in an Alzheimer Model of Mice. ACS Chem Neurosci 2020;11:4098–4110.

[62] Du X, Li H, Wang Z, et al. Selenoprotein P and selenoprotein M block Zn2+-mediated Aβ42 aggregation and toxicity†. Metallomics 2013;5:861–870.

[63] Yamaguchi S, Miura C, Kikuchi K, et al. Zinc is an essential trace element for spermatogenesis. Proc Natl Acad Sci U S A 2009;106:10859–10864.

[64] Sensi SL, Paoletti P, Koh J-Y, et al. The neurophysiology and pathology of brain zinc. J Neurosci 2011;31:16076–16085.

[65] Urbano T, Vinceti M, Mandrioli J, et al. Selenoprotein P Concentrations in the Cerebrospinal Fluid and Serum of Individuals Affected by Amyotrophic Lateral Sclerosis, Mild Cognitive Impairment and Alzheimer's Dementia. Int J Mol Sci 2022;23:.

[66] Cuajungco MP, Lees GJ. Zinc and Alzheimer's disease: is there a direct link? Brain Res Brain Res Rev 1997;23:219–236.

[67] Kiyohara ACP, Torres DJ, Hagiwara A, et al. Selenoprotein P Regulates Synaptic Zinc and Reduces Tau Phosphorylation. Front Nutr 2021;8:683154.

[68] Yamazaki Y, Zhao N, Caulfield TR, et al. Apolipoprotein E and Alzheimer disease: pathobiology and targeting strategies. Nat Rev Neurol 2019;15:501–518.

[69] Xu H, Gupta VB, Martins IJ, et al. Zinc affects the proteolytic stability of Apolipoprotein E in an isoform-dependent way. Neurobiol Dis 2015;81:38–48.

[70] Zwolak I. The Role of Selenium in Arsenic and Cadmium Toxicity: an Updated Review of Scientific Literature. Biol Trace Elem Res 2020;193:44–63.

[71] Shahid MA, Balal RM, Khan N, et al. Selenium impedes cadmium and arsenic toxicity in potato by modulating carbohydrate and nitrogen metabolism. Ecotoxicol Environ Saf 2019;180:588–599.

[72] Klaassen CD, Liu J, Diwan BA. Metallothionein protection of cadmium toxicity. Toxicol Appl Pharmacol 2009;238:215–220.

[73] Liu X, Hu Q, Yang J, et al. Selective cadmium regulation mediated by a cooperative binding mechanism in CadR. Proceedings of the National Academy of Sciences 2019;116:20398–20403.

[74] Nair PS, Robinson WE. Cadmium binding to a histidine-rich glycoprotein from marine mussel blood plasma: potentiometric titration and equilibrium speciation modeling. Environ Toxicol Chem 2001;20:1596–1604.

[75] Sasakura C, T. Suzuki K. Biological interaction between transition metals (Ag, Cd and Hg), selenide/sulfide and selenoprotein P. J Inorg Biochem 1998;71:159–162.

[76] Katakura M, Sugawara N. Preventive Effect of Selenium against the Testicular Injury by Cadmium. Nippon Eiseigaku Zasshi (Japanese Journal of Hygiene) 1999;54:481–489.

[77] Xiong L, Bin Zhou, Young JL, et al. Exposure to low-dose cadmium induces testicular ferroptosis. Ecotoxicol Environ Saf 2022;234:113373.

[78] Ramírez-Acosta S, Uhlírová R, Navarro F, et al. Antagonistic Interaction of Selenium and Cadmium in Human Hepatic Cells Through Selenoproteins. Front Chem 2022;10:891933.

[79] Tolbatov I, Marrone A. Selenocysteine of thioredoxin reductase as the primary target for the antitumor metallodrugs: A computational point of view. J Organomet Chem 2022;965–966:122330.

[80] Chaudiere J, Tappel AL. Interaction of gold(I) with the active site of selenium-glutathione peroxidase. J Inorg Biochem 1984;20:313–325.

[81] Rigobello MP, Messori L, Marcon G, et al. Gold complexes inhibit mitochondrial thioredoxin reductase: consequences on mitochondrial functions. J Inorg Biochem 2004;98:1634–1641.

[82] Omata Y, Folan M, Shaw M, et al. Sublethal concentrations of diverse gold compounds inhibit mammalian cytosolic thioredoxin reductase (TrxR1). Toxicol In Vitro 2006;20:882–890.

[83] Prast-Nielsen S, Cebula M, Pader I, et al. Noble metal targeting of thioredoxin reductase--covalent complexes with thioredoxin and thioredoxin-related protein of 14 kDa triggered by cisplatin. Free Radic Biol Med 2010;49:1765–1778.

[84] Arnér ES, Holmgren A. Physiological functions of thioredoxin and thioredoxin reductase. Eur J Biochem 2000;267:6102–6109.

[85] Casini A, Hartinger C, Gabbiani C, et al. Gold(III) compounds as anticancer agents: Relevance of gold–protein interactions for their mechanism of action. J Inorg Biochem 2008;102:564–575.

[86] Barnard PJ, Berners-Price SJ. Targeting the mitochondrial cell death pathway with gold compounds. Coord Chem Rev 2007;251:1889–1902.

[87] Rackham O, Shearwood A-MJ, Thyer R, et al. Substrate and inhibitor specificities differ between human cytosolic and mitochondrial thioredoxin reductases: Implications for development of specific inhibitors. Free Radic Biol Med 2011;50:689–699.

[88] Bindoli A, Rigobello MP, Scutari G, et al. Thioredoxin reductase: A target for gold compounds acting as potential anticancer drugs. Coord Chem Rev 2009;253:1692–1707.

[89] Marzano C, Gandin V, Folda A, et al. Inhibition of thioredoxin reductase by auranofin induces apoptosis in cisplatin-resistant human ovarian cancer cells. Free Radic Biol Med 2007;42:872–881.

[90] Urig S, Fritz-Wolf K, Réau R, et al. Undressing of phosphine gold(I) complexes as irreversible inhibitors of human disulfide reductases. Angew Chem Int Ed Engl 2006;45:1881–1886.

[91] You BR, Park WH. Auranofin induces mesothelioma cell death through oxidative stress and GSH depletion. Oncol Rep 2016;35:546–551.

[92] Freire Boullosa L, Van Loenhout J, Flieswasser T, et al. Auranofin reveals therapeutic anticancer potential by triggering distinct molecular cell death mechanisms and innate immunity in mutant p53 non-small cell lung cancer. Redox Biol 2021;42:101949.

[93] Li H, Hu J, Wu S, et al. Auranofin-mediated inhibition of PI3K/AKT/mTOR axis and anticancer activity in non-small cell lung cancer cells. Oncotarget 2016;7:3548–3558.

[94] Ott I, Gust R. Non platinum metal complexes as anti-cancer drugs. Arch Pharm 2007;340:117–126.

[95] Liu W, Gust R. Metal N-heterocyclic carbene complexes as potential antitumor metallodrugs. Chem Soc Rev 2012;42:755–773.

[96] Rahman MM, Hossain KFB, Banik S, et al. Selenium and zinc protections against metal-(loids)-induced toxicity and disease manifestations: A review. Ecotoxicol Environ Saf 2019;168:146–163.

[97] Zwolak I, Zaporowska H. Selenium interactions and toxicity: a review. Selenium interactions and toxicity. Cell Biol Toxicol 2012;28:31–46.

[98] Burns FJ, Rossman T, Vega K, et al. Mechanism of selenium-induced inhibition of arsenic-enhanced UVR carcinogenesis in mice. Environ Health Perspect 2008;116:703–708.

[99] Battin EE, Zimmerman MT, Ramoutar RR, et al. Preventing metal-mediated oxidative DNA damage with selenium compounds†. Metallomics 2011;3:503–512.

[100] Naderi M, Puar P, Zonouzi-Marand M, et al. A comprehensive review on the neuropathophysiology of selenium. Sci Total Environ 2021;767:144329.

[101] Du X, Zheng Y, Wang Z, et al. Inhibitory Act of Selenoprotein P on Cu+/Cu2+-Induced Tau Aggregation and Neurotoxicity. Inorg Chem 2014;53:11221–11230.

Review https://metallomicsresearch.brte.org

Methods for recovering and recycling selenium from wastewater and soil

Osamu Otsuka[1,2*], Mitsuo Yamashita[1]

[1] Rare Metal Bio Research Center, Shibaura Institute of Technology, 307 Fukasaku, Minuma-ku, Saitama-city, Saitama 337-8570, Japan

[2] KFC Ltd., 1-19 Ookuwa, Kazo-city, Saitama 347-0010, Japan

Abstract

The high toxicity of soluble selenium (Se) has led to the establishment of environmental standards in Japan. Consequently, various methods for recovering Se from wastewater and contaminated soil have been developed and applied. Despite the recovery and recycling potential of Se after wastewater and/or soil treatment, Se recycling has rarely been mentioned in previous studies. Therefore, a recycling method for Se proposed by the authors is outlined here. Briefly, the selenate contained in wastewater was converted into solid elemental Se or volatile dimethyl diselenide via *Pseudomonas stutzeri* NT-I metabolism, recovered, purified to high-purity elemental Se, and recycled. The advantages and disadvantages of this recycling method are discussed, as well as those of other recovery and recycling treatment. Overall, Se in soils and wastewater can be recovered by choosing a treatment method suitable for each condition and Se species.

Key words: Selenium contamination, Selenium recycling, *Pseudomonas stutzeri* NT-I, biomineralization, biovolatilization, physicochemical methods

Statements about COI: The authors declare no conflict of interest associated with this manuscript.

Introduction

A recycling-oriented society in which the environment is considered, aiming at the elimination of fossil fuel dependence and reduction of global greenhouse gas effects, is required internationally. In line with this, in September 2015, the United Nations Summit adopted several Sustainable Development Goals (SDGs). As a result, research and development efforts have focused not only on reducing the cost of energy while improving its use, but also on saving resources and energy. Rare metals have supported both high-performance and environmentally compatible technologies, such as regenerative energy use (SDG 7 - Affordable and Clean Energy) and production (SDG 12 - Responsible Consumption and Production) with the premise of recycling. Unlike the common metals used in large quantities, rare metals are often used in small amounts to improve technological performance and designated as “industrial vitamins” because of their distinctive properties and essential role in electronic devices.

Selenium (Se) is a rare metal and an essential trace element for both plants and animals [1]. The antioxidant effect of Se in the human body has driven its use as a raw material in therapeutic drugs such as anticancer drugs [2]. However, Se may be toxic

*Correspondence:
Osamu Otsuka
KFC Ltd.
1-19 Ookuwa, Kazo-city, Saitama 347-0010, Japan
Tel: +81 480 76 0095 Fax: +81 480 65 8608
E-mail: ootsuka.osamu@kfc-net.co.jp

Received: October 24, 2022
Accepted: January 20, 2023
Released online: January 31, 2023

Table 1. | Laws and reference values for selenium in Japan

Target	Low name	reference value
water	Basic Environment Law Water Supply Act Sewerage Law	0.01 mg/L
	Water Pollution Control Law	0.1 mg/L
soil	Soil Contamination Countermeasures Law	0.01 mg/L (soil elution standard), 150 mg/kg (soil content standard)

to the human body if taken in excess. It is known that chronic ingestion of Se at 400 μg/day or more causes gastrointestinal disorders and peripheral neuropathy in adult human, and acute toxic effects, such as severe gastrointestinal disorders and dyspnea, when ingested at higher dosages (e.g., in g/day) [3]. As an important industrial raw material for advanced industries, Se is mainly smelted as a by-product from electrolytic slimes of copper [4]. Previously used as a semiconductor with rectifying effects, Se is now used as a material for copper indium gallium selenide (CIGS) photovoltaic panels. Recent studies have developed CIGS photovoltaic cells with conversion efficiencies exceeding 34%, and the practical application of photovoltaic cells with such high conversion efficiencies has become more realistic despite their low-cost and low-resource use [5].

Thus, Se has a variety of uses and an increase in its demand is expected in the future. With the expansion of Se production and application, industrial wastewater containing this metal at concentrations high enough to be considered non-natural [6] and the increasing possibility of Se leak into the environment have to be considered. However, it is difficult for purifying, recovering, and reusing the Se contained in industrial wastewater. This is because industrial wastewater contains impurity ions such as As, Fe, Cu and S and the others in addition to selenium [7, 8]. In industrial wastewater, Se occurs mostly in the form of selenate [Se(VI)] or selenite [Se(IV)] oxyanions, which are detrimental to organisms at low levels. For instance, the half-lethal dose (LD50) of oral administration in rats is 1.6 mg/kg for selenate and 10 mg/kg for selenite, which is comparable to the LD50 of arsenic, regarded as a severe venom [9–11]. The Japanese government has focused on the toxicity of Se and has legislated on the Se standards for water, soil, and air (**Table 1**). Currently, Se refining processes and thermal power plants generate wastewater containing high concentrations of soluble seleno-oxyanions [12]. Physicochemical treatments, such as coprecipitation, have been implemented to treat wastewater containing Se and allowed achieving Se levels in solution under 0.1 mg/L before discharge (**Figure 1**). For soluble Se, physicochemical treatment methods for selenate in particular are still being investigated but a treatment combining ion exchange and precipitation methods for high Se concentration has been proposed [13–17]. Although the purpose of these treatment methods is to remove Se, there are few reports on the recovery, purification, and recycling of removed Se.

Because Se is present at trace concentrations not only in wastewater but also in the natural environment (e.g., in volcanic sediments), naturally-derived Se is widely distributed in Japan, which has many volcanos [18–21]. Japan's soil contamination controls and environmental basic laws establish the standard levels for Se and the countermeasures to be applied when the levels are exceeded, even for naturally-derived Se. Excavation muck, such as that from tunnel construction, is likely to contain Se

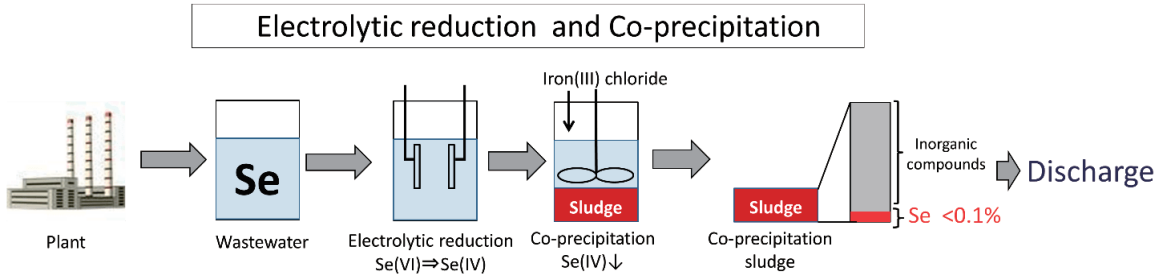

Figure 1. | Overview of the selenium (Se) treatment by co-precipitation method

Table 2. | Chemical reaction and valence of Se

Reaction No.	Starting material	Valence	Purification method	Reaction	Refined product
1	Se(VI)	VI	Addition of Barium (II)	$Ba^{2+} + SeO_4^{2-} \rightarrow BaSeO_4$	$BaSeO_4$
2			Boil in concentrated HCl	$H_2SeO_4 + 2HCl \rightarrow H_2SeO_3 + Cl_2 + H_2O$	Se(IV)
3	Se(IV), SeO_2	IV	Addition of Barium (II)	$Ba^{2+} + SeO_3^{2-} \rightarrow BaSeO_3$	$BaSeO_3$
4			Addition of Ascorbic acid	Ascorbic acid + SeO_3^{2-} →Dehydroascorbic acid + Se(0)	Se(0)
5			Addition of $Na_2S_2O_4$	$H_2SeO_3+Na_2S_2O_4 \rightarrow Se(0)+Na_2SO_4 + SO_2 + H_2O$	Se(0)
6			Addition of KI	$H_2SeO_3 + 4KI + 4HNO_3 \rightarrow Se(0) + 2I_2 + 4KNO_3 + 3H_2O$	Se(0)
7	Bioselenium	0	Oxidizing roasting	$Se(0) \rightarrow SeO_2$	SeO_2

[22, 23] leading to increased construction costs and delayed construction periods due to the countermeasures that need to be applied. In the natural environment, Se is found at low concentrations, unlike that observed for industrial wastewater, and thus the recycling of environmental Se has not been examined. If no regulated substances, such as Se, are included in the materials discharged from tunnel construction, the soil is reused (e.g., embankment materials) however, if Se is present in the soil, even after it has been treated, it may leach back into the environment and worsen the health damages to the soil. Therefore, the soil itself is not reused and is treated as waste.

In Japan, most of the Se produced is exported as elemental Se or selenium dioxide to foreign countries. In this review, "recycling" is defined as the conversion to pure Se compounds that are on the market. Therefore literature on Se compounds obtained by conventional treatment methods and Se recycling methods are outlined, and the authors' recycling method is introduced.

Recovery and recycling of Se in solution

Se recovery using physicochemical treatment

Ion exchange [13, 17] and adsorbent [16, 24] methods have been studied as physicochemical treatments for Se. Shi et al. reported Se removals of 96% in 100 μg/L Se-containing wastewater by using strongly basic anion-exchange resins [13]. Although Se in an ion exchange membrane after treatment has not been mentioned, a solution that has been membrane-concentrated as a selenate or a selenite solution can be recovered by desorption from an ion exchange membrane.

A method for recovering barium selenate ($BaSeO_4$) is via precipitation from a selenate solution [25]; it can then be further reduced to selenite by using a reducing agent[26]. $BaSeO_4$ can be recovered from a selenate solution containing little contaminants by adding barium chloride as a precipitate (**Table 2, Reaction 1**). Moreover, $BaSeO_4$ can be recycled because it is distributed at a price equivalent to elemental Se. However, it should be noted that the products of these reactions may compete with Se and considered as impurities if arsenic and sulfate ions are contaminants in the solutions. Selenate reduction to selenite (**Table 2, Reaction 2**) is also effective because it increases Se purification (**Table 2, Reactions 3-6**).

There is also a method by which a selenite solution is precipitated to recover barium selenite ($BaSeO_3$) and further reduced to elemental Se. Like selenate solutions, selenite solutions can be purified to $BaSeO_3$ by the addition of barium chloride [27]. However, when arsenic and sulfate ions are also contained as contaminants, this reaction may lead to impurities in the final product. It is also possible to reduce $BaSeO_3$ to elemental Se by adding ascorbic acid and sodium sulfite [28]. The reduction and recovery of selenite at room temperature yields amorphous Se, which exhibits the same red color as elemental Se. Amorphous Se and iodine are precipitated by adding potassium iodide to a selenite solution under acidic conditions. As the precipitated iodine volatilizes as hydrogen iodide when sodium sulfite is added, elemental Se can be recovered by solid-liquid separation.

Table 3. | Bacterial treatment technology for waste water containing selenium

Processing method	Additive	Initial Se concentration (mM)	Recovery Se	Se purity of the recovered product	Selenium purity after refined	reference
Batch reactor	rice straw	0.01	Bioselenium	208μg/L	–	[54]
Sludge-blanket reactor	*Thauera selenatis*	0.01	Bioselenium	237 μg/L	–	[30]
Upflow Anaerobic Sludge Bed reactor	*Sulfurospirillum barnesii*	0.01	Bioselenium in polyacrylamide	1194 mg/kg	–	[31]
Membrane biofilm reactor	methane oxidizing consortium	0.01	Bioselenium	–	–	[55]
Membrane biofilm reactor	anaerobic biofilm	0.03	Bioselenium	–	–	[56]
Membrane biofilm reactor	methane oxidizing consortium	0.06	Bioselenium	–	–	[57]
Biotrickling filter	activated sludge	0.09	Bioselenium	–	–	[58]
Upflow Anaerobic Sludge Bed reactor	granularbsludge	0.13	Bioselenium	437mg/g	–	[59]
Batch reactor	*Pseudomonas stutzeri* NT-I	0.50	Bioselenium	30%	99%	[33], [34]
			Mehtlseleninic adic	0.04%	99%	

Se recovery via microbial metabolism

By using the metabolism of bacteria to recover Se, a specific reaction is used, and as a result, the recovered product has fewer contaminants than the product obtained by physicochemical means. In addition to elemental selenium, the sludge mixture also contains bacteria cells, hereafter referred to as "bioselenium". The elemental Se that can be recovered by microbial metabolism also has antimicrobial activity inhibiting the viability of an *Escherichia coli* [29]. However, if it cannot be purified elemental selenium from bioselenium, it will not be reused. Selenium treatments utilizing specific Se metabolic pathways and recycling methods from recovered materials are discussed below.

Recovery and recycling by biomineralization

Reports of selenium wastewater treatment using microbial mineralization are shown in **Table 3**. Cantafio et al. recovered elemental selenium in a 186 day operation in selenium wastewater treatment using a sludge-blanket reactor by *Thauera selenatis*. The collected sludge mixture at this time contained selenium at a concentration of 0.237 mg/L (0.0000237%) [30]. Lenz et al. immobilized *Sulfurospirillum barnesii* with acrylamide and recovered elemental selenium in an Upflow Anaerobic Sludge Bed reactor. Elemental selenium was concentrated in acrylamide gels with a maximum Se concentration of 1194 mg/kg (0.1194%) in the sludge mixture after 58 days of incubation. Lenz et al. has proposed a purification process that uses the melting point difference between selenium and acrylamide gels to thermally dissolve the gel and purify Se from the gel [31]. A report using *Pseudomonas stutzeri* NT-I reports a series of steps in selenium wastewater treatment and selenium recycling from the recovered material [32–34]. This bacterium, which was isolated from the wastewater ditch-bottom sewage of a metal-recycling plant, reduced the Se in solution to elemental Se. In fact, *P. stutzeri* NT-I can reduce selenate and selenite in aqueous solution to non-toxic and insoluble elemental Se. Dimethyl diselenide (DMDSe) was biosynthesized from elemental Se with further *P. stutzeri* NT-I cultivation [32]. Taking advantage of the Se biomineralization ability of *P. stutzeri* NT-I, we recovered bioselenium at 87.8% and 78.8% of the initial concentration from simulated and real wastewater, respectively.

Bioselenium collected by centrifugation was red and X-ray diffraction analysis suggested the presence of amorphous Se [34]. Elemental Se in bioselenium is known to change its crystal structure depending on the drying temperature [34]. Bioselenium dried at 40 °C exhibited a red color (amorphous Se, red bioselenium) while bioselenium dried at 60 °C exhibited a black color (trigonal Se). In addition to Se, six other inorganic components are present in bioselenium: calcium, potassium, magnesium, sodium, phosphorus, and sulfur (**Table 4**).

Washing with hydrochloric acid and ethanol could concentrate the recovered bioselenium up to a Se concentration of 90%. However, contaminants could not be completely removed due to organic molecules derived from bacterial metabolism. For elemental Se, the retail price does not change depending on its crystalline structure but the higher the purity, the higher the price.

Table 4. | Elemental analysis of selenium (Se) recovery (%) from wastewater treated with *P. stutzeri* NT-I [36], [37]

N.D. : Not detected

Element	Biomeneralization			Biovolatilization	
	Bioselenium	Refined SeO_2	Refined Se(0)	Methylseleninic Acid	Refined Se(0)
Calcium	0.3-0.4	0.1	N.D.	N.D.	N.D.
Potassium	0.9-1.1	0.2	N.D.	N.D.	N.D.
Magnesium	0.3 -0.4	N.D.	N.D.	N.D.	N.D.
Sodium	0.9 -1.1	0.3	< 0.1	N.D.	0.4
Phosphorus	1.9 -4.2	N.D.	N.D.	N.D.	N.D.
Sulfur	1.8 -2.7	0.7	N.D.	0.03	N.D.
Selenium	11-14	99	99	0.04	99

As the purity of commercially available elemental Se is at least 99%, it is necessary to increase the purity of the recovered Se to 99% or more for recycling. Bioselenium is largely comprised of microbial-derived organic matter, which originate water and carbon dioxide by perfect combustion under pure oxygen. These organic substances can be easily removed from bioselenium; thus, if Se volatilization and separation from bioselenium is achieved, high-purity Se can be expected as well as its recycling. Therefore, selenium dioxide purification from bioselenium by oxidative roasting was attempted (**Table 2, Reaction 7**) [34]. Conditions of oxidized roasting were investigated, and selenium dioxide with 99% purity could be recovered when the Se in bioselenium was sufficiently oxidized (700 ℃, pure oxygen, gas flow at 100 mL/min). In addition, regardless of the Se crystal structure in bioselenium, selenium dioxide could also be recovered as amorphous and trigonal Se. The recovered selenium dioxide had a purity of 99% or more, but sulfur and calcium, which are thought to be derived from bacteria, were included as contaminants. Selenium dioxide was dissolved in water to form a selenite solution, which was then reduced to elemental Se by sodium sulfite. The sulfur and calcium contained in selenium dioxide were then removed from the purified elemental Se (**Table 2, Reaction 5**), and Se purity was further increased (**Table 4**). The purified elemental Se is equivalent in purity to the commercial elemental Se and may be reused for industrial materials and recycled. There are many reports on Se treatment methods using biomineralization (**Figure 2**). The Se in the sludge mixture may therefore be recovered as high-purity selenium dioxide by oxidative roasting.

Recovery and recycling using biovolatilization

Kagami et al. reported that *P. stutzeri* NT-I was able to reduce elemental Se to dimethyl diselenide (DMDSe) [35], meaning this unique bacterium carries out all reactions from selenate to DMDSe in a single cell. DMDSe is highly volatile and is easily removed from solutions. Kagami et al. also reported that Se in aqueous solution could be volatilized at 7.6 μmol/L/h in a flask and 14 μmol/L/h in Jarfarmenter culture. Gas-phase analysis showed that, in addition to DMDSe, dimethyl selenide (DMSe), dimethyl selenosulfide (DMSeS), and dimethyl disulfide (DMDS) were included in the gas phase of *P. stutzeri* NT-I culture. Using the Se vaporization ability of *P. stutzeri* NT-I, we recovered 71.2% and 38.9% of the initial Se concentration in nitric acid solution from simulated and real wastewater, respectively [33]. The only metallic elements detected in the nitric acid traps recovered in both simulated and real wastewater were Se and sulfur (**Table 4**). DMDSe in nitric acid becomes nonvolatile methylseleninic acid [36], which is difficult to use in the industry. Therefore, we tried to convert it into resource-valuable elemental Se (**Figure 3**). Methylseleninic acid recovered from the simulated wastewater contained 0.04% of Se and 0.03% of sulfur. A nitric acid solution containing methylseleninic acid was neutralized with sodium hydroxide; after adding hydrogen peroxide, the mixture was heated at 70 ℃ for 60 min for oxidation and conversion of methylseleninic acid into selenate. Subsequently, hydrogen chloride was added to reduce selenate and convert it into selenite (**Table 2, Reaction 2**). Finally, the reduction and conversion of ascorbic acid to elemental Se allowed the recovery of more than 99% pure Se (**Table 2, Reaction 4**).

Summary of wastewater treatment methods

When Se is physicochemically treated, contaminants may be easily included in the recovered Se compound due to non-specific reactions and therefore the purity of final product becomes low. On the contrary, microbial treatment can recover Se by specific reactions and less contaminants are therefore expected in the Se compound recovered; in addition, the purity of the final product becomes high. In particular, in the treatment using *P. stutzeri* NT-I, Se was recovered from wastewater by Se biomineralization and biovolatilization, and the recovered material was successfully recycled to elemental Se by further physicochemical treatment (**Figure 2, Figure 3**). However, microbial treatment takes longer than physicochemical treatment, which is a disadvantage of this method.

Different from the recycling of Se, research on the synthesis of high-value-added products by bacteria was also carried out. Kuroda et al., for example, synthesized bismuth selenide, which is used as a thermo-electroconversion element, by culturing *P. stutzeri* NT-I with selenite and bismuth mixed solutions [37]. Thus, instead of recovering only Se from wastewater, it is possible to simultaneously treat wastewater and synthesize bismuth selenide, a high-value-added product.

When Se wastewater is treated and the recovered Se is recycled, it is necessary to examine the final purified product morphology and the contaminants contained in Se wastewater via combined analyses.

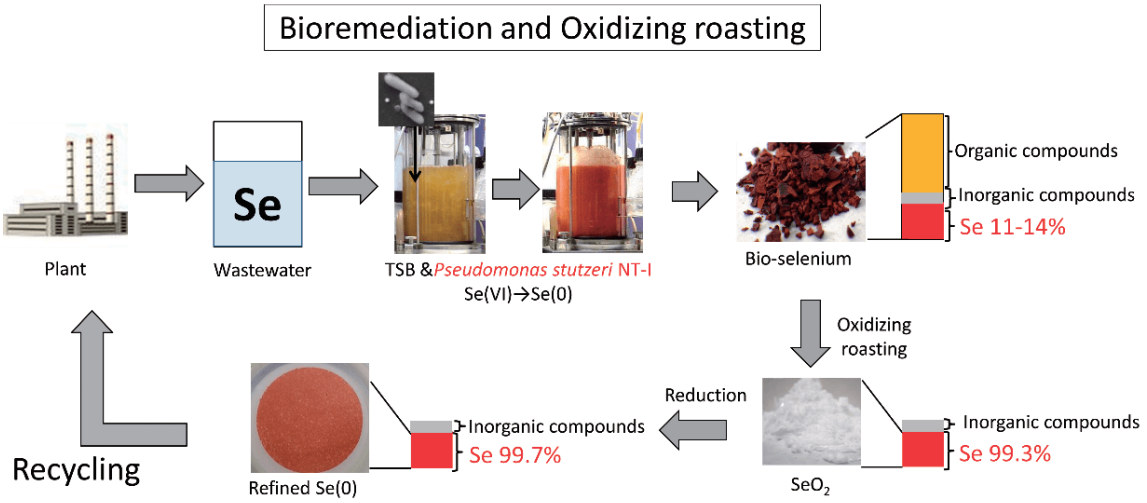

Figure 2. | Overview of the selenium (Se) treatment by Bioremediation using *Pseudomonas stutzeri* NT-I

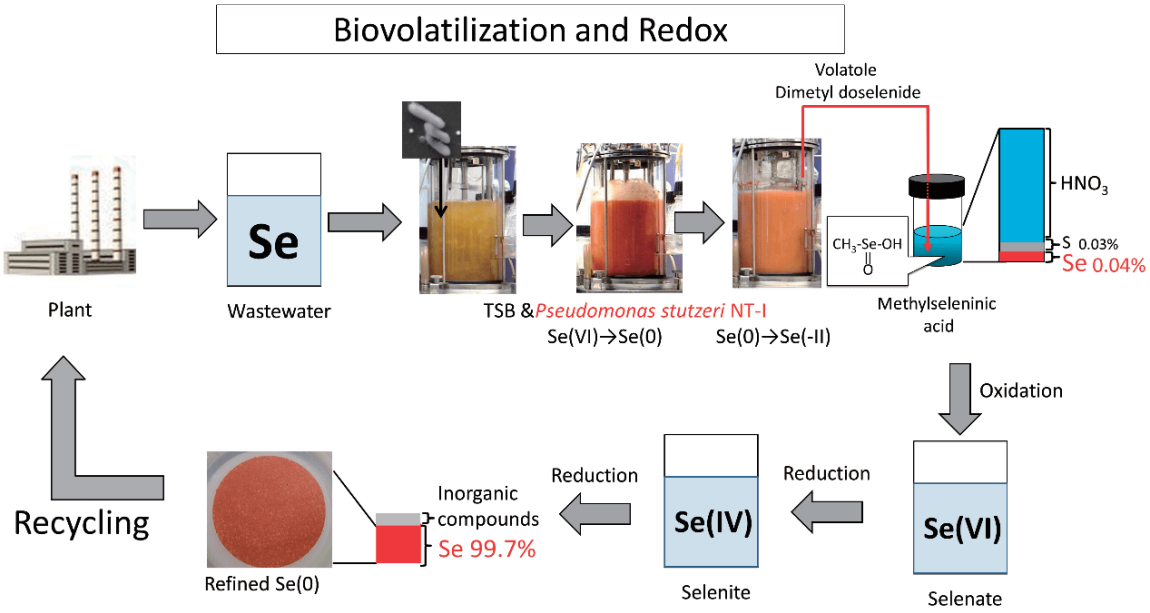

Figure 3. | Overview of the selenium (Se) treatment by Biovolatilization using *Pseudomonas stutzeri* NT-I

Se treatment methods for contaminated soil

The difficult processing of selenate is also a social problem concerning soil treatment. In Japan, the revision of the soil contamination control law in 2010 implied acting on metal concentration in soil exceeding the environmental standard, even for naturally-derived metals including arsenic, boron, cadmium, chromium, fluorine, mercury, lead, and Se. In many cases, heavy metals of natural origin are detected in workers handling large amounts of soil and sand, and the prolongation of the construction period due to countermeasures together with the cost of treatments have become a problem. Selenate in particular has attracted attention because of its low reactivity and difficulty in treatment. Therefore, the following sections outline the treatment methods used in Japan for Se-containing soil and introduce a new soil treatment method currently being examined by the authors.

Water-deprivation containment

Soils containing Se have undergone "water-deprivation containment" in which water-deprivation sheets were laid around contaminated soils to achieve environmental standards [38–41]. Physically intercepting the contact between rainwater and contaminated soil using impermeable sheets also prevents the leaching of heavy metals in contaminated soil. This is an excellent technique that can respond to all concentrations of contamination because it prevents stormwater from entering the soil. At present, it is mainstream to lay a total of five layers (three layers of protective mats plus two layers of impervious sheets) but applying this arrangement to cover the bottom, side, and top of contaminated soil presents a high work burden and large amount of material used, which leads to high treatment costs. Water-soluble Se contained in the soil remains in situ in the same form even after containment but when water-deprivation sheets surrounding contaminated soils are damaged due to earthquakes or other natural occurrences, the water-soluble Se may leak. Thus, the water-deprivation containment method continues to pose the risk of Se leakage. Furthermore, if water-soluble Se remains in the soil, soil cannot be reused.

Insolubilization

As the cost of "water-deprivation containment" is high, the heavy metal insolubilization treatment, which has a 2-day curing period and low cost, has gained increasing attention. This insolubilization method can reduce the solubility of Se in soil by mixing drugs and other substances at concentrations adjusted to the amount of contaminated soil [42, 43]. In the case of selenite contamination, it has been shown to exerts a substantial effect. However, selenate in soil as well as in wastewater has low reactivity with drugs, and therefore a large amount of chemicals is required to meet environmental standards increasing the cost of soil treatment using this method. Although the insolubilization method can prevent the leaching of Se from contaminated soil, it poses the risk of re-elution of the Se remaining in the soil. Therefore, soils contaminated with Se and treated by insolubilization cannot be reused to prevent the spread of health hazards.

Soil washing

The soil washing technique can reduce the amount of heavy metals in contaminated soil by using water and/or solvents in the total amount of contaminated soil [44, 45]. By washing out water-soluble Se from the soil and further separating the fine granules that tend to elute rapidly, the residual amount of Se in the soil becomes lower than the environmental standard while the cleaning solution (water/solvent) contains a large amount of Se at low concentration. Because the water-soluble Se is removed by this process, the soil can be reused. Although not suitable for vegetation, this soil can be used industrially for embankments as organic components and other compounds are also washed out together with Se.

Adsorption layer method

The adsorption layer method can reduce the heavy metal concentration of leached water passed through an adsorption layer consisting of an adsorbent and a base material [46, 47]. For instance, when the leachate of excavation muck passes through an adsorption layer laid in the bottom of the contaminated soil due to rainfall, it can react with the adsorbent in the adsorption layer, which reduces the concentration of heavy metals in the leachate. In recent years, a sheet-like adsorption layer containing a standardized adsorbent has been developed, and an increasing number of treatment cases have used this method characterized by low work-load and relatively low cost because it is not necessary to treat the whole soil. As Se in the contaminated soil moves along with rainwater to the adsorption layer, water-soluble Se is also removed over time. However, as there is no method of

evaluating if water-soluble Se has been completely removed from the contaminated soil, the excavation muck is not reused.

Biological metabolism method

Microbial metabolism-based (bioremediation) and plant metabolism-based (phytoremediation) methods have been attempted to insolubilize Se in selenate-contaminated soils that are difficult to treat using other methods [48–50]. However, these methods take longer to achieve the desired result when compared with existing engineering methods. Since *P. stutzeri* NT-I has a fast selenate reduction rate at 8.8×10^{-16} mol/h/cell, we considered using the bacterium as an alternative to non-specific drugs currently used for insolubilizing Se in soil. The experiments in which selenate in soils could be insolubilized by *P. stutzeri* NT-I are described below [51].

Tunnel excavation mucks were collected and used to simulate contaminated soil. The harvested excavation shears were crushed and partitioned to produce samples of 1–2 mm in diameter. When the soil dissolution test was carried out using these soil samples, the Se concentration did not exceed the environmental standard. According to the Ministry of the Environment, Se concentration in the eluted soil cannot exceed approximately 10 times the environmental reference value to be considered as natural Se contamination. Therefore, we added an aqueous sodium selenate solution to our soil samples so that the soluble Se concentration was less than ten times the environmental standard value (soil elution in mg/L); thus, simulating natural Se contamination.

To investigate Se mass balance in soil, a *P. stutzeri* NT-I suspension (optical density at 600 nm = 1.0; pH 7.0) was added at 100% to 100 g of simulated contaminated soil and allowed to stand at 38 °C. *P. stutzeri* NT-I reduces selenate to insoluble elemental Se in aqueous solution but also to DMDSe. As *P. stutzeri* NT-I reduces selenate to at least elemental Se in the soil. The phase change of soluble Se in the simulated contaminated soil after adding *P. stutzeri* NT-I was therefore investigated over time (**Figure 4**). When only sterile medium was added to the simulated contaminated soil, the Se concentration remained almost constant, but the environmental standard value was achieved in 72 h after *P. stutzeri* NT-I addition (**Figure 4 (a)**). In addition, a marked decrease in soluble Se concentration and increase in insoluble Se concentration was observed 24 h after *P. stutzeri* NT-I addition (**Figure 4 (b)**); 72 h after adding *P. stutzeri* NT-I, 94% of soluble Se was removed. This removal rate was the highest among the conditions tested so far. Analysis showed that approximately 5% of the initial concentration was detected as soluble Se and 49% as insoluble Se 72 h after *P. stutzeri* NT-I addition. Therefore, about 46% of the soluble Se in the initial soil was likely removed via *P. stutzeri* NT-I metabolism.

The Se species in the gas phase of the tested soils were measured by gas chromatograph-mass spectrometer (GC-MS), but Se metabolites such as DMDSe were not detected. However, the previous findings suggest that the soluble Se in soil was reduced to DMDSe via the high Se vaporization capacity of *P. stutzeri* NT-I [35], which could convert 82% of the initial Se concentration

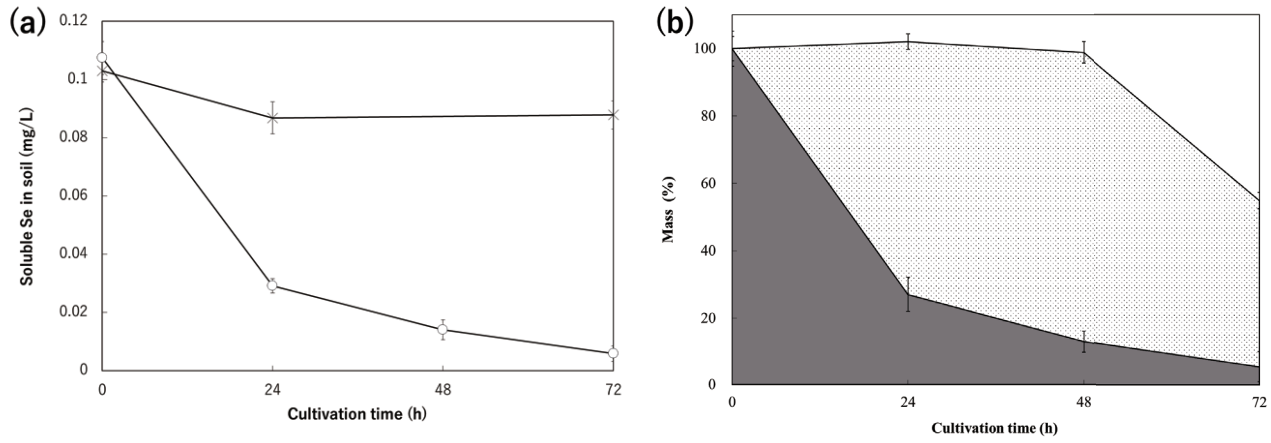

Figure 4. **Soil purification test of simulated contaminated soil**
(a) Time course of the selenium amount of soil elution.
(Open circles): addition of *P. stutzeri* NT-I; (Cross marks): addition of sterile medium (without *P. stutzeri* NT-I).
(b) Mass balance (%). Black area: soluble selenium; shaded area: insoluble selenium

in aqueous solution to DMDSe in 48 h. However, the synthesis of DMDSe by *P. stutzeri* NT-I is strongly influenced by aeration volume; the DMDSe recovery rate in the flask test without aeration was 76% but when forced aeration was used with a culture device the recovery rate increased to 82%. Therefore, forced aeration of contaminated soil by pumping may facilitate Se elimination by *P. stutzeri* NT-I. These results indicate that bacterial treatment of Se-contaminated soils not only insolubilizes the selenate in soil, but also removes Se from soils by reducing it to DMDSe. As DMDSe is synthesized in the 48 h after treatment with *P. stutzeri* NT-I and Se is removed, the soil can be reused as noncontaminated soil faster than when treated by the adsorption layer method. Because only Se is specifically removed from the soil after bacterial treatment, it can potentially be reused as a vegetation soil. Therefore, the removal of Se by *P. stutzeri* NT-I may be the most efficient treatment for naturally occurring Se-contaminated soils in Japan. However, several problems remain to be solved in the practical application of microbial treatment, such as the effect of the input microorganisms on the surrounding ecosystem.

A new treatment method to enrich metal-contaminated soil has been proposed for treated soils that can be used for supporting vegetation. It consists of flower remediation, adding the value of landscape beautification to metal-treated soil [52, 53]. Treatment of heavy metal-contaminated soils, such as those contaminated by cadmium and lead, are currently being considered. Flower remediation of Se-contaminated soil may also be possible, as several plants capable of metabolizing Se have been reported, and therefore this treatment method should be carefully examined.

Summary of soil treatment methods

Selenium-containing soil treatment also has advantages and disadvantages. The impervious sheet method can physically enclose, but there is a risk of the selenium inside leaking out if the sheet avoids it. Although the insolubilization method has a low risk of selenium leakage, it requires the chemical to be mixed with the whole soil and the construction is complicated. Soil washing has a low risk of selenium leakage, but it also has a risk of secondary contamination from the low-concentration selenium solution produced by washing. The adsorbed layer method is easy to construct, but there is a risk of leakage if selenium above the assumed concentration is piled on the adsorbed layer. Treatment using biological metabolism is easy to install, but there are still issues to be overcome before commercialization. In construction sites where large amounts of soil are transferred, such as tunnel excavation sites, natural Se-contaminated soil is produced. Treatment conditions (season, amount of soil, area available for treatment, cost, and surrounding environment) vary from site to site, and therefore the treatments that can be applied also differ. Thus, not all naturally occurring Se-contaminated soils can be reused after treatment.

Conclusions and perspectives

It has become established that selenium, in particular selenate, is difficult to treat, and the goal is to achieve environmental standards both for selenium-containing water and soil treatment. In addition, Se is cheaper than other rare metals and no significant profit can be expected when it is recycled. However, the recycling of rare metals is important to fulfill the SDGs established by the United Nations, and the recovery and reuse of Se is no exception. As outlined, there are several methods for Se treatment and further purification of the recovered Se compounds. At present, it is possible to retain the resource value of the recovered Se by selecting a suitable treatment method based on the properties of the Se-containing waste.

References

[1] S. J. Fairweather-Tait *et al.*, "Selenium in Human Health and Disease," *Antioxid. Redox Signal.*, vol. 14, no. 7, pp. 1337–1383, 2011, doi: DOI: 10.1089/ars.2010.3275.

[2] L. Kuršvietienė, A. Mongirdienė, J. Bernatonienė, J. Šulinskienė, and I. Stanevičienė, "Selenium Anticancer Properties and Impact on Cellular Redox Status," *Antioxidants*, vol. 9, no. 1, p. 80, Jan. 2020, doi: 10.3390/antiox9010080.

[3] M. Bajaj, E. Eiche, T. Neumann, J. Winter, and C. Gallert, "Hazardous concentrations of selenium in soil and groundwater in North-West India," *J. Hazard. Mater.*, vol. 189, no. 3, pp. 640–646, May 2011, doi: 10.1016/j.jhazmat.2011.01.086.

[4] C. Wang, "Selenium minerals and the recovery of selenium from copper refinery anode slimes," J. *South. Afr. Inst. Min. Metall.*, vol. 116, no. 6, pp. 593–600, 2016, doi: 10.17159/2411-9717/2016/v116n6a16.

[5] F. Ahamd, A. Lakhtakia, and P. B. Monk, "Double-absorber thin-film solar cell with 34% efficiency," *Appl. Phys. Lett.*, vol. 117, no. 3, p.

033901, Jul. 2020, doi: 10.1063/5.0017916.

[6] V. Mavrov, S. Stamenov, E. Todorova, H. Chmiel, and T. Erwe, "New hybrid electrocoagulation membrane process for removing selenium from industrial wastewater," *Desalination*, vol. 201, no. 1–3, pp. 290–296, Nov. 2006, doi: 10.1016/j.desal.2006.06.005.

[7] S. Soda *et al.*, "Biotreatment of Selenium Refinery Wastewater Using Pilot-Scale Granular Sludge and Swim-Bed Bioreactors Augmented with a Selenium-Reducing Bacterium *Pseudomonas stutzeri* NT-I," *Jpn. J. Water Treat. Biol.*, vol. 48, no. 2, pp. 63–71, 2012, doi: 10.2521/jswtb.48.63.

[8] L. C. Tan, Y. V. Nancharaiah, S. Lu, E. D. van Hullebusch, R. Gerlach, and Piet. N. L. Lens, "Biological treatment of selenium-laden wastewater containing nitrate and sulfate in an upflow anaerobic sludge bed reactor at pH 5.0," *Chemosphere*, vol. 211, pp. 684–693, Nov. 2018, doi: 10.1016/j.chemosphere.2018.07.079.

[9] A. S. Mueller and J. Pallauf, "Compendium of the antidiabetic effects of supranutritional selenate doses. In vivo and in vitro investigations with type II diabetic db/db mice," *J. Nutr. Biochem.*, vol. 17, no. 8, pp. 548–560, Aug. 2006, doi: 10.1016/j.jnutbio.2005.10.006.

[10] A. S. Muller, E. Most, and J. Pallauf, "Effects of a supranutritional dose of selenate compared with selenite on insulin sensitivity in type II diabetic dbdb mice," *J. Anim. Physiol. Anim. Nutr.*, vol. 89, no. 3–6, pp. 94–104, Apr. 2005, doi: 10.1111/j.1439-0396.2005.00559.x.

[11] S. Biswas, G. Talukder, and A. Sharma, "Selenium salts and chromosome damage," *Mutat. Res. Toxicol. Environ. Mutagen.*, vol. 390, no. 3, pp. 201–205, May 1997, doi: 10.1016/S1383-5718(97)00004-1.

[12] P. K. Petrov, J. W. Charters, and D. Wallschläger, "Identification and Determination of Selenosulfate and Selenocyanate in Flue Gas Desulfurization Waters," *Environ. Sci. Technol.*, vol. 46, no. 3, pp. 1716–1723, Feb. 2012, doi: 10.1021/es202529w.

[13] Y. S. Shi, Y. Z. Shi, and L. Wang, "Removal of Se(VI) from Raw Water by Ion Exchange Process," *Adv. Mater. Res.*, vol. 430–432, pp. 941–948, Jan. 2012, doi: 10.4028/www.scientific.net/AMR.430-432.941.

[14] M. Malhotra, M. Pal, and P. Pal, "A response surface optimized nanofiltration-based system for efficient removal of selenium from drinking Water," *J. Water Process Eng.*, vol. 33, p. 101007, Feb. 2020, doi: 10.1016/j.jwpe.2019.101007.

[15] Y. K. Kharaka, G. Ambats, T. S. Presser, and R. A. Davis, "Removal of selenium from contaminated agricultural drainage water by nanofiltration membranes," *Appl. Geochem.*, vol. 11, no. 6, pp. 797–802, Nov. 1996, doi: 10.1016/S0883-2927(96)00044-3.

[16] S. O. Okonji, J. A. Dominic, D. Pernitsky, and G. Achari, "Removal and recovery of selenium species from wastewater: Adsorption kinetics and co-precipitation mechanisms," *J. Water Process Eng.*, vol. 38, p. 101666, Dec. 2020, doi: 10.1016/j.jwpe.2020.101666.

[17] T. Nishimura, H. Hashimoto, and M. Nakayama, "Removal of Selenium(VI) from Aqueous Solution with Polyamine-type Weakly Basic Ion Exchange Resin," *Sep. Sci. Technol.*, vol. 42, no. 14, pp. 3155–3167, Oct. 2007, doi: 10.1080/01496390701513107.

[18] T. Mizutani, K. Kanaya, and T. Osaka, "Map of Selenium Content in Soil in Japan.," *J. Health Sci.*, vol. 47, no. 4, pp. 407–413, 2001, doi: 10.1248/jhs.47.407.

[19] H. Yamada, A. Kamada, M. Usuki, and J. Yanai, "Total selenium content of agricultural soils in Japan," *Soil Sci. Plant Nutr.*, vol. 55, no. 5, pp. 616–622, Oct. 2009, doi: 10.1111/j.1747-0765.2009.00397.x.

[20] Y. Kang, N. Nozato, K. Kyuma, and H. Yamada, "Distribution and forms of selenium in paddy soil," *Soil Sci. Plant Nutr.*, vol. 37, no. 3, pp. 477–485, Sep. 1991, doi: 10.1080/00380768.1991.10415061.

[21] Y. Kang, H. Yamada, K. Kyuma, and T. Hattori, "Speciation of selenium in soil," *Soil Sci. Plant Nutr.*, vol. 39, no. 2, pp. 331–337, Jun. 1993, doi: 10.1080/00380768.1993.10417004.

[22] T. Hosokawa, K. Sugai, and M. Yamazaki, "Identification and Countermeasure of Tunnel Excavation Muck Leaching Heavy Metal-Yukisawa-Daini-Tunnel, in Nihonkai-Engan Tohoku Expressway from Oodate to Kosaka Section-," *J. Jpn. Soc. Eng. Geol.*, vol. 47, no. 6, pp. 346–353, 2007, doi: 10.5110/jjseg.47.346.

[23] Y. Itaya and K. Kuninishi, "Development of selenium insolubilized material eluted from tunnel excavation rock," *Jpn. Geotech. J.*, vol. 15, no. 3, pp. 435–440, Sep. 2020, doi: 10.3208/jgs.15.435.

[24] K. Tokunaga and Y. Takahashi, "Effective Removal of Selenite and Selenate Ions from Aqueous Solution by Barite," *Environ. Sci. Technol.*, vol. 51, no. 16, pp. 9194–9201, Aug. 2017, doi: 10.1021/acs.est.7b01219.

[25] D. Rai *et al.*, "Thermodynamic model for the solubility of $BaSeO_4$ (cr) in the aqueous Ba^{2+}-SeO_4^{2-}-Na^+-H^+-OH^--H_2O system: Extending to high selenate concentrations," *Radiochim. Acta*, vol. 102, no. 9, pp. 817–830, Sep. 2014, doi: 10.1515/ract-2013-2206.

[26] H. Satake and S. Ikeda, "Differential Determination of Selenite and Selenate by Amperometric Titration," *NIPPON KAGAKU KAISHI*, no. 9, pp. 1393–1397, 1984, doi: https://doi.org/10.1246/nikkashi.1984.1393.

[27] R. Hata, T. Nishimura, and Y. Umetsu, "Solubility and Stability Regions of Barium Selenites and Barium Selenates in Aqueous Solution at 25 °C," *Can. Metall. Q.*, vol. 43, no. 1, pp. 57–66, Jan. 2004, doi: 10.1179/cmq.2004.43.1.57.

[28] Sakurai H. and Hirokawa K., "Precipitation behavior of metallic selenium and tellurium in aqueous solutions.," *BUNSEKI KAGAKU*, vol. 45, no. 8, pp. 799–804, 1996, doi: 10.2116/bunsekikagaku.45.799.

[29] J. T. Tendenedzai, E. M. N. Chirwa, and H. G. Brink, "Enterococcus spp. Cell-Free Extract: An Abiotic Route for Synthesis of Selenium Nanoparticles (SeNPs), Their Characterisation and Inhibition of Escherichia coli," *Nanomaterials*, vol. 12, no. 4, p. 658, Feb. 2022, doi:

10.3390/nano12040658.

[30] A. W. Cantafio, K. D. Hagen, G. E. Lewis, T. L. Bledsoe, K. M. Nunan, and J. M. Macy, "Pilot-Scale Selenium Bioremediation of San Joaquin Drainage Water with Thauera selenatis," *Appl. Environ. Microbiol.*, vol. 62, no. 9, pp. 3298–3303, Sep. 1996, doi: 10.1128/aem.62.9.3298-3303.1996.

[31] M. Lenz, A. M. Enright, V. O'Flaherty, A. C. van Aelst, and P. N. L. Lens, "Bioaugmentation of UASB reactors with immobilized Sulfurospirillum barnesii for simultaneous selenate and nitrate removal," *Appl. Microbiol. Biotechnol.*, vol. 83, no. 2, pp. 377–388, May 2009, doi: 10.1007/s00253-009-1915-x.

[32] M. Kuroda *et al.*, "Characterization of Pseudomonas stutzeri NT-I capable of removing soluble selenium from the aqueous phase under aerobic conditions," *J. Biosci. Bioeng.*, vol. 112, no. 3, pp. 259–264, Sep. 2011, doi: 10.1016/j.jbiosc.2011.05.012.

[33] O. Otsuka and M. Yamashita, "Selenium recovery from wastewater using the selenate-reducing bacterium Pseudomonas stutzeri NT-I," *Hydrometallurgy*, vol. 197, p. 105470, Nov. 2020, doi: 10.1016/j.hydromet.2020.105470.

[34] O. Otsuka, Y. Yanaba, T. Yoshikawa, and M. Yamashita, "Fundamental Studies on Oxidizing Roasting of the 'Bioselenium,'" *Mater. Trans.*, vol. 57, no. 7, pp. 1183–1191, 2016, doi: 10.2320/matertrans.M2016060.

[35] T. Kagami *et al.*, "Effective selenium volatilization under aerobic conditions and recovery from the aqueous phase by Pseudomonas stutzeri NT-I," *Water Res.*, vol. 47, no. 3, pp. 1361–1368, Mar. 2013, doi: 10.1016/j.watres.2012.12.001.

[36] L. Winkel, J. Feldmann, and A. A. Meharg, "Quantitative and Qualitative Trapping of Volatile Methylated Selenium Species Entrained through Nitric Acid," *Environ. Sci. Technol.*, vol. 44, no. 1, pp. 382–387, Jan. 2010, doi: 10.1021/es902345m.

[37] M. Kuroda *et al.*, "Biosynthesis of bismuth selenide nanoparticles using chalcogen-metabolizing bacteria," *Appl. Microbiol. Biotechnol.*, vol. 103, no. 21–22, pp. 8853–8861, Nov. 2019, doi: 10.1007/s00253-019-10160-2.

[38] B. Abbar, A. Alem, A. Pantet, S. Marcotte, N.-D. Ahfir, and D. Duriatti, "Experimental investigation on removal of suspended particles from water using flax fibre geotextiles," *Environ. Technol.*, vol. 38, no. 23, pp. 2964–2978, Dec. 2017, doi: 10.1080/09593330.2017.1284270.

[39] B. Abbar *et al.*, "Nonwoven flax fibres geotextiles effects on solute heavy metals transport in porous media," *Environ. Technol.*, vol. 41, no. 16, pp. 2061–2072, Jul. 2020, doi: 10.1080/09593330.2018.1555284.

[40] H. Wu *et al.*, "Review of Application and Innovation of Geotextiles in Geotechnical Engineering," *Materials*, vol. 13, no. 7, p. 1774, Apr. 2020, doi: 10.3390/ma13071774.

[41] T. Katsumi, T. Invui, and M. Kamon, "In-Situ Containment For Waste Landfill and Contaminated Sites," in *Advances in Environmental Geotechnics*, Y. Chen, L. Zhan, and X. Tang, Eds. Berlin, Heidelberg: Springer Berlin Heidelberg, 2010, pp. 248–258. doi: 10.1007/978-3-642-04460-1_17.

[42] N. T. Basta and S. L. McGowen, "Evaluation of chemical immobilization treatments for reducing heavy metal transport in a smelter-contaminated soil," *Environ. Pollut.*, vol. 127, no. 1, pp. 73–82, Jan. 2004, doi: 10.1016/S0269-7491(03)00250-1.

[43] C. S. Lwin, B.-H. Seo, H.-U. Kim, G. Owens, and K.-R. Kim, "Application of soil amendments to contaminated soils for heavy metal immobilization and improved soil quality—a critical review," *Soil Sci. Plant Nutr.*, vol. 64, no. 2, pp. 156–167, Mar. 2018, doi: 10.1080/00380768.2018.1440938.

[44] X. Guo, Z. Wei, Q. Wu, C. Li, T. Qian, and W. Zheng, "Effect of soil washing with only chelators or combining with ferric chloride on soil heavy metal removal and phytoavailability: Field experiments," *Chemosphere*, vol. 147, pp. 412–419, Mar. 2016, doi: 10.1016/j.chemosphere.2015.12.087.

[45] R. A. Wuana, F. E. Okieimen, and J. A. Imborvungu, "Removal of heavy metals from a contaminated soil using organic chelating acids," *Int. J. Environ. Sci. Technol.*, vol. 7, no. 3, pp. 485–496, Jun. 2010, doi: 10.1007/BF03326158.

[46] J. Mo, G. Flores, T. Inui, and T. Katsumi, "Hydraulic and sorption performances of soil amended with calcium-magnesium composite powder against natural arsenic contamination," *Soils Found.*, vol. 60, no. 5, pp. 1084–1096, Oct. 2020, doi: 10.1016/j.sandf.2020.05.007.

[47] O. Otsuka *et al.*, "Fundamental Study of Adsorption Thin Layers for Safe Storage of Heavy Metal Contaminated Soil," in *Advances in Sustainable Construction and Resource Management*, vol. 144, H. Hazarika, G. S. P. Madabhushi, K. Yasuhara, and D. T. Bergado, Eds. Singapore: Springer Singapore, 2021, pp. 467–476. doi: 10.1007/978-981-16-0077-7_40.

[48] M. C. Zambonino *et al.*, "Green Synthesis of Selenium and Tellurium Nanoparticles: Current Trends, Biological Properties and Biomedical Applications," *Int. J. Mol. Sci.*, vol. 22, no. 3, p. 989, Jan. 2021, doi: 10.3390/ijms22030989.

[49] S. L. Wadgaonkar, Y. V. Nancharaiah, G. Esposito, and P. N. L. Lens, "Environmental impact and bioremediation of seleniferous soils and sediments," *Crit. Rev. Biotechnol.*, vol. 38, no. 6, pp. 941–956, Aug. 2018, doi: 10.1080/07388551.2017.1420623.

[50] L. C. Tan, Y. V. Nancharaiah, E. D. van Hullebusch, and P. N. L. Lens, "Selenium: environmental significance, pollution, and biological treatment technologies," *Biotechnol. Adv.*, vol. 34, no. 5, pp. 886–907, Sep. 2016, doi: 10.1016/j.biotechadv.2016.05.005.

[51] O. Otsuka and M. Yamashita, "Development of technology to purify selenium-contaminated soil using metal biotechnology (Metallbiotechnology wo katsuyoushita seren osenn dojou no joukagijutu kaihatsu)," *Bull. Iron Steel Inst. Jpn.*, vol. 26, no. 6, pp. 351–357, 2022.

[52] F. T. Davies, J. D. Puryear, R. J. Newton, J. N. Egilla, and J. A. Saraiva Grossi, "Mycorrhizal fungi enhance accumulation and tolerance of chromium in sunflower (Helianthus annuus)," *J. Plant Physiol.*, vol. 158, no. 6, pp. 777–786, Jan. 2001, doi: 10.1078/0176-1617-00311.

[53] C.-C. Lin, H.-Y. Lai, and Z.-S. Chen, "Bioavailability Assessment and Accumulation by Five Garden Flower Species Grown in Artificially Cadmium-Contaminated Soils," *Int. J. Phytoremediation*, vol. 12, no. 5, pp. 454–467, Jul. 2010, doi: 10.1080/15226510903213985.

[54] Y. Zhang and W. T. Frankenberger, "Factors affecting removal of selenate in agricultural drainage water utilizing rice straw," *Sci. Total Environ.*, vol. 305, no. 1–3, pp. 207–216, Apr. 2003, doi: 10.1016/S0048-9697(02)00479-5.

[55] C.-Y. Lai *et al.*, "Selenate and Nitrate Bioreductions Using Methane as the Electron Donor in a Membrane Biofilm Reactor," *Environ. Sci. Technol.*, vol. 50, no. 18, pp. 10179–10186, Sep. 2016, doi: 10.1021/acs.est.6b02807.

[56] S. Xia, X. Xu, and L. Zhou, "Insights into selenate removal mechanism of hydrogen-based membrane biofilm reactor for nitrate-polluted groundwater treatment based on anaerobic biofilm analysis," *Ecotoxicol. Environ. Saf.*, vol. 178, pp. 123–129, Aug. 2019, doi: 10.1016/j.ecoenv.2019.04.005.

[57] J.-H. Luo, H. Chen, S. Hu, C. Cai, Z. Yuan, and J. Guo, "Microbial Selenate Reduction Driven by a Denitrifying Anaerobic Methane Oxidation Biofilm," *Environ. Sci. Technol.*, vol. 52, no. 7, pp. 4006–4012, Apr. 2018, doi: 10.1021/acs.est.7b05046.

[58] T. Eregowda, E. R. Rene, and P. N. L. Lens, "Bioreduction of selenate in an anaerobic biotrickling filter using methanol as electron donor," *Chemosphere*, vol. 225, pp. 406–413, Jun. 2019, doi: 10.1016/j.chemosphere.2019.02.158.

[59] T. Zeng, E. R. Rene, Q. Hu, and P. N. L. Lens, "Continuous biological removal of selenate in the presence of cadmium and zinc in UASB reactors at psychrophilic and mesophilic conditions," *Biochem. Eng. J.*, vol. 141, pp. 102–111, Jan. 2019, doi: 10.1016/j.bej.2018.10.013

Regular article https://metallomicsresearch.brte.org

Bioavailability of selenium from selenotrisulfides in primary cultured neuronal cells

Sakura Yoshida[1*], Ryosuke Mori[1], Risako Hayashi[1], Takeshi Fuchigami[2], Akira Toriba[1], Morio Nakayama[1], Mamoru Haratake[3*]

[1] Graduate School of Biomedical Sciences, Nagasaki University, 1–14 Bunkyo-machi, Nagasaki 852–8521, Japan
[2] Graduate School of Medical Sciences, Kanazawa University, Kakuma-machi, Kanazawa 920–1192, Japan
[3] Faculty of Pharmaceutical Sciences, Sojo University, 4–22–1 Ikeda, Kumamoto 860–0082, Japan

Summary

Selenium plays vital roles as a defense against oxidative stress in the central nervous system. This essential micronutrient is transported to the brain in the form of selenoprotein P. Additionally, small molecular-mass selenium compounds are also suggested to participate in supplying selenium to the brain, although its definitive transport pathways to the brain still remain unclear. Selenotrisulfide (–S–Se–S–, STS) is a metabolic intermediate of selenium and can react with free cysteine (Cys) thiols in proteins through the thiol-exchange reaction (R–S–Se–S–R' + R"–SH → R–S–Se–S–R" + R'–SH). These reactions of free Cys thiols in human hemoglobin (Hb) and serum albumin (HSA) with STS are involved in the selenium metabolic and/or transport pathway in red blood cells. In this study, rat dorsal root ganglion (DRG) neurons are supplemented with STS species including STSs bound to HSA and Hb to determine the selenium utilization efficiency from STS species. After incubation with STS species for 72 h, the cellular selenium concentration and activity of selenium-dependent glutathione peroxidase in DRG neurons increased as well as those incubated with selenious acid. Selenium from STS is thought to be absorbed and utilized for the selenoprotein synthesis in neurons.

Key words: selenium, selenotrisulfide, neuron, brain, protein thiol

*Correspondence:
Sakura Yoshida, Ph.D. Assistant professor
Department of Hygienic Chemistry, Graduate School of Biomedical Sciences, Nagasaki university
1-14 Bunkyo-machi, Nagasaki 852-8521, Japan
Tel/Fax. +81 95 819 2443, E-mail: yoshida-s@nagasaki-u.ac.jp

Mamoru Haratake, Ph.D. Professor
Faculty of Pharmaceutical Sciences, Sojo University
4-22-1 Ikeda, Kumamoto 860-0082, Japan
Tel/Fax. +81 96 326 3816, E-mail: haratake@ph.sojo-u.ac.jp

Received: October 07, 2022
Accepted: December 09, 2022
Released online: January 12, 2023

Statements about COI: The authors declare no conflict of interest associated with this manuscript.

Introduction

Selenium plays vital roles in the brain [1, 2]. Relatively higher amounts of lipids and vigorous oxygen consumption in the brain are supposed to cause numerous amounts of peroxides including phospholipid peroxides. Because excess amounts of peroxides could cause various diseases, such as cerebrovascular diseases and neurodegenerative diseases [3–5], antioxidative selenoproteins, such as glutathione peroxidases (GPxs) and thioredoxin reductases, are suppose to be important in the brain. The importance of selenium in the brain is also suggested from the fact that the selenium concentration in the brain is less vulnerable compared to other peripheral organs/tissues though the mechanism of selenium retention has not been fully

elucidated [6, 7]. Selenoprotein P (SelP) in blood is reported to play a key role in the systematic delivery of selenium to the brain [8–11]. However, there is a possibility that small molecular-mass selenium species are involved in the SelP-independent selenium transport pathway to the brain.

Selenotrisulfide (R–S–Se–S–R', STS) is thought to be one of the key metabolic intermediates of selenium [12]. STS can react with protein by the free cysteine (Cys) thiols through the thiol-exchange reaction (R–S–Se–S–R' + Protein-Cys–SH → Protein-Cys–S–Se–S–R + R'–SH). We have developed a comprehensive method to detect STS reactive protein from the organ/tissue of rodents using penicillamine selenotrisulfide (PenSSeSPen) and MALDI TOF mass spectrometry [13–16]. With this methodology, liver fatty acid binding protein, cystatin-12 precursor and myoglobin were identified to bind selenium via selenotrisulfide bonds in the liver, brain and heart of rat, respectively. Generally, STS species with small molecular-mass thiols, such as glutathione, are chemically unstable under physiological conditions. However, selenium bound to protein via STS is relatively more stable compared to STS with small molecular-mass thiols [17, 18]. There is a possibility that these STS reactive proteins can participate in the transport and/or metabolic pathways of the selenium in biological systems.

In this study, primary cultured dorsal root ganglion (DRG) neurons of rats were incubated with PenSSeSPen and protein bound STS to elucidate the involvement of STS species in the selenium transport to neuronal cells. DRG neurons can be easily obtained from adult rats and have the same biological features as the brain neurons. We previously demonstrated that selenium from selenious acid (SA) and seleno-L-methionine (SeMet) was absorbed into DRG neurons and utilized to increase the cellular GPx activity [19]. Human hemoglobin (Hb) and human serum albumin (HSA) were used as models of the STS reactive protein. Hb has free Cys thiols in its β-subunits and mediates the selenium metabolism in red blood cells (RBCs) [17, 20]. Free Cys thiol in HSA promotes the efflux of selenium from RBCs to plasma [18]. These proteins seemed to have suitable characteristics as STS reactive proteins, such that they can react with STS and stably retain selenium in its molecules. Their large molecular mass also made it easy to modify these proteins with small molecular-mass STS compounds. In addition, the selenium absorption character in DRG neurons from STS compounds was compared to human hepatoma cells.

Materials and Methods

Materials

Selenious acid (SA), seleno-L-methionine (SeMet), glutathione in the reduced form (GSH) and hydrogen peroxide were purchased from Nacalai Tesque, Inc. (Kyoto, Japan). L-Penicillamine (Pen), human serum albumin (HSA, 66,400 Da), human hemoglobin (Hb, 64,500 Da) and matrix-assisted laser desorption ionization time of flight-mass spectrometry (MALDI TOF-MS)-grade sinapinic acid were purchased from the Sigma Co. (St. Louis, MO, U.S.A.) and 2,3-diaminonaphthalene (DAN) was from Dojindo Molecular Technologies, Inc. (Kumamoto, Japan). Nicotinamide adenine dinucleotide phosphate in the reduced form (NADPH) and glutathione reductase (GR) were from the FUJIFILM Wako Pure Chemical Corporation (Osaka, Japan). The water used throughout this study (>18 MΩ cm) was generated by a Milli-Q Reference system (Millipore Corp., Billerica, MA, U.S.A.). All other chemicals were of commercial reagent or special grade and used as received.

Preparation of selenotrisulfide compounds

Thiol can react to form selenotrisulfide (STS) by the Painter reaction [6, 12]. According to this reaction procedure, L-penicillamine selenotrisulfide (PenSSeSPen) was synthesized as follows. An equal volume of 1 mM SA solution and a 4 mM Pen solution were mixed and allowed to react with stirring for 2 h at room temperature and left overnight at 4 °C. The resulting snow-white precipitate was isolated and carefully washed twice with cold water and methanol. The obtained material was dried in a desiccator at room temperature for 24 h or longer, then stored at −20 °C until used. Elemental analysis (%), calcd for $C_{10}H_{20}N_2O_4S_2Se$: C 31.97, H 5.33, N 7.46, Se 21.04, found: C 31.13, H 5.86, N 7.24, Se 21.89. $[\alpha]_D$, +7.07. λ_{max} in deionized water 266 nm (ε_{mM}: 1.47). MALDI TOF-MS (positive ion mode), calcd for $C_{10}H_{20}N_2O_4S_2{}^{80}Se$ 376.2, found *m/z* 376.3.

An equal volume of 3 mM HSA and 6 mM dithiothreitol (DTT) were mixed in 66 mM phosphate buffer (pH 7.4) and allowed to react for 90 min at room temperature. The reaction mixture was dialyzed overnight against 6.6 mM phosphate buffer (pH 7.4) at 4 °C to remove any unreacted DTT using the dialysis tube Spectra/Por Membrane (regenerated cellulose, molecular mass cutoff; 6–8 kDa, Spectrum Laboratories, Inc.). Reduced HSA was incubated with PenSSeSPen for 30 min followed by dialysis under the same conditions. STS containing HSA (HSA-SSeSPen) was concentrated and dried by lyophilization. Hb was

reduced with 12 mM DTT, and STS containing Hb (Hb-SSeSPen) was prepared by the same procedure as the HSA-SSeSPen.

Ultrafiltration

Ultrafiltration of HSA-SSeSPen and Hb-SSeSPen was performed by an Amicon Ultra Ultracel-30K [molecular-mass cut-off (MMCO) 30 kDa, Millipore Corp.]. After centrifugation at 7,500 *g*, 4 °C for 20 min, the selenium concentration in the filtrate was determined.

MALDI TOF mass spectrometry of selenotrisulfide conjugated protein

The HSA samples were digested with trypsin (0.2 mg/mL in water) at 37 °C for 1 h before the mass spectrometric analysis. An excess amount of sinapinic acid was suspended in 34% (v/v) acetonitrile and 0.067% trifluoroacetic acid for preparation of the matrix solution. After centrifugation at 7,500 *g* for 3 min, the obtained supernatant was mixed with the HSA and Hb samples in a 3 to 1 ratio by volume, and an aliquot was applied to an AnchorChip target (Bruker Daltonics, Inc., Bremen, Germany). Mass spectra were acquired in the linear positive ion mode using an Ultraflex III MALDI TOF/TOF-MS (Bruker Daltonics, Inc.).

Animals

Three-week old male Wistar rats were purchased from CLEA Japan, Inc. (Tokyo, Japan). The rats were housed on a 12-h light/ 12-h dark schedule at 25 ± 2 °C and 60% relative humidity, and were freely given deionized water and a regular CE-2 diet (CLEA Japan, Inc.). All experiments with the live animals were performed in compliance with the guidelines of the Nagasaki University on Animal Care and Use, and the institutional committee approved the experimental protocols.

Cell culture

Rat dorsal root ganglional neurons were excised from 3–6 week-old Wistar rats according to a previously described procedure [19]. Briefly, the spinal column was excised from the rat under isoflurane anaesthesia. The dorsal root ganglia (DRG) from the spinal cord were cut into small pieces in an ice cold Hanks balanced salt solution and incubated with 0.15% collagenase (from *Streptomyces parvulus*, 400–500 units/mg, Wako Pure Chemical Ind.) for 2 h, then with a mixture of 0.05% trypsin (from porcine pancreas, 1000–2000 units/mg, Nacalai Tesque, Inc.) and 0.02% EDTA for 1 h. After washing twice with medium, the treated DRG were plated into poly-L-lysine coated dishes. The DRG neurons were cultured in Dulbecco's modified Eagle medium (DMEM, FUJIFILM Wako Pure Chemical Corporation) containing 10% fetal bovine serum (FBS, Sigma Co.) supplemented with 100 IU/mL penicillin and 100 μg/mL streptomycin (FUJIFILM Wako Pure Chemical Corporation) at 37 °C and 5% CO_2 with humidity for 7–10 days before use until the dendrites of the neurons well developed. The selenium compounds, including the synthesized STS species, were dissolved in the medium to make the final selenium concentration of 1.0 μM. After incubation for the indicated period, the DRG neurons were washed 3 times with Hanks balanced salt solution followed by treatment with 0.25% trypsin. The detached DRG neurons were collected and lysed by sonication. Human hepatoma (HepG2) cells were purchased from the Japanese Collection of Research Bioresources (JCRB) cell bank. The HepG2 cells were cultured and treated under the same conditions as the DRG neurons except for using phosphate buffered saline (PBS, calcium and magnesium free) instead of Hanks balanced salt solution.

Determination of cellular glutathione peroxidase activity

The cellular GPx activity was measured by monitoring the absorbance at 340 nm due to the NADPH [21]. The cell lysate was combined with sodium azide (1 mM), a GR solution (1 unit/mL), a reduced GSH solution (1 mM) and an NADPH solution (0.2 mM) in 66 mM phosphate buffer (pH 7.4). The reaction was initiated by the addition of a hydrogen peroxide solution (0.25 mM). Absorbance at 340 nm was recorded every 1 min just after mixing by inversion. The GPx activity was calculated using the following equation (1) as μmoles of NADPH oxidized per minute, where ΔA_{SAM} is the decrease in the absorbance at 340 nm of the sample solutions between 15 and 75 s after the addition of the substrates, ΔA_{BLK} is the decrease in absorbance at 340 nm per minute of the solutions using the 66 mM phosphate buffer instead of the sample solutions, 10 is the dilution factor, ε_{mM} is the extinction coefficient for the 1 mM NADPH solution (6.22 mM^{-1} cm^{-1}), and c is the protein content (mg/mL).

$$\text{GPx activity} = (\Delta A_{SAM} - \Delta A_{BLK}) \times 10/\varepsilon_{mM}/c \quad (1)$$

Determination of selenium and protein thiol concentrations

After acid digestion with a 1 : 4 mixture by volume of perchloric acid and nitric acid, the selenium concentrations in the specimens were fluorometrically determined using DAN [22]. The selenium standard solution for atomic absorption spectrometry (1000 mg/L in 0.1 mol/L nitric acid, Kanto Chemical Co., Inc., Tokyo, Japan) was used as the standard material for preparation of the calibration curve (1-10 pgSe/mL). An FP-6600 fluorometer (JASCO Corporation, Tokyo, Japan) was used for measurement of the fluorescence intensity (Ex: 375 nm, Em: 520 nm). The protein concentrations in the specimens were measured by the Lowry method using bovine serum albumin (Nacalai Tesque, Inc.) as the standard [23]. The protein thiol concentrations were colorimetrically determined using 5,5'-dithiobis(2-nitrobenzoic acid) (DTNB, Sigma Co.) [24]. An equal volume of a 1 mM DTNB solution in a 66 mM phosphate buffer (pH 7.4) was added to the sample solution, then incubated for 30 min. The absorbance at 450 nm was recorded by a V-660 spectrometer (JASCO Corp.). GSH was used as the standard compound for preparation of the calibration curve.

Statistical analysis

All data are presented as the mean and standard deviation (SD). Statistical analyses were performed using PRISM 4 (GraphPad Software, Inc., La Jolla, CA, U.S.A.). Statistically significant differences between the controls and selenium-treated groups were determined by one-way ANOVA using the Tukey method. Comparisons were considered to be statistically significant at $P < 0.05$.

Results and discussion

PenSSeSPen is a model compound of GSSeSG, which was an important intermediate in the metabolism of selenious acid [12, 25], and efficiently used to investigate the selenium metabolic pathway and selenium reactive proteins [13-16, 20, 26]. Because PenSSeSPen is also effective in restoring the organ/tissue selenium concentration and hepatic GPx activity of dietary selenium deficient mice [6], there was a possibility that PenSSeSPen was absorbed and utilized as the selenium source compound in cultured cells. Both HSA and Hb can participate in the thiol-exchange reaction with PenSSeSPen to form the asymmetric STS (HSA-Cys34-SSeSPen and Hb-βCys93-SSeSPen, respectively) [17, 18]. One HSA molecule contains 35 Cys residues and 34 of them were involved in the 17 intramolecular disulfide bonds. Only one Cys residue at amino acid position 34 (Cys34) is free and can participate in the thiol-exchange reaction with selenotrisulfide to form HSA-Cys34-SSeSR. HSA with the free Cys thiol promotes efflux of the selenium from red blood cells (RBC) in a thiol concentration dependent manner. Selenium bound to HSA via STS can be transported to isolated rat hepatocytes [18]. On the other hand, Hb has one free Cys residue in each β subunit (Cysβ93). These free Cys thiols can also react with STS and form Hb-Cysβ93-SSeSR. Selenium bound to Hb is transferred to the free Cys thiol in anion exchanger-1 in the RBC membrane [26, 27]. These reactions of the free Cys thiols in Hb are involved in the release of selenium from the RBC. Because both HSA and Hb can bind selenium and participate in the RBC membrane transport of selenium, these proteins appeared to be suitable as model proteins transferring selenium to cultured cells in this study.

Since Cys34 in HSA is usually oxidized, reduction with DTT was carried out before the treatment with PenSSeSPen. The reduction of HSA was confirmed by determination of the thiol content in HSA [**Figure 1 (a)**]. The protein thiol content in HSA increased from 0.22 to 1.0 in the 1 HSA molecule after reduction with DTT. For further confirmation of the reduction of Cys34 of HSA, HSA before and after reduction with DTT was digested with trypsin followed by a MALDI TOF mass spectrometric analysis. The mass spectral peaks of the free-Cys containing fragments were specified by the molecular mass gain

Table 1. Selenium content in PenSSeSPen treated HSA or Hb and selenium filtration rate with MMCO 30 kDa membrane after 72-h incubation in PBS.

	Se (mol/mol-protein)	Se filtered (%)
HSA	0.56 ± 0.06	35.5 ± 8.6
Hb	0.59 ± 0.02	28.3 ± 6.6

Data are mean ± SD (n = 4).

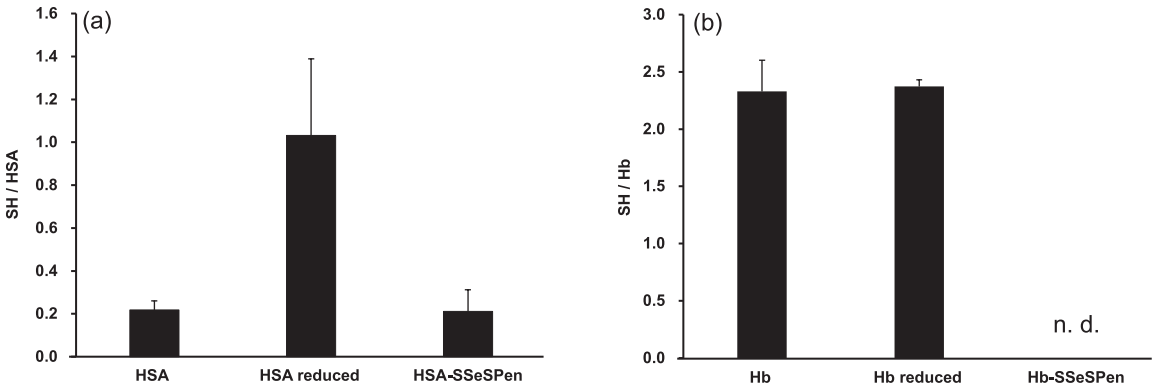

Figure 1. Thiol content in HSA (a) and Hb (b). HSA and Hb were reduced with DTT followed by treatment with PenSSeSPen. Data are mean ± SD (n = 3), n. d., not determined.

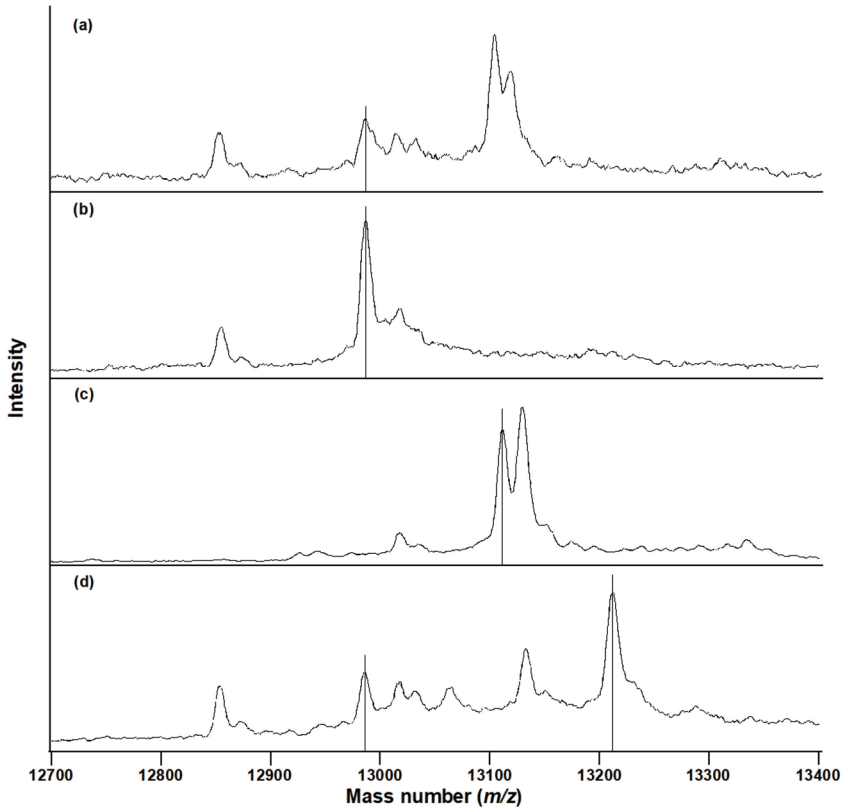

Figure 2. MALDI TOF mass spectrometric analysis of Cys34 fragment of HSA digested with trypsin. (a) non-treated HSA, (b) DTT-reduced HSA, (c) NEM-treated HSA and (d) PenSSeSPen-treated HSA. Solid lines were drawn at *m/z* 12,986 (Cys34 fragment, reduced form), *m/z* 13,112 (NEM-adduct), *m/z* 13,212 (SeSPen-adduct).

in *m/z* by 125 after alkylation with the thiol-specific *N*-ethylmaleimide (NEM) in comparison to the reduced HSA [**Figures 2 (b) and (c)**]. After digestion with trypsin, the fragment peak containing Cys34 could be detected at *m/z* 13,105 and *m/z* 12,986 in the mass spectrum of the non-reduced HSA and DTT reduced HSA, respectively [**Figures 2 (a) and (b)**]. The difference in these molecular masses of 119 was near the molecular mass of Cys (Mw: 121.16). These facts suggested that the reduction with DTT was effective to reduce thiol in Cys34 and the non-reduced HSA used in this study might be oxidized with Cys. After PenSSeSPen treatment of the reduced HSA, the thiol content in HSA decreased to 0.21 while selenium bound to HSA was calculated to be 0.56 in 1 molecule of HSA [**Figure 1 (a), Table 1**]. In the case of the PenSSeSPen-treated HSA, the molecular mass of the Cys34 containing fragment shifted by 226 (*m/z* 13,212) which corresponded to the molecular mass of selenenyl

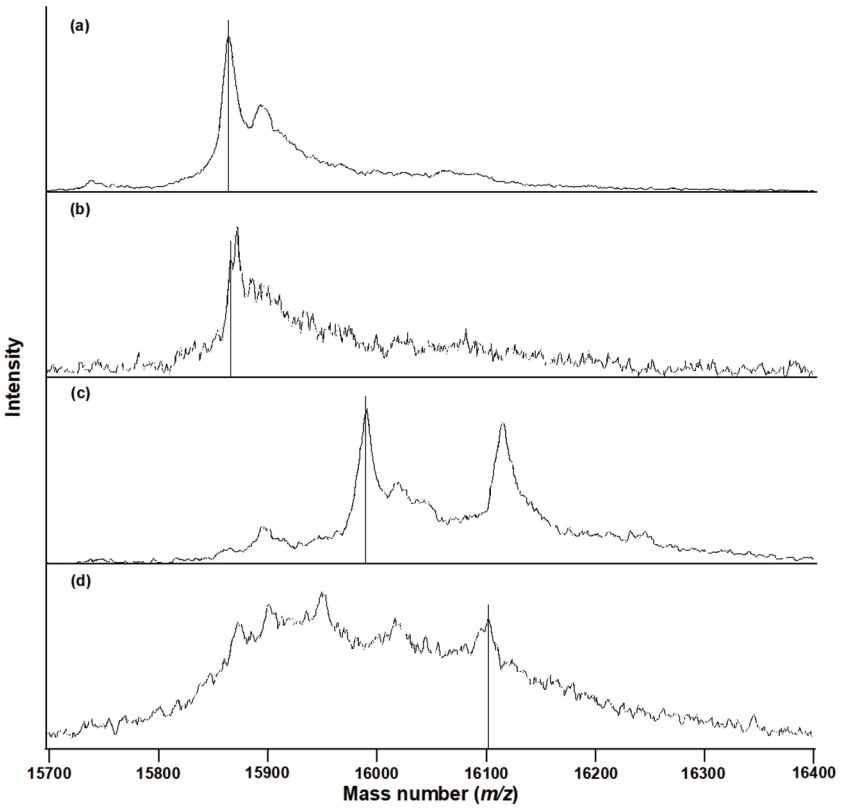

Figure 3. MALDI TOF mass spectrometric analysis of Hb β-subunit. (a) non-treated Hb, (b) DTT-reduced Hb, (c) NEM-treated Hb and (d) PenSSeSPen-treated Hb. Solid lines were drawn at *m/z* 15,864 (Hb β-subunit, reduced form), *m/z* 15,990 (NEM-adduct), *m/z* 16,099 (SeSPen-adduct).

penicillamine (−Se−S−Pen) [**Figure 2 (d)**]. These results indicated that a new STS bond was formed in the Cys34 of HSA through the thiol-exchange reaction (PenSSeSPen + HSA-Cys34−SH → HSA-Cys34-SSeSPen + Pen−SH). According to the thiol determination and mass spectrometric analysis of the PenSSeSPen-treated HSA, a considerable amount of unreacted free thiol remained in the HSA after the PenSSeSPen treatment [**Figures 1 (a) and 2 (d)**]. Additionally, the peak shift at *m/z* 13,133 in the mass spectrum of the PenSSeSPen-treated HSA suggested the formation of a disulfide bond in Cys34 with Pen (HSA-Cys34-SS-Pen). These facts seemed to contribute to the difference in the thiol content of the reduced HSA (1.0 mol/mol-HSA) and selenium content in the PenSSeSPen-treated HSA (0.56 ± 0.06 mol-Se/mol-HSA).

Human Hb-SSeSPen was also prepared by a procedure similar to the HSA-SSeSPen. Because Hb is composed of double sets of α- and β-subunits, there are 2 free Cys thiols in 1 Hb molecule (Cysβ93). Reduction of Hb with DTT did not affect the thiol content in Hb [**Figure 1 (b)**]. These data coincided with the result of the mass spectrometric analysis of the non-reduced and DTT reduced Hb, in which peaks corresponding to the Hb β-subunit were observed at *m/z* 15,864 in the mass spectra of both the non-reduced and reduced Hb [**Figures 3 (a) and (b)**]. The mass spectral peak of the Hb β-subunit at *m/z* 15,864 was specified by the molecular mass gain in *m/z* by 125 after treatment with NEM [**Figure 3 (c)**]. Thiols in Hb seemed to be less susceptive to oxidation compared to those in HSA. After treatment with PenSSeSPen, the thiol content in Hb decreased and could not be determined by the DTNB method [**Figure 1 (b)**]. However, the selenium bound to Hb was 0.59 ± 0.02 mol-Se/mol-Hb, which suggested only 30% of the thiol in the Hb molecules participated in the binding of selenium (**Table 1**). A peak shift corresponding to the −Se−S−Pen moiety was observed at *m/z* 16,099 in the mass spectrum of the PenSSeSPen-treated Hb [**Figure 3 (d)**]. These results demonstrated the occurrence of the thiol-exchange reaction (PenSSeSPen + Hb-Cysβ93−SH → Hb-Cysβ93-SSeSPen + Pen−SH). The formation of a disulfide bond with Pen was also suggested by the peak shift at *m/z* 16,019 in the mass spectrum of the PenSSeSPen-treated Hb and this seemed to be related to the lower selenium content than that which was estimated from the thiol content of Hb (2.0 mol/mol-Hb).

The stability of the STS-bound HSA and Hb was evaluated by ultrafiltration. Generally, STS compounds with small molecular-

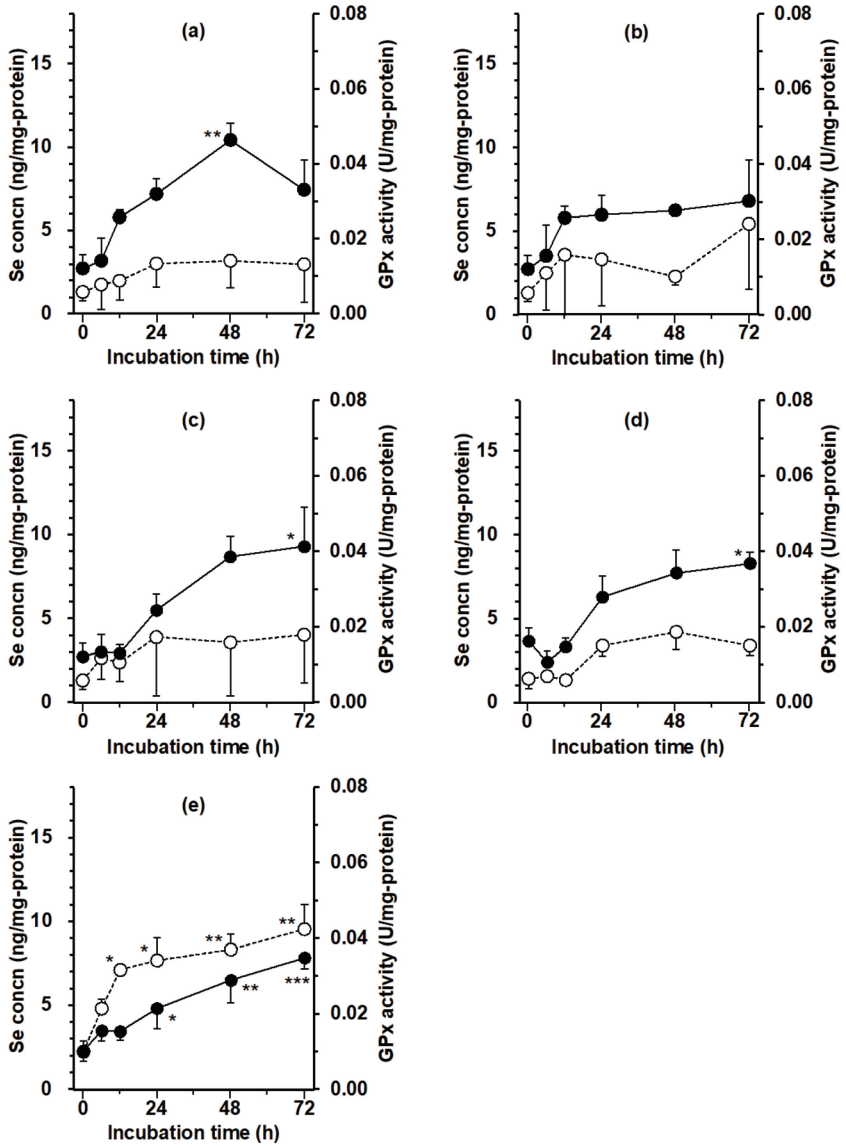

Figure 4. Changes in cellular selenium concentration (open circles) and GPx activity (closed circles) of DRG neurons incubated with SA (a), SeMet (b), PenSSeSPen (c), HSA-SSeSPen (d) and Hb-SSeSPen (e). Selenium concentrations in the culture media were 1.0 μM. Data express mean ± SD (n = 3). *, **, ***, significantly different from the value at time 0 h with $P < 0.05$, < 0.01, < 0.001 (ANOVA with a Tukey test).

mass thiols are liable to decompose and become red elemental selenium at physiological pH *in vitro.* The prepared HSA-SSeSPen and Hb-SSeSPen were each dissolved in PBS and incubated for 72 h followed by ultrafiltration with membrane MMCO 30 kDa. Selenium released from the HSA-SSeSPen and Hb-SSeSPen was calculated as 35.5 and 28.3% of the total selenium bound to the protein before incubation, respectively (**Table 1**). Because most of the selenium was proved to remain on the membrane, the protein bound STS appeared to be stable during the incubation time.

To evaluate the selenium absorption and utilization efficiency in cultured cells, the PenSSeSPen and protein bound STS were added to the medium for culture of the DRG neurons to make the final selenium concentration 1.0 μM, then incubated for 6-72 h. SA and SeMet were utilized as the standard selenium compound. Changes in the cellular selenium concentration and cellular GPx activity depended on the incubation time and the types of selenium species supplemented to the culture media. During the incubation time of 6–24 h, an increase in the cellular selenium concentration along with the incubation time was observed in all the DRG neurons supplemented with the selenium species (**Figure 4**). Although it was not significant, incubation with the selenium species other than Hb-SSeSPen kept the cellular selenium concentration at about 3–4 ng-Se/mg-protein during the incubation time of 24–72 h. A significant increase in the cellular selenium concentration was observed only in the Hb-SSeSPen-

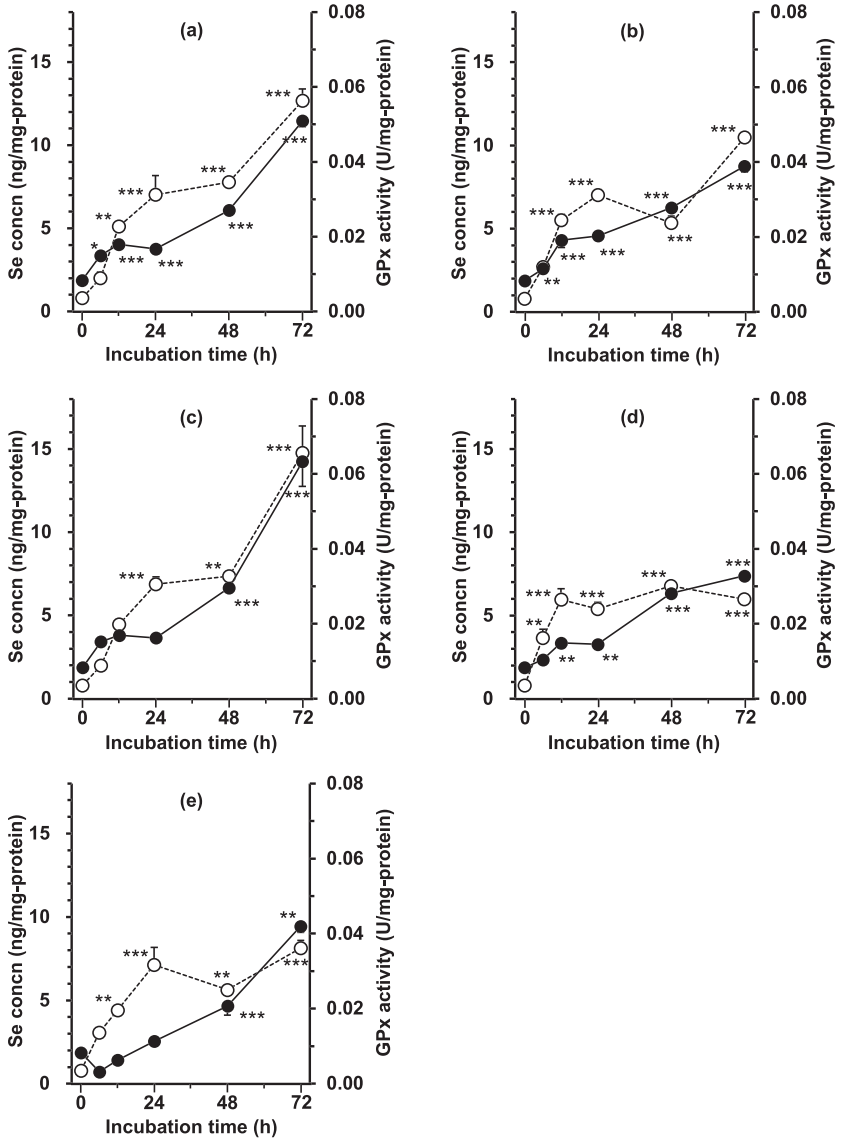

Figure 5. Changes in cellular selenium concentration (open circles) and GPx activity (closed circles) of HepG2 cells incubated with SA (a), SeMet (b), PenSSeSPen (c), HSA-SSeSPen (d) and Hb-SSeSPen (e). Selenium concentrations in the culture media were 1.0 μM. Data express mean ± SD (n = 3). *, **, ***, significantly different from the value at time 0 h with $P < 0.05$, < 0.01, < 0.001 (ANOVA with a Tukey test).

supplemented DRG neurons incubated for more than 24 h [**Figure 4 (e)**]. These data indicated that selenium from STS could be absorbed into the DRG neurons as well as SA and SeMet. The cellular GPx activity in the DRG neurons supplemented with the STS species increased in a time dependent manner. After incubation with the selenium for 72 h, the cellular GPx activity of the DRG neurons supplemented with PenSSeSPen or HSA-SSeSPen was higher than those with SA, SeMet or Hb-SSeSPen. On the other hand, the GPx activity of the DRG neurons supplemented with SA or SeMet increased faster and indicated higher values at the incubation time of 12 h. In the DRG neurons incubated for 72 h, selenium from PenSSeSPen and HSA-SSeSPen was presumed to be more effectively utilized for the synthesis of the GPx than the other selenium species. On the other hand, Hb-SSeSPen seemed to be less effective to raise the GPx activity in the DRG neurons although a remarkable increase in the cellular selenium concentration compared to the other 4 selenium species was observed. This might be due to the adhesion of Hb to the cell surface since the DRG neuron adhered the petri dish looked slightly reddish after 3 washings with Hanks balanced salt solution (data not shown). There was a possibility that selenium from Hb-SSeSPen nonspecifically bound to cell surface was not effectively absorbed into the DRG neurons and utilized for the GPx synthesis. Consequently, selenium from the STS species absorbed into the DRG neurons was suggested to be utilized for the synthesis of selenoproteins. Only the SeMet treatment did

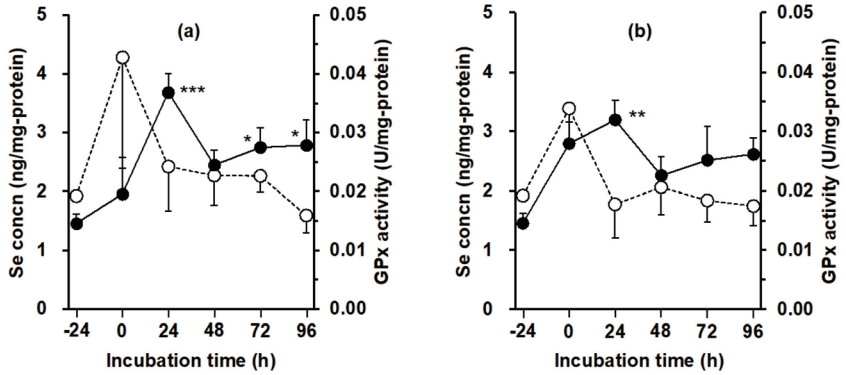

Figure 6. Changes in cellular selenium concentration (open circles) and GPx activity (closed circles) of DRG neurons incubated with PenSSeSPen (a) and HSA-SSeSPen (b). DRG neurons were incubated in 10% FBS-containing DMEM during time 0 to 96 h subsequent to 1.0 μM selenium supplemented medium during time −24 to 0 h. Data express mean ± SD (n = 3). *, **, ***, significantly different from the value at time 0 h with $P < 0.05$, < 0.01, < 0.001 (ANOVA with a Tukey test).

not cause a significant increase in the cellular GPx activity of the DRG neurons during the 72-h incubation. A similar tendency was observed when other cell lines were incubated with SeMet [28, 29]. Because SeMet is misincorporated into proteins instead of methionine and cannot be directly utilized for selenoprotein biosynthesis [30], the bioavailability of SeMet was presumed to be lower than that of the SA and STS species.

Human hepatoma (HepG2) cells were incubated with selenium species under the same conditions as the DRG neurons to examine the effect of the cell type on the selenium bioavailability from the STS species. HepG2 cells that originated from liver cancer and immortalized might have different selenium absorption and metabolic pathways from the primary cultured DRG neurons. The selenium concentration of all the HepG2 cells incubated with selenium species significantly increased after the 24-h incubation and the values were higher than that of the DRG neurons supplemented with the same selenium species except for Hb-SSeSPen (**Figure 5**). The HepG2 cells incubated with SA and PenSSeSPen exhibited a similar increasing pattern of the cellular selenium concentration and higher cellular selenium concentration [**Figures 5 (a) and (c)**]. On the other hand, the cellular selenium concentration of the HepG2 cells supplemented with HSA-SSeSPen and Hb-SSeSPen was lower than that of the HepG2 cells incubated with other selenium species including PenSSeSPen [**Figures 5 (d) and (e)**]. These data suggested that selenium absorption mechanisms from the STS species in the DRG neurons and HepG2 cells might be different. In animals, the liver is the main organ to synthesize SelP; plasma selenoprotein transports selenium from the liver to the brain and other peripheral organs [8, 9]. Because the HepG2 cells are reported to synthesize and secrete SelP [31, 32], they might be able to absorb a greater amount of selenium compared to the DRG neurons. While PenSSeSPen-supplemented HepG2 cells indicated the highest cellular GPx activity after the 72-h incubation, the increase in the cellular GPx activity of the HepG2 cells supplemented with HSA-SSeSPen and Hb-SSeSPen was lower than that of the PenSSeSPen or SA supplemented cells. This might be caused by the lower level of selenium in the protein bound STS supplemented HepG2 cells. Although the efficiency of the selenium absorption and utilization was different, selenium from the STS species appeared to be absorbed and utilized to increase the cellular GPx activity in the HepG2 cells as well as the DRG neurons. A future study will be needed to reveal the cause of these differences in the selenium utilization efficiency between the DRG neurons and HepG2 cells.

In our previous research, the DRG neurons incubated with SA or SeMet for 24 h could retain the increased cellular GPx activity for the following 96 h in the SA or SeMet free media [19]. This characteristic selenium retention behavior of the DRG neurons may be associated with the homeostatically maintained store of selenium in the brain at the whole-body level. In this study, we examined whether selenium from the STS species would be retained in the DRG neurons. DRG neurons were first incubated in the PenSSeSPen or HSA-SSeSPen-supplemented media prepared to make the selenium concentration 1.0 μM for 24 h, then incubated in STS free media for the following 96 h. After a 24-h incubation (at incubation time 0 h) with the STS species, both the DRG neurons supplemented with PenSSeSPen and HSA-SSeSPen showed an increased cellular selenium concentration (**Figure 6**). The highest cellular GPx activity was observed at 24 h after the removal of the STS species from the media in both

DRG neurons. While the selenium concentration in the DRG neurons rapidly decreased to the basal level (at incubation time −24 h), the cellular GPx activity was maintained at a higher level than that before the STS species supplementation. These facts suggested that selenium from PenSSeSPen and HSA-SSeSPen was retained in the DRG neurons and utilized to maintain the cellular GPx activity. The cellular selenium concentration in the DRG neurons after removal of the STS species was extremely low, but the GPx activity was kept at a higher level. This was probably because the amount of selenium utilized for the GPx activity was much lower than that stored in the DRG neurons. This also corresponded to the fact that there was not a correlation between the increase in the cellular selenium concentration and GPx activity in the DRG neurons (**Figure 4**). Actually, the SA supplementation at 0.1 μM was sufficient to raise the cellular GPx activity to the same level as that of the DRG neurons supplemented with 1.0 μM SA in our previous study [19]. The increase in the extremely small amount of cellular selenium was presumed to be sufficient to raise the GPx activity in the DRG neurons for at least 96 h.

In conclusion, we prepared the protein-bound STS species, HSA-SSeSPen and Hb-SSeSPen, in this study. Although selenium absorption and utilization mechanisms were thought to be different between the cell types and among the selenium source compounds, selenium from PenSSeSPen, HSA-SSeSPen and Hb-SSeSPen was absorbed into both the DRG neurons and HepG2 cells and utilized for increasing the cellular GPx activity. STS compounds including the STS bound to protein were proved to be utilized as a selenium source for the selenoprotein synthesis in both cells.

Acknowledgement

This study was supported by The Uehara Memorial Foundation. This study was the result of using research equipment shared in the MEXT Project for promoting public utilization of the advanced research infrastructure (Program for supporting introduction of the new sharing system) Grant number JPMXS0422500320.

References

[1] Rayman MP: Selenium and human health. Lancet 379: 1256-1268, 2012.

[2] Solovyev N, Drobyshev E, Blume B, Michalke B: Selenium at the neural Barriers: A review. Frontiers in Neuroscience 15: 630016, 2021.

[3] Boudina S, Abel ED: Mitochondrial uncoupling: A key contributor to reduced cardiac efficiency in diabetes. Physiology 21: 250-258, 2005.

[4] Otani K, Shichita T: Cerebral sterile inflammation in neurodegenerative diseases. Inflammation and Regeneration 40: 28, 2020.

[5] Reichert CO, de Freitas FA, Sampaio-Silva J, Rokita-Rosa L, de Lima Barros P, Levy D, Bydlowski SP: Ferroptosis mechanisms involved in neurodegenerative disease. International Journal of Molecular Sciences 21: 8765, 2020.

[6] Haratake M, Ono M, Nakayama M: Penicillamine selenotrisulfide as a selenium-source in mice. Journal of Health Science 50: 366-371, 2004.

[7] Zhang Y, Zhou Y, Schweizer U, Savaskan NE, Hua D, Kipnis J, Hatfield DL, Gladyshev VN: Comparative analysis of selenocysteine machinery and selenoproteome gene expression in mouse brain identifies neurons as key functional sites of selenium in mammals. The Journal of Biological Chemistry 283: 2427-2438, 2008.

[8] Hill KE, Zhou J, McMahan WJ, Motley AK, Atkins JF, Gesteland RF, Burk RF: Deletion of selenoprotein P alters distribution of selenium in the mouse. The Journal of Biological Chemistry 278: 13640-13646, 2003.

[9] Olson GE, Winfrey VP, NagDas SK, Hill KE, Burk RF: Apolipoprotein E receptor-2 (ApoER2) mediates selenium uptake from selenoprotein P by the mouse testis. The Journal of Biological Chemistry 282: 12290-12297, 2007.

[10] Valentine WM, Abel TW, Hill KE, Austin LM, Burk RF: Neurodegeneration in mice resulting from loss of functional selenoprotein P or its receptor apolipoprotein E receptor 2. Journal of Neuropathology and Experimental Neurology 67: 68-77, 2008.

[11] Burk RF, Hill KE, Motley AK, Winfrey VP, Kurokawa S, Mitchell SL, Zhang W: Selenoprotein P and apolipoprotein E receptor-2 interact at the blood-brain barrier and also within the brain to maintain an essential selenium pool that protects against neurodegeneration. The FASEB Journal 28: 3579-3588, 2014.

[12] Self WT, Tsai L, Stadtman TC: Synthesis and characterization of selenotrisulfide derivatives of lipoic acid and lipoamide. Proceedings of the National Academy of Sciences of the United States of America 97: 12481-12486, 2000.

[13] Hori E, Yoshida S, Haratake M, Ura S, Fuchigami T, Nakayama M: An effective method for profiling the selenium-binding proteins using its reactive metabolic intermediate. Journal of Biological Inorganic Chemistry 20, 781-789, 2015.

[14] Yoshida S, Hori E, Ura S, Haratake M, Fuchigami T, Nakayama M: Comprehensive Analysis of Selenium-Binding Proteins in the Brain Using Its Reactive Metabolite. Chemical & Pharmceutical Bulletin 64: 52-58, 2016.

[15] Hori E, Yoshida S, Fuchigami T, Haratake M, Nakayama M: Cardiac myoglobin participates in the metabolic pathway of selenium in rats. Metallomics 10: 614-622, 2018.

[16] Yoshida S, Yamamoto A, Masumoto H, Fuchigami T, Toriba A, Haratake M, Nakayama M: Peptidyl-prolyl *cis-trans* isomerase A participate in the selenium transport into the rat brain. Journal of Biological Inorganic Chemistry 26: 933-945, 2021.

[17] Haratake M, Fujimoto K, Ono, M, Nakayama M: Selenium binding to human hemoglobin via selenotrisulfide. Biochimica et Biophysica Acta 1723: 215-220, 2005.

[18] Haratake M, Hongoh M, Miyauchi M, Hirakawa R, Ono M, Nakayama M: Albumin-mediated selenium transfer by a selenotrisulfide relay mechanism. Inorganic Chemistry 47: 6273-6280, 2008.

[19] Haratake M, Koga K, Inoue M, Fuchigami T, Nakayama M: Absorption and retention characteristics of selenium in dorsal root ganglion neurons. Metallomics 3: 1019-1026, 2011.

[20] Haratake M, Fujimoto K, Hirakawa R, Ono, M, Nakayama M: Hemoglobin-mediated selenium export from red blood cells. Jornal of Biological Inorganic Chemistry 13: 471-479, 2008.

[21] Flohé L, Günzler WA: Assays of glutathione peroxidase. Methods in Enzymology 105: 114-121, 1984.

[22] Watkinson JH: Fluorometric determination of selenium in biological material with 2,3-diaminonaphthalene. Analytical Chemistry 38: 92-97, 1966.

[23] Lowry OH, Resebrough NJ, Farr AL, Randall RJ: Protein measurement with the Folin phenol reagent. The Journal of Biological Chemistry193: 265-275, 1951.

[24] Ellman GL: A colorimetric method for determining low concentrations of mercaptans. Archives of Biochemistry and Biophysics 74, 443-450, 1958.

[25] Ganther HE: Selenium metabolism, selenoproteins and mechanisms of cancer prevention: complexities with thioredoxin reductase. Carcinogenesis 20, 1657-1666, 1999.

[26] Hongoh M, Haratake M, Fuchigami T, Nakayama M: A thiol-mediated active membrane transport of selenium by erythroid anion exchanger 1 protein. Dalton Transactions 41: 7340-7349, 2012.

[27] Haratake M, Hongoh M, Ono M, Nakayama M: Thiol-dependent membrane transport of selenium through an integral protein of the red blood cell membrane. Inorganic Chemistry 48: 7805-7811, 2009.

[28] Yoshida S, Iwataka M, Fuchigami T, Haratake M, Nakayama M: *In vitro* assessment of bioavailability of selenium from a processed Japanese anchovy, Niboshi: Food Chemistry 269: 436-441, 2018.

[29] Iwataka M, Yoshida S, Koga K, Fuchigami T, Haratake M, Nakayama M: Separation of selenium species in Japanese littleneck clam 'Asari' (*Ruditapes philippinarum*) and *in vitro* assessment of their bioavailability. BPB Reports 1: 40-46, 2018.

[30] Schrauzer GN: Selenomethionine: A review of its nutritional significance, metabolism and toxicity. The Journal of Nutrition 130: 1653-1656, 2000.

[31] Dreher I, Schmutzler C, Jakob F, Köhrle J: Expression of selenoproteins in various rat and human tissues and cell lines. Journal of Trace Elements in Medicine and Biology 11: 83-91, 1997.

[32] Renko K, Martitz J, Hybsier S, Heynisch B, Voss L, Everley RA, Gygi SP, Stoedter M, Wisniewska M, Köhrle J, Gladyshev VN, Schomburg L: Aminoglycoside-driven biosynthesis of selenium-deficient selenoprotein P. Scientific Reports 7: 4391, 2017.